博士論文

Comparative Analysis of Sequential Time Discount Rate in Differential Disastrous Networks

(異なる災害時ネットワークにおける逐次時間割引率の比較分析)

WADIYA RALLAGE SAMAL SANJEEWA DHARMARATHNA

ワディヤ ララゲ サマル サンジューワ ダルマトゥナ

Comparative Analysis of Sequential Time Discount Rate in Differential Disastrous Networks

(異なる災害時ネットワークにおける逐次時間割引率の比較分析)

WADIYA RALLAGE SAMAL SANJEEWA DHARMARATHNA

ワディヤ ララゲ サマル サンジューワ ダルマトゥナ

Dissertation submitted in partial fulfillment
of the requirements for the degree of

DOCTOR OF PHILOSOPHY

in

CIVIL ENGINEERING

東京大学大学院工学系研究科

社会基盤学専攻

Department of Civil Engineering
Graduate School of Engineering
The University of Tokyo, Japan

August 20, 2018

Dedicated to my wonderful parents, without whom

I wouldn't have come this far.

To my loving wife and son, who are always

there for me.

Comparative Analysis of Sequential Time Discount Rate in Differential Disastrous Networks

Wadiya Rallage Samal Sanjeewa Dharmarathna

Doctor of Philosophy

Department of Civil Engineering

The University of Tokyo

August 2018

Supervisor: Prof. Eiji Hato

Abstract

Transportation networks are subjected to significant delays and caused operational irregularities due to both natural or man-made extremes. Natural extremes could either be unexpected like earthquake, fire, landslide or expected like heavy rainfall, flood, snowfall. Respectively, man-made events also either could be unexpected such as explosion, terrorist attack, vehicular collision or expected such as end of a famous game (e.g. world cup final), protesting rally, famous festival and so forth. Even though the severity of these events are different to each other, occurrence of such events often disturbed the normal travel plans of the people and are forced to make in-situ decisions on their route choices. Identifying the altering travelers' decision-making dynamics and degree of network cognition together with their travel behavior under these circumstances has a paramount importance in saving lives of disaster victims, saving travel time and fuel of travelers, and reducing environmental pollution which could create due to a congested network.

With the vast development in the field of computer technology, solving complex mathematical problems become easier. Correspondingly, number of modeling tools have been developed to appropriately assess and mitigate the prevailing issues in transport planning. But when it comes to address the transportation problems in unexpected or disastrous situations, such tools are limited in the literature. Hence, this study is focused the evaluate the sensitivity, stability, performance and applicability in real disaster situations of such a modeling tool, $\beta -$ scaled recursive logit ($\beta -$SRL) model, which could describe the travelers route choice behavior in such conditions. The model falls to the category of Markovian route choice models and the route choice behavior is described through the sequential time discount rate (β) which is recognized as a generalization of drivers' decision-making dynamics and a representation of the degree of spatial cognition of networks.

Chapter 3 presents the model framework of the $\beta -$SRL and the sensitivity analysis. The model corresponds to a dynamic discrete choice model and the path choice is formulated as a sequence of link choices under the umbrella of Markovian route choice models. At each node in the network, the individual is expected to choose the utility-maximizing link,

where the utility is the sum of the instantaneous link cost, the maximum expected utility to the destination and iid extreme value type I error terms. The sensitivity of the sequential time discount rate in describing the route choices was tested by using a hypothetical network with changing link costs at different locations of the network.

Parameter stability is essential for drawing conclusions or making inference on estimation results. Hence, chapter 4 is designed to test the stability of the sequential time discount rate under different network conditions. It was initially tested under moving time and random sampling under different sampling rates as 10 trips, 20 trips and 30 trips per sample. Then the same random sampling technique was applied under the criteria, in different time zones considering morning peak, day peak and evening peak, in unsteady state by considering the cumulative link delay time of trips under the categories less than 5 minutes, between 5 – 10 minutes and over 10 minutes and in different areas (networks) such as Toyosu where some events of the 2020 Olympic games will be conducted, city center of Tokyo basically in an area inside of ring road 8, and in suburbs or considering an area outside of the ring 8 road. Overall results showed that β – SRL model estimate better results under all 03 categories while 20 trips and 30 trips samples always provide stable and reliable results compare to the 10 trips samples. Further, the improvements of the results from 10 trips samples to 20 trips samples was larger in comparison with the improvements from the 20 trips samples to 30 trips samples.

Understanding mathematical characteristics and model performances are paramount importance in explaining model estimations under different network conditions. Hence chapter 5 was designed to scrutinize the matrix formations in intermediate steps of solving β −SRL model. In addition, the model performances were discussed under four different scenarios. The value functions with respect to each link of the considered network can be determined by solving the system of non-liner equations with the sequential time discount rate. Hence, such a system of non-liner equations was determined based on a hypothetical network and their elementary basis changes under the key solving steps were discussed in detail. Thereafter the model performances were discussed based on normalized network, scaled network, extended network and number of links per trip. Results under the normalized network showed assigning similar probabilities for choosing the links under the lower values of sequential time discount rate while the route choice probabilities also normalized when the sequential time discount rate gets higher values. Further sequential time discount rate produces lower values at normalized networks. The analysis based on scaled network showed that the results are holding the equivalent differences property between the alternatives. Lower sequential time discount rates were observed in the extended networks as it kept the original route choices unchanged. The results based on the influence of the number of links per trip showed that the model performance become more consistent and the estimations become more stable when estimating the samples having trips with their number of links per trip is more than 50 links.

Chapter 6 includes a comparative analysis of network behavior under two distinct and divergent disasters, the great east Japan earthquake and a torrential downpour. Probe taxi data collected under the aforementioned disaster conditions and normal days as one week after each disaster were used for the analysis. Route choice characteristics were visualized

by making a cross sectional analysis and travel behavior under each disastrous conditions were compared with a normal day variations. During both disasters that altered the normal city life, drivers had to change their original travel plans and choose alternatives. The sequential time discount rate was estimated together with two other parameters, travel time and right turn dummy variable in both circumstances. The estimated values of sequential time discount rate indicated the transition of drivers' decision-making process from global decisions to myopic decisions. In addition, the estimated values of travel time parameter under both events indicated the difficulty for drivers to evaluate travel time properly, under the congestions. The estimations of right turn dummy variable showed an increasing difficulty of making right-turns under both disaster scenarios.

Acknowledgements

Being a Ph.D. student at the University of Tokyo was a magnificent as well as challenging experience to me. During the past three years, many people were instrumental directly and indirectly in shaping up my academic career. It was hardly possible for me to thrive in my doctoral work without the precious support of those personalities. Here is a small tribute to all those people.

First of all, it is a genuine pleasure to express my deep sense of thanks and gratitude to my supervisor, Prof. Dr. Eiji Hato, for sacrificing his valuable time and passing on his vast knowledge in guiding me through the entire process. I'm incredibly grateful for his invaluable suggestions, detailed explanations and constructive criticisms throughout the past three years which helped me getting through the journey of my PhD thesis. I'm also thankful to Assoc. Prof. Yusuke Hara for his useful advices and provision of all facilities for my research in Transportation Research and Infrastructure Planning Laboratory.

I am very grateful to my thesis reading committee Prof. Dr. Takashi Oguchi, Prof. Dr. Riki Honda, Prof. Dr. Takashi Fuse and Assoc. Prof. Dr. Kiyoshi Takami for their valuable comments and remarks on my thesis. I would also like to thank Dr. Sachiyo Fukuyama and Dr. Yuki Oyama for their kind helps during the process. My appreciation also extends to my laboratory colleagues at TRIP lab and BinN lab, who assisted for my research in various occasions and also helped to sustain a positive atmosphere.

Living in Japan was a unique experience and it was highly supported by the Japanese host family. Hence, I really appreciate the kind support given by Ms. Akiko Suzuki of the host family program office and my own host family, the family of Assoc. Prof. Uchimura Taro. Also I would like to extend my appreciation to Shirokane Himawari day nursery and Tender loving day care nursery for caring my son throughout this hard living period.

I am grateful to my parents who are waiting at 7000 miles away, for their love, support, perfect understanding and encouragement that inspired me and strengthened me throughout my stay in Japan. I could never come to this level without their sacrifices and guidance. Also, I need to thank my 5-year-old son, who made lot of sacrifices from his childhood due to my busy schedules. His love and joy kept me mentally stronger in every hard time. I really appreciate the help of my wife, who also completing her PhD with me on same time, at same department. Her understanding, suggestions and encouragement also played a huge role in this achievement.

Finally, I would like to acknowledge the Ministry of Education, Culture, Sports, Science and Technology, Japan (MEXT) for providing me with the Monbukagakusho scholarship to pursue my PhD in Japan and The University of Tokyo for giving me the admission.

Table of Contents

List of Figures

List of Tables

List of Abbreviations

CDF	**C**umulative **D**istribution **F**unction
CF	**C**ommonality **F**actor
CI	**C**ongestion **I**ndex
CNL	**C**ross **N**ested **L**ogit
CV	**C**oefficient of **V**ariation
DU	**D**iscounted **U**tility
GEV	**G**eneral **E**xtreme **V**alue
GNL	**G**eneralized **N**ested **L**ogit
GPS	**G**lobal **P**ositioning **S**ystem
GRL	**G**eneralized **R**ecursive **L**ogit
IIA	**I**ndependence of **I**rrelevant **A**lternatives
iid	**i**ndependent and **i**dentically **d**istributed
IPCC	**I**ntergovernmental **P**anel on **C**limate **C**hange
JST	**J**apan **S**tandard **T**ime
LK	**L**ogit **K**ernel
LRT	**L**ight **R**ail **T**ransit
MCA	**M**arkov **C**hain **A**ssignment
MERS	**M**iddle **E**ast **R**espiratory **S**yndrome
MLE	**M**aximum **L**ikelihood **E**stimation
MNL	**M**ulti**N**omial **L**ogit
MNP	**M**ulti**N**omial **P**robit
NL	**N**ested **L**ogit
PCL	**P**aired-**C**ombinatorial **L**ogit
PDF	**P**robability **D**ensity **F**unction
PSL	**P**ath **S**ize **L**ogit
RL	**R**ecursive **L**ogit
RSD	**R**elative **S**tandard **D**eviation
RT	**R**ight **T**urn
RUM	**R**andom **U**tility **M**aximization
SD	Standard Deviation
SEM	**S**tandard **E**rror of the **M**ean

SUE	**S**tochastic **U**ser **E**quilibrium
TT	**T**ravel **T**ime
β **−SRL**	β **− S**caled **R**ecursive **L**ogit

List of Symbols

β	sequential time discount rate
a	link
c	travel cost
d	destination link
n	traveler
$p(./.)$	conditional probability
r	route
u	utility
v	deterministic utility
x	attribute
ε	error terms
θ	parameter
C_n	choice set of traveler n
V_{FF}	free flow speed
$\mathbb{P}(.)$	probability function
VAR	variance
A	set of links
$E[.]$	expected value function
G	graph
I	identity matrix
LL	value of log-likelihood function at the estimated parameters
$LL(.)$	log-likelihood function
Lc	value of log-likelihood function when all the parameters
N	set of nodes
S	state
V	average link speed
$V(.)$	value function

1 Introduction

1.1 Background

Exploring the governing formula of "how people make choices" has been an eager topic among the researchers in the arena of economics, transportation and urban planning, psychology, and so forth. With vast improvements in the field of computer technology (software, modeling and programming), numerical computations have become speedy and effortless. Correspondingly, many mathematical tools and analytical frameworks have been developed and used more frequently for solving people's choice problems. Travel behavior has neither different as it is a sub-topic in human behavior and follows the similar characteristics.

Traveling is one of the leading day-to-day activity of people which constantly maintained its significance since early in the history of discipline, with diverse improvements. People travels for various purposes, using different modes in complex networks for fulfilling their daily requirements. Increasing population together with excessive automobile usage, demanded by the growing travel needs, create congestions in traffic networks and cost man hours, fuel. This has become a serious environmental problem in both terms of noise and emissions of chemical substances, and a safety concern in many large cities in the world. Correspondingly, Intergovernmental Panel on Climate Change (IPCC) too has recommended for procuring low-emission vehicles in government purchases (IPCC, 2015).

Scope of the travel behavior analysis is expanded over individuals and households' movements and discussed through the sub-topics mode choice, destination choice, route choice, and beyond. These discussions have been generated challenging headaches on researchers working in transportation researches, due to the massive number of selfish travelers making their own decisions for personal satisfaction in highly correlated large choice sets. Accordingly, a host of models and frameworks have been developed for understanding these complexities.

This thesis is organized for scrutinizing route choice characteristics and understanding abnormal travel behaviors under differential disastrous conditions in densified networks. Road networks are frequently subjected to natural and man-made disasters such as earthquakes, extreme weather events (hurricanes, tornadoes, floods, snowfall etc.), crashes, terrorist incidents and so forth. All these disturbances cause significant delays and operational irregularities in traffic networks. Further, occurrence of such events disturbed the normal travel plans of people and more often they are forced to make in-situ decisions on their route choice. Under these circumstances, identifying the altering travelers' decision-making dynamics and degree of network cognition is very important, and this research investigate them.

Japan is geographically located in the Ring of Fire and lies at the confluence of four plates namely, Eurasian plate and North American plate from the north, Pacific plate from the east and Philippine sea plate from the south, causes the island vulnerable to natural

disasters. Together with, the increasing trend of days having precipitation over 100 and 200 mm per year (Hashida, 2016) and frequent earthquakes highlighted the necessity of disaster preparedness in transport systems. Given the fact that future weather will become more extreme, it is vital for transport planners and policy-makers to understand how they influence on travel behavior, to achieve a sustainable transport system (Liu, Susilo, & Karlstrom, 2017).

1.2 Research objectives

Understanding unsteady travel behavior in disastrous networks has a paramount importance in saving lives of disaster victims, saving travel time and fuel of travelers, and reducing environmental pollution which could create due to the congested network, through minimizing the network delays and operational irregularities caused by the disaster and its impacts. In the literature, studies have been done based on the disastrous networks, but many of such are steady state analysis (Giuliano & Golob, 1998; Iida, Kurauchi, & Shimada, 2000; Minhans, 2008; Helton, Kemp, & Walton, 2013; Lee, Zheng, Kashfi, Chia, & Yi, 2013). Further, it was highlighted the problems such the data limitations and their accuracy. Specially in the case of using questionnaire survey data of a disaster travel behavior, they could be affected by the memory decay and the emotional trauma of the event. As a solution, probe data can be presented as a good reliable data where it gives the Global Positioning System (GPS) trajectories of the travel paths. Probe data has been an emerging and encouraging data source among the transportation researchers (Miwa, Sakai, & Morikawa, 2004; Sun & Fu, 2007; Uno, Karauchi, Tamura, & Iida, 2009; Hunter, Herring, Abbeel, & Bayen, 2009; Shafique, Hato, & Yaginuma, 2014) but they were very less used in the case of understanding travel behavior in disaster conditions. With that background, this research is set up to make a comparative analysis on differential disastrous networks by using probe taxi data based on sequential time discount rate which was estimated as a parameter in an unsteady travel behavior model called $\beta-$Scaled recursive logit model (Oyama, Chikamatsu, Shoji, Hato, & Koga, 2016). In order to succeed the aforementioned purposes, the following objectives were set up for the study;

1. Illustrate the behavior of sequential time discount rate through a sample sensitivity analysis
2. Accomplish a comparative study on stability of sequential time discount rate subjected to;
    - Moving time
    - Sampling rate
    - Peak hour periods
    - Unsteady state
    - Different networks

    and find out the answers to the questions;

a) How many trips are needed for stable estimations under recursive logit framework?
b) Does it stable under different traffic conditions?
c) What are the characteristics of sequential time discount rate?

3. Estimation results of sequential time discount rate is strongly related with the link usage. Hence, identify the mathematical characteristics of value function of β −SRL model and carryout model performance analyses through normalized network, scaled network, extended network and based on the number of links per trip.

4. Carrying out a comparative study on two differential distinct disasters focusing on;
    - Exploring link speed characteristics in time-space
    - Scrutinizing trajectory patterns and their behavior
    - Analyzing travel behavior through parameter estimation

1.3 Thesis structure

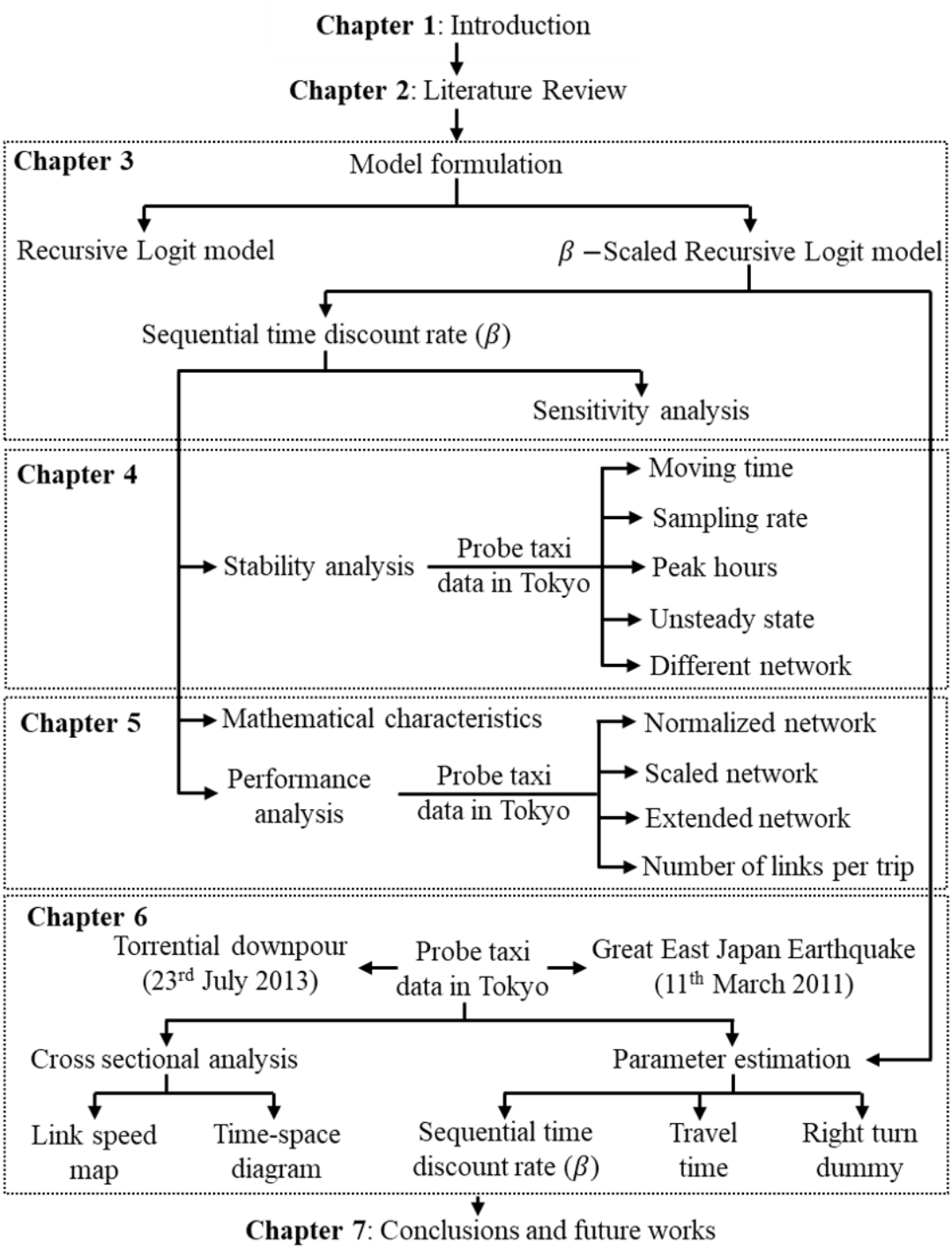

Figure 1.1 Thesis organization

2 Literature review

2.1 Overview of route choice modeling

Travel behavior analyses are basically focused on answering the questions;

- Why people travel (purposes)?
- Where do they go?
- When was the trip made?
- Which transportation mode was used?
- Which route was taken?

First two questions address the demand factors and their effected areas respectively. The rest of three questions are related to understanding infrastructure usage and visualize transportation network at different instances. A better overview on this topic can be found in Bovy and Stern (Bovy & Stern, 1990) which is considered as the first book that entirely devoted for this subject.

This thesis is basically focused on the last of the aforementioned questions, i.e. investigate the route choice behavior especially under the disastrous conditions in damaged networks. A route choice model predicts the selection probability of any given path connecting an origin and a destination, based on travelers' characteristics and routes' specifications. This is often confused with the route find problem where the shortest or the most reliable route is found based on the given origin and destination. This is used in many mobile applications such as google maps, best route finder, route planner and beyond. Whereas route choice models identify the route that a given traveler would take under the associated circumstances.

Disastrous networks are expected to cause significant delays and operational irregularities in traffic networks and cost human lives, in addition to, consume time, fuel and increase environmental pollution. Further, understanding the mechanism and identifying the anomalous driving behavior have become essential for smoothing the traffic flow and securing the road capacity for emergency and evacuation vehicles. Even though it is very important to carry out this sort of researches, they are very limited and slapped due to the lack of proper data. Under the normal circumstances, it is not given the immediate priority to collect accurate real time data within the disaster period and consecutive few hours (Iida, Karauchi, & Shimada, 2000). But such data becomes very crucial for comprehensive studies.

In addition to the aforementioned reasons specially under the disastrous conditions, modeling route choice behavior becomes essential in order to assess drivers' consciousness of route characteristics, to predict future traffic conditions on transportation networks, to predict drivers' behavior under different policy measures, to delineate the effect of traffic information, and to enhance the route choice part of traffic assignment methods. However, modeling route choice behavior is problematic due to massive number of selfish travelers making their own decisions for fulfillment of their

personal requirements in complex networks. Technically, given the complexity of representing human behavior, the lack of drivers' knowledge about the network composition, the uncertainty about drivers' perceptions of route characteristics and the unavailability of exact information about drivers' preferences cause problems in modeling route choice behavior (Prato, 2009).

2.2 Modeling concepts

2.2.1 Shortest path problem

Finding the shortest path in a transport network that a traveler can achieve his destination from a given origin with a minimum travel time or travel cost is considered as the simplest form of the route choice model. The problem is formulated as;

$$r = arg \min_{r}\{c_r\} \tag{2.1}$$

where r represents a route in the network and can be detailed as a sequence of links.

$$r = \left(a_1, \dots, a_j, \dots, a_J\right) \tag{2.2}$$

c_r is the cost of route r and a_j are sequence of links. Now, considering a directed connected graph, $G = (N, A)$ as a transportation network where N and A denotes the set of nodes and set of links respectively, the number of paths is $|A| \times |A| \times \dots \times |A| = |A|^J$. This is often uncountable. Dijkstra's algorithm (Dijkstra, 1959) is used for solving the single-source shortest path issues having positive link costs. Since travelers hardly get the perfect information of the traveling network and are heterogeneous, it is problematic to hypothesize that the shortest path issue reflects their route choice decisions. Hence, the discrete choice framework is often used for analyzing the route choice problem in order to describe the individual traveler's decision-making mechanisms.

2.2.2 Multinomial logit model

The multinomial logit (MNL) model is one of the most commonly used models in practice due to its simplicity. However, it is kept within bounds due the assumption that the error terms are identically and independently distributed (i.i.d.) which doesn't satisfy in the case of route choice scenario as the paths are naturally overlapping. The model has a long history since Prof. R. Duncan Luce proposed it as a theory of psychological choice behavior in 1959. Moving in to the mathematical formulations, discrete choice analysis which is built on the principle of random utility maximization (RUM) [(McFadden D. , 1978), (Ben-Akiva & Lerman, 1985)] is used as the framework for probabilistic route choice models. The argument when an individual n chooses a route r where $\tilde{u}_{nr}$ is the utility can be represented as;

$$r = arg \max_{r \in C_n}\{\tilde{u}_{nr}\} \tag{2.3}$$

C_n is the choice set for individual n and it is defined by the researcher. $\tilde{u}_{nr}$ includes the unobserved characteristics to the researcher and it is considered as a stochastic variable. The utility component of route r is supposed to be consist with deterministic component u_{nr} and the error component ε_{nr};

$$\tilde{u}_{nr} = u_{nr} + \varepsilon_{nr} \tag{2.4}$$

The deterministic component comprises the route attributes such as distance, travel time, number of right/left turns and beyond while the error component covers the model uncertainty.

Based on the random utility approach proposed by Manski (Manski, 1977) in the concept of consumer theory and as visualized the Eq. (2.3), subjects are expected to maximize their random utilities when choosing their routes. Accordingly, the route choice models determine the probability of the routes that contained in the choice set. Hence, the probability that subject n chooses route r can be expressed as;

$$P(r|C_n) = \mathbb{P}[u_{nr} > u_{ns}; r \neq s, \forall s \in C_n] \tag{2.5}$$

Separating the deterministic and error terms;

$$P(r|C_n) = \mathbb{P}[u_{nr} + \varepsilon_{nr} > u_{ns} + \varepsilon_{ns}; r \neq s, \forall s \in C_n] \tag{2.6}$$

Then, rearranging with the error terms;

$$P(r|C_n) = \mathbb{P}[\varepsilon_{nr} > u_{ns} - u_{nr} + \varepsilon_{ns}; r \neq s, \forall s \in C_n] \tag{2.7}$$

Based on the specific assumptions on the joint distribution of the disturbances, any particular multinomial choice model can be derived by using Eq. (2.7) [Refer (Ben-Akiva & Lerman, 1985) for more details]. Considering the joint probability distribution of all error terms, $f(\varepsilon_{nr}; r \in C_n)$, Eq. (2.7) can be re-arrange as;

$$P(r|C_n) = \int_{\varepsilon_{n1}=-\infty}^{\infty} \int_{\varepsilon_{n2}=-\infty}^{u_{n1}-u_{n2}+\varepsilon_{n1}} \dots \int_{\varepsilon_{n|C_n|}=-\infty}^{u_{n1}-u_{n|C_n|}+\varepsilon_{n1}} f(\varepsilon_{nr}; r \in C_n) d\varepsilon_{n|C_n|} \dots d\varepsilon_{n2} d\varepsilon_{n1} \tag{2.8}$$

By taking the partial derivative of Eq. (2.8) with respect to ε_{nr};

$$F_r(\varepsilon_{nr}; r \in C_n) = \frac{\partial F(\varepsilon_{nr}; r \in C_n)}{\partial \varepsilon_{nr}} \tag{2.9}$$

where $F(\varepsilon_{nr}; r \in C_n)$ is the joint distribution function of errors.

The MNL follows specific assumptions as the error components are extreme-value (or Gumbel) distributed, the error components are i.i.d. distributed across alternatives and observations/individuals. Accordingly, the cumulative distribution function (CDF) and the probability density function (PDF) are formulated as follows respectively;

$$F(\varepsilon_{nr}) = exp\left[-exp^{-\mu(\varepsilon_{nr}-\eta)}\right], \qquad \mu > 0, \tag{2.10}$$

$$f(\varepsilon_{nr}) = \mu exp^{-\mu(\varepsilon_{nr}-\eta)}.exp\left[-exp^{-\mu(\varepsilon_{nr}-\eta)}\right] \tag{2.11}$$

where η is the location parameter, that is the mode of the distribution. μ is a positive scale parameter which implies the degree of variation of ε_{nr}. The mean is $\eta + \gamma/\mu$, where γ is the Euler constant (~ 0.577) and the variance is $\pi^2/6\mu^2$. Then the MNL model is derived by substituting Eq. (2.10) and Eq. (2.11) on Eq. (2.8).

$$P(r|C_n) = \frac{exp(\mu u_{nr})}{\sum_{s \in C_n} exp(\mu u_{ns})} \tag{2.12}$$

MNL is largely been discussed among the researchers due to its independence from irrelevant alternatives property (IIA). The property states that for any individual, the ratio of the probabilities of choosing two alternatives is independent of the presence of any other alternative. Even though it looks like a simple property, it has some important consequences. In some occasions, it could generate some odd or erroneous predictions. Red bus/blue bus paradox is one of the famous examples.

2.2.3 Other related models

As stated, because of the i.i.d. assumption on the error component, biases could exist in parameters that estimated through the MNL model when the routes are overlapped between alternatives in transportation networks (Jin, Yao, Zhang, & Liu, 2017). As a result, a host of revised models were proposed to minimize the problems generated by the path overlapping in route choice. A deterministic correction, named Commonality Factor (CF), was first proposed by the Cascetta et al. in 1996 (Cascetta, Nuzzolo, Russo, & Vitetta, 1996). It is an attribute, which includes in the deterministic part of the utility and derived the C-Logit model. The value of CF for a particular path was proportional to its overlapping with remaining paths in the choice set.

Three years later, a model called Path Size Logit (PSL) (Ben-Akiva & Bierlaire, 1999) was proposed with a similar concept to the C-Logit model. In PSL model, correction for the path overlapping was obtained by adding Path Size (PS) attribute to the deterministic part of the utility. An important discovery was made and started a new chapter in the field by McFadden in 1978 with the introduction of General Extreme Value (GEV) models which allowed various flexible modeling structures. Models such as Nested Logit (NL) model (Ben-Akiva & Lerman, 1985), Cross Nested Logit (CNL) model (Vovsha & Bekhor, 1998), Paired-Combinatorial Logit (PCL) model (Koppelman & Wen, 2000), and the Generalized Nested Logit (GNL) model (Bekhor & Prashker, 2001) were introduced. Further improvements were being made with the proposals of Multinomial Probit (MNP) model (Bolduc & Ben-Akiva, 1991), and it's modified applications such as (Yai, Iwakura, & Morichi, 1997), correlation structure (Frejinger & Bierlaire, 2007), and Logit Kernel (LK) model (Bekhor, Ben-Akiva, & Ramming, 2002).

2.2.4 Maximum likelihood estimation

Maximum likelihood estimation (MLE) is the process that many route choice models mainly adopted for estimating their parameters. MIE strives to determine parameter values that maximize the likelihood function defined in each model based on given observations. Under the scenario that an individual n chooses a route r from the choice set C_n can be mathematically formulated as;

$$\max_{\theta} LL(\theta) = \log\left(\prod_{n=1}^{N}\prod_{r\epsilon C_n} P_n(r|C_n;\theta)^{\delta_r^n}\right)$$

$$= \sum_{n=1}^{N}\sum_{r\epsilon C_n} \delta_r^n \log P_n\,(r|C_n;\theta) \qquad (2.13)$$

where δ_r^n is equal to one if the individual n chooses the route r and zero otherwise. Travelers route choice preferences can be determined by solving the above formulation defined in Eq. (2.13).

2.2.5 Markovian route choice models

A Markov process is a memoryless process which is capable of being in multiple states. Further, it can make transitions between those states, where the respective state variable and transition probabilities rely only upon the current state of the system. This property is named as Markov property in probability theory and statistics, and the name was given on honor to the Russian mathematician Andrei Andreyevich Markov**.** Markovian models follow the Markov property and it is a very crucial stochastic process in the contest of route choice modeling. Markov property for a stochastic process, say $\{X_n; n = 0,1,2, \dots\}$ in a discrete state space S, can be formulated as follows;

$$\mathbb{P}(X_{n+1} = j|X_n = i, X_{n-1} = i_{n-1}, \dots, X_0 = i_0) = \mathbb{P}(X_{n+1} = j|X_n = i) \qquad (2.14)$$

where $j, i, i_{n-1}, \dots, i_0 \in S$ are state variables. As the Eq. (2.14) implies, the states $X_{n-1} = i_{n-1}, \dots, X_0 = i_0$ are not going to make any impact on the future state of the process as it is only depend on the current state, $X_n = i$. When the stochastic process is stationary or homogenous, it can be explained through the transition probability matrix $\mathbf{P}(|S| \times |S|)$. Accordingly, Eq. (2.14) reduces to transition probability or becomes an entry;

$$\mathbb{P}(X_{n+1} = j|X_n = i) = p(j|i) \qquad \forall n \qquad (2.15)$$

And the transition probability satisfies;

$$p(j|i) \geq 0, \qquad \sum_{j \in S} p(j|i) = 1 \tag{2.15}$$

Now, by adopting the Chapman-Kolmogorov principle, and $p^m(j|i)$ is the m^{th} step transition probability;

$$p^{m+n}(j|i) = \sum_{k \in S} p^m(k|i)\, p^n(j|k) \tag{2.16}$$

Accordingly, the below relationship can be derived.

$$p^n(j|i) = \big(p(j|i)\big)^n \tag{2.17}$$

Hence, once the transition probability matrix **P** is derived**,** it is possible to calculate the transition probability of any step.

When it comes to solving the route choice problem in transportation networks, it is possible to consider a path as a set of continuous nodes (links) and the route choice probability can be explained as the state transition probabilities by considering states as nodes (links). Markovian route choice models follow this concept in their modeling.

Consider the below example showed in Figure 2.1,

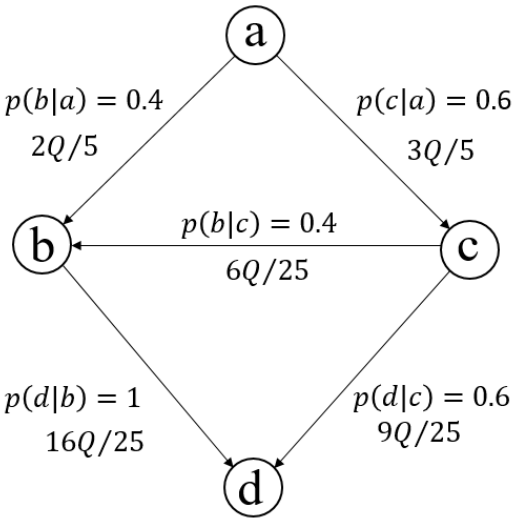

Figure 2.1 Transition probabilities in a sample network

Figure 2.1 illustrates the transition probabilities and respective traffic flows for a sample traffic flow Q departing from node "a". It is hypothesized that the flow patterns follow the Markov property and accordingly, it is notable that the principle of flow conservation has achieved at every node. Hence, the flow conservation can be formulated as:

$Q_{origin} - Q_{destination} = 0$ for all nodes.

Accordingly, it is possible to formulate the interrelationship between the link flows and their transition probability as below;

$$p(j/i) = \frac{x_{ij}}{\sum_{j'} x'_{ij'}} \tag{2.18}$$

where x_{ij} represents the link flows.

Then the path probability can be determined as a product of the transition probabilities by using Eq. (2.17);

$$\mathbb{P}\big(r = [i_0, \dots, i_J]\big) = \prod_{j=0}^{J-1} p\big(i_{J+1} | i_J\big) \tag{2.19}$$

Some of the key development stages of Markovian models for solving the route choice problem are shown in Figure 2.2

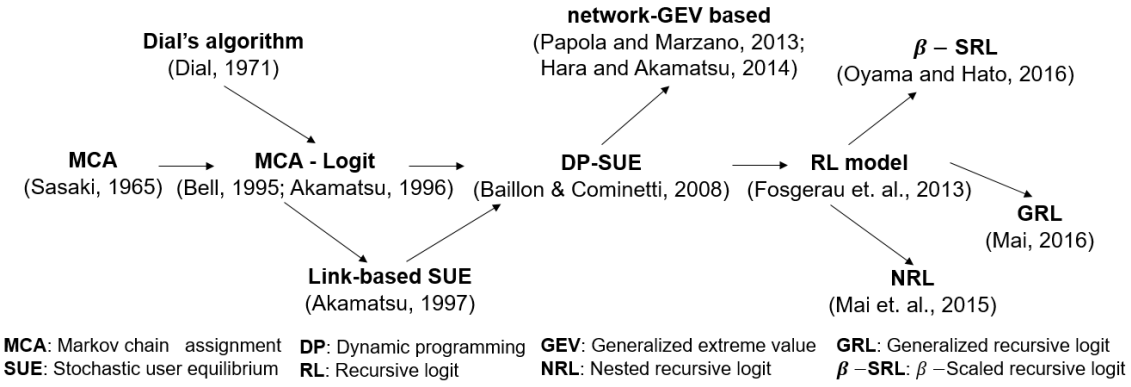

Figure 2.2 Key development stages of Markovian models for solving route choice problem

2.2.6 Sequential time discount rate

Link choice decisions occurring at different times (at different nodes) when completing a path in a road network are plausible to consider as intertemporal choices, given the fact that choices at one time influence the links availability at other nodes in time. Intertemporal choices are being discussed by the economists from a long history and milestoned with the introduction of discounted utility (DU) model (Samuelson, 1937). DU model is a generalized model of intertemporal choice where Samuelson compressed all the psychological concerns discussed over the previous century into a single parameter and called the discount rate. Per se person's intertemporal utility function $U^t(c_t, \dots \dots, c_T)$ is represented as the following functional form:

$$U^t(c_t, \dots\dots, c_T) = \sum_{k=0}^{T-t} D(k)u(c_{t+k}) \tag{2.18}$$

where $D(k) = \left(\frac{1}{1+\rho}\right)^k$.

$u(c_{t+k})$ is the person's cardinal instantaneous utility function, $t + k$ is well-being in period and $D(k)$ is the person's discount function, the relative weight she attaches in period t, to well-being in period $t + k$. ρ is the discount rate (Frederick, Loewenstein, & O'Donoghue, 2002).

Since then, discount rate is being a popular topic in the field of economics based on various monetary aspects in different time frames such as positive time preference (positive discount rate) (Olson & Bailey, 1981), constant discount rate (Kirby & Marakovic, 1995), uniform or differential discounting (Severens & Milne, 2004), preference reversals (Green, Fristoe, & Myerson, 1994) and so forth. Meanwhile, researchers in other fields also have attempted to understand the discounting of non-monetary and mixed-outcomes. Temporal discounting for health and money (Chapman & Elstein, 1995), delayed discounting for additive substances (Bickel & Johnson, 2003) are some of the such examples.

Drivers discount the travel time when making link choice decisions at each node and hence, the aforementioned concept can be adopted in solving route choice problems. Since route choice is a link by link (node by node) process over the time frame, discount rate becomes sequential time discount rate. Oyama et al. (Oyama, Chikamatsu, Shoji, Hato, & Koga, 2016) generalized the recursive logit (RL) model (Fosgerau, Frejinger, & Karlstrom, 2013) by incorporating the sequential time discount rate and referred as β – scaled recursive logit model (β – SRL). β – SRL model follows the Markovian approach, which assess the path choice probabilities as the products of link transition probabilities and avoids the necessity to enumerate path set. The approach has initially been applied for traffic assignment and recently been highlighted due to its consistency with logit type route choice modeling without path enumeration.

2.3 Travel behavior in disrupted networks

Steady travel behavior of a transportation network could disturb and become unsteady due to natural or man-made extremes. Natural extremes could either be unexpected like earthquakes, fire, landslides or expected like heavy rainfalls, floods, snowfalls. As same as, man-made events also either could be unexpected such as explosions, terrorist attacks, vehicular collisions or expected such as end of famous games (e.g. world cup final), protesting rallies, famous festivals and so forth. Even though the severity of these events are different to each other, the effectiveness of transportation systems can be remarkably enhanced through sufficient planning and training, capacity and demand management

processes such as signal coordination retiming, elimination of conflict points, route closures, contraflow, evacuation phasing and forced movements (Matherly, et al., 2013).

Once a disaster is being occurred on a traffic network, it is important to investigate the system capacity to bounce back or the system resilience [e.g. (Barker, Ramirez-Marquez, & Rocco, 2013; Nogal, O'Connor, Caulfield, & Martinez-Pastor, 2016; Faturechi & Hooks, 2014)]. But enhancing resilience is highly depending on the budget availability and implementation activities (Liao, Hu, & Ko, 2018). Hence, scrutinized travel behavior analysis on distinct divergent disastrous networks are needed for avoiding unnecessary disadvantages for road users and minimizing the system recovery periods.

Travel behavior in a normal network is influenced by the network familiarity (Young, Mackenzie, Davies, & Crundall, 2017), attitudes (Mohamed & Bromfield, 2017), beliefs (Hamilton, Peden, Keech, & Hagger, 2018), location (Stanojevic, Lajunen, Jovanovic, Sarbescu, & Kostadinov, 2018) and driving professionalism (Maslac, Antic, Pesic, & Milutinovic, 2017). But in a disastrous network, these factors could be less benefited as the traveler's decision-making mechanism alters from global decisions to myopic decisions due to the congestion and less information about forth links. In the literature, studies have been carried out based on various network disrupted conditions including both hypothetical and real disruptions, and some are listed in Table 2.1.

Table 2.1 List of studies that have carried out based on disrupted network conditions

Event	Main focus	Analysis/Model	Data/ Data source	Respective literature
Hyogoken-Nanbu (Kobe) earthquake 1995	Post-disaster system performance	Develop post-disaster system performance measures	Detector counts	(Chang & Nojima, 2001)
Hurricane Katrina, Gulf Coast, United States 2005	Evacuation planning and management	Data analysis	Traffic detector data	(Wolshon, Catarella-Michel, & Lambert, 2006)
The Beijing 2008 Summer Olympic Games	Travel characteristics of local Beijing residents and spectators in game time	Beijing Olympic transport model (BOTM)	Questionnaire survey	(Yan, Yang, & Fu, 2010)
Collapse of I-35W bridge over Mississippi river	Investigate aggregate traffic patterns and underlying travelers preference	Regression analysis	Loop detector, bus ridership and survey data	(Zhu, Levinson, Liu, & Harder, 2010)
Incident data from December 2007 to September 2008 at motorway A13, Delft in the Netherlands	Travel behavior under exceptional conditions	Data analysis	Loop detectors data, Questionnaire and simulator set-up	(Knoop, Hoogendoorn, & Zuylen, 2010)
Researcher defined network conditions	Vulnerability of road network under disruptions	Grid-based analysis	Swedish national travel demand model system	(Jenelius & Mattsson, 2012)
Road maintenance, City of York, England 2000 – 2001	Check the forecasting ability of equilibrium model due to systematic change in network	Graphical methods and maximum likelihood estimation	License plate survey	(Watling, Milne, & Clark, 2012)

Event	Main focus	Analysis/Model	Data/ Data source	Respective literature
Construction of the West LRT line in Calgary, Alberta, Canada 2010 – 2012	Investigate ravel behavioral effects of the reduction in traffic capacity	Statistical analysis, MNL and SPSS	Questionnaire survey	(Kattan, De Barros, & Saleemi, 2013)
Floods at Jalan P. Ramlee road in Malaysia in 2013	Generating route choice alternative maps during floods	GIS based analysis	Manually taken traffic volume data	(Othman & Hamid, 2014)
Hurricane Irene (2011) and Sandy (2012)	Quantitative analysis of traffic patterns and highway disruptions	Traffic pattern analysis and evacuation response models	Multiple traffic and event data	(Li, Ozbay, & Bartin, 2015)
Based on prevailing weather condition and it's forecast at mass rapid transit stations, Singapore	Effect of weather conditions and weather forecast on cycling travel behavior	Logistic regression model and analysis	Questionnaire survey	(Meng, Zhang, Wong, & Au, 2016)
Middle East Respiratory Syndrome (MERS) outbreak in South Korea in 2015	Influence of public fear of a pandemic disease on travel behavior	Data analysis	Smart card transaction data, land values and MERS hotspots data	(Kim, Cheon, Choi, Joh, & Lee, 2017)
Based on the past flood experiences of individual households in Bangladesh	Interrelationship between changes in travel behavior and job and residential location under flood disasters	Structural equation modeling (AMOS), SPSS software	Stated preference survey data	(Lu, Zhang, & Rahman, 2017)
MacArthur Maze collapse 2007	Evaluate the impacts of closure on Bay Area Rapid Transit and remaining freeway system	Analyze the effect on BART and toll bridges	Empirical data	(Oh, Chung, Park, Kim, & Kang, 2017)

Most of the above studies have conducted based on steady state analysis and focusing towards evacuation or post disaster evaluations. But, in order to have a proper understanding on travel behavior within the disaster phase and immediately after the disaster, an unsteady modeling approach is needed and this research provides it. Marsden et al. suggested based on the evidence on behavioral responses under disrupted transport networks that travelers are supposed to take a decision on whether to continue to do the activity or change the destination for that activity, use the same mode or change it, continue the journey or not, re-organize the activity or postpone, cancel the activity when they dealing with a damaged network (Marsden, Anable, Shires, & Docherty, 2016). All these decisions are individual based and taken according to the situation where each individual face in. Along with, in order to assess travelers' consciousness of route characteristics, to predict future traffic conditions on transportation networks, to predict travelers' behavior under different policy measures, and to delineate the effect of traffic information, to enhance the route choice part of traffic assignment methods, modeling travelers' route choice behavior becomes mandatory.

2.4 Data scarcity and probe data

Having an accurate completed data set is key for conducting a comprehensive research. Traffic conditions are extremely transient specially surrounding the affected structures after natural or manmade disasters. Hence, collecting real time data become more difficult though they are very important for inclusive studies. On the other hand, it is not given the immediate priority to collect data just after the occurrence of a disaster (Iida, Kurauchi, & Shimada, 2000), sharing and coordinating of information during disasters (Bharosa, Lee, & Janssen, 2010; Steenbruggen, Nijkamp, Smits, & Mohabir, 2012). Hence, those data limitations frustrate inclusive studies (Giuliano & Golob, 1998).

The data collected through questionnaire surveys (Helton, Kemp, & Walton, 2013) and travel surveys (Giuliano & Golob, 1998) might have accuracy problems due to memory decay and emotional trauma of the disaster. Hence collecting accurate data under disastrous conditions becomes bit worried and difficult. Meanwhile, data collection techniques have been improved over the past six decades from face-to-face interviews or paper-and-pencil interviews to collecting from social media (Hara, 2015; Maghrebi, Abbasi, Rashidi, & Waller, 2015), open street map (Bono & Gutierrez, 2011) and probe technology (Shafique & Hato, 2016).

Probe person technologies are defined as "integrated technologies designed for recording people's awareness and behaviors in real urban space" in Japan society of traffic engineers probe research group website (Hato, 2007). Coming in to the contest of probe taxi data which this study use, it comprises global positioning system (GPS) trajectories of taxi trips. Probe data provides highly accurate and detailed data for comprehensive researches and hence, it is being widely used in transportation studies around the world. Route identification and travel time prediction using probe car data (Miwa, Sakai, & Morikawa, 2004), predicting bus arrival time (Sun & Fu, 2007) and evaluating road network from the viewpoint of travel time stability and reliability (Uno, Karauchi,

Tamura, & Iida, 2009) using probe bus data, path and travel time inference from probe taxi data (Hunter, Herring, Abbeel, & Bayen, 2009) are some of the examples. But comparative studies on describing unsteady travel behavior under differential disastrous networks based on probe data are very limited in the literature for the best of my knowledge and that is one of the gap which this thesis is filled on. Khan et al. have made a traffic congestion analysis by using probe taxi data (Khan, Wisetjindawat, Fujita, & Suzuki, 2013) but that is very different from our research.

3 Model framework and sensitivity analysis

Sequential time discount rate is estimated through the β – scaled recursive logit model (Oyama, Chikamatsu, Shoji, Hato, & Koga, 2016) as a generalization of drivers' decision-making dynamics and a representation of degree of spatial cognition of networks. β – SRL model is a generalized version of recursive logit model (Fosgerau, Frejinger, & Karlstrom, 2013). Mathematical formulation of RL model and β – SRL model are described in detail under this chapter.

3.1 Recursive logit model

The RL corresponds to a dynamic discrete choice model and the path choice is formulated as a sequence of link choices. At each node in the network, the individual chooses the utility-maximizing link, where the utility is the sum of the instantaneous link cost, the maximum expected utility to the destination and i.i.d. extreme value type I error terms. Therefore, attributes of the RL model are attributes of the links in the network and they are specified to be link-additive, such that the utility of a path is the sum of the utility of each link in the path (Zimmermann, Mai, & Frejinger, 2017). The formulation of the model is described below in detail.

The road network is considered as a directed connected graph, $G = (A, N)$ where A and N denote the set of links and the set of nodes respectively. More precisely, a set of absorbing links without successors, corresponding to the observed destinations, is added to A. Network nodes are junctions, interchanges, origins and destinations of trips. Links are denoted as $a_{j+1},\ a_j \in A$. Each link pair (a_j, a_{j+1}) where $a_{j+1} \in A(a_j)$, has a deterministic utility component $v(a_{j+1}|a_j)$, based on the attributes $x(a_{j+1}|a_j)$ of the link pair. Hence, considering an individual n, traveling in the aforementioned network, the instantaneous random utility of a link a_{j+1} conditionally on being in state a_j can be defined as;

$$u_n(a_{j+1}|a_j) = v_n(a_{j+1}|a_j) + \mu\varepsilon_n(a_{j+1}) \tag{3.1}$$

where $\varepsilon_n(a_{j+1})$ are independent and identically distributed (i.i.d.) extreme value type I error terms with zero mean and μ is a fixed scale parameter. The full utility of link a_{j+1} conditionally on being in state a_j is determined by sum of the instantaneous utility $u_n(a_{j+1}|a_j)$ associated with each link pair and maximum expected downstream utility to the destination link d, denoted as a value function $V_n^d(a_j)$ and defined by the Bellman equation (Bellman, 1957).

$$V_n^d(a_j) = \mathrm{E}\left[\max_{a_{j+1}\in A(a_j)}\{v_n(a_{j+1}|a_j) + V_n^d(a_{j+1}) + \mu\varepsilon_n(a_{j+1})\}\right] \quad \forall a_j \epsilon A \tag{3.2}$$

Hence, upon observing the random term $\varepsilon_n(a_{j+1})$, the individual chooses in $A(a_j)$ the link a_{j+1} which maximizes $u_n(a_{j+1}|a_j) + V_n^d(a_{j+1})$.

The probability of choosing a link a_{j+1} given state a_j conditionally on going to destination d is determined by the multinomial logit model and is shown in equation 3.3

$$P_n^d(a_{j+1}|a_j) = \frac{e^{\frac{1}{\mu}\{v_n(a_{j+1}|a_j)+V_n^d(a_{j+1})\}}}{\sum_{a'_{j+1}\in A(a_j)} e^{\frac{1}{\mu}\{v_n(a'_{j+1}|a_j)+V_n^d(a'_{j+1})\}}} \tag{3.3}$$

In this case the value function is the logsum;

$$V_n^d(a_j) = \begin{cases} \mu\, log \sum_{a_{j+1}\in A} \delta(a_{j+1}|a_j) e^{\frac{1}{\mu}\{v_n(a_{j+1}|a_j)+V_n^d(a_{j+1})\}}, & a_j \in A \\ 0, & a_j = d \end{cases} \tag{3.4}$$

where $\delta(a_{j+1}|a_j)$ is an indicator that equals one if $a_{j+1} \in A(a_j)$ and zero otherwise. $V_n^d(d)$ is set to zero as the destination link d has no outgoing link.

The Bellman equation have to be solved in order to calculate the link choice probabilities. Hence, equation 3.4 is transformed by taking the exponential,

$$e^{\frac{V_n^d(a_j)}{\mu}} = \begin{cases} \sum_{a_{j+1}\in A} \delta(a_{j+1}|a_j) e^{\frac{1}{\mu}\{v_n(a_{j+1}|a_j)+V_n^d(a_{j+1})\}}, & a_j \in A \\ 1, & a_j = d \end{cases} \tag{3.5}$$

Further, the matrix $\mathbf{z}(|\tilde{A}| \times 1)$ and $\mathbf{M}(|\tilde{A}| \times |\tilde{A}|)$ are defined as entries,

$$z_{a_j} = e^{\frac{V_n^d(a_j)}{\mu}}, M_{a_j a_{j+1}} = \delta(a_{j+1}|a_j) e^{\frac{v_n(a_{j+1}|a_j)}{\mu}} \tag{3.6}$$

The value functions are the solutions to the following equation;

$$\mathbf{z} = \mathbf{M}\mathbf{z} + \mathbf{b} \tag{3.7}$$

where $\mathbf{b}(|\tilde{A}| \times 1)$ is a vector with zero value for all steps except for the destination, which is equal to one (Fosgerau, Frejinger, & Karlstrom, 2013).

The equation 3.7 can be reformulated as below;

$$(\boldsymbol{I} - \boldsymbol{M})\mathbf{z} = \mathbf{b} \tag{3.8}$$

Where an identity matrix is denoted by $\boldsymbol{I}$. Correspondingly, if $(\boldsymbol{I}-\boldsymbol{M})$ is invertible, the system has a solution. If so, the value function for each destination can be determined by solving a system of linear equations.

3.2 β – scaled recursive logit model

Oyama et al. (Oyama, Chikamatsu, Shoji, Hato, & Koga, 2016) included the concept of sequential time discount rate (β), as a generalization of drivers' decision-making dynamics and a representation of the degree of spatial cognition of networks, as a parameter in RL model. Accordingly, the equation 3.2 was re-formulated;

$$V_n^d(a_j) = \mathrm{E}\left[\max_{a_{j+1}\in A(a_j)}\left\{v_n(a_{j+1}|a_j) + \beta V_n^d(a_{j+1}) + \mu\varepsilon_n(a_{j+1})\right\}\right] \quad \forall a_j \epsilon A \qquad (3.9)$$

β is the sequential time discount rate of the value function, and it is assumed to be vary between zero and one.

Accordingly, the probability of choosing a link a_{j+1} given state a_j conditionally on going to destination d is determined by the multinomial logit model and the equation 3.3 was re-formulated as shown in equation 3.10

$$P_n^d(a_{j+1}|a_j) = \frac{e^{\frac{1}{\mu}\{v_n(a_{j+1}|a_j)+\beta V_n^d(a_{j+1})\}}}{\sum_{a'_{j+1}\in A(a_j)} e^{\frac{1}{\mu}\{v_n(a'_{j+1}|a_j)+\beta V_n^d(a'_{j+1})\}}} \qquad (3.10)$$

The decision-making dynamic of a driver is expected to be illustrated through the variation of sequential time discount rate and is graphically represented in Figure 3.1

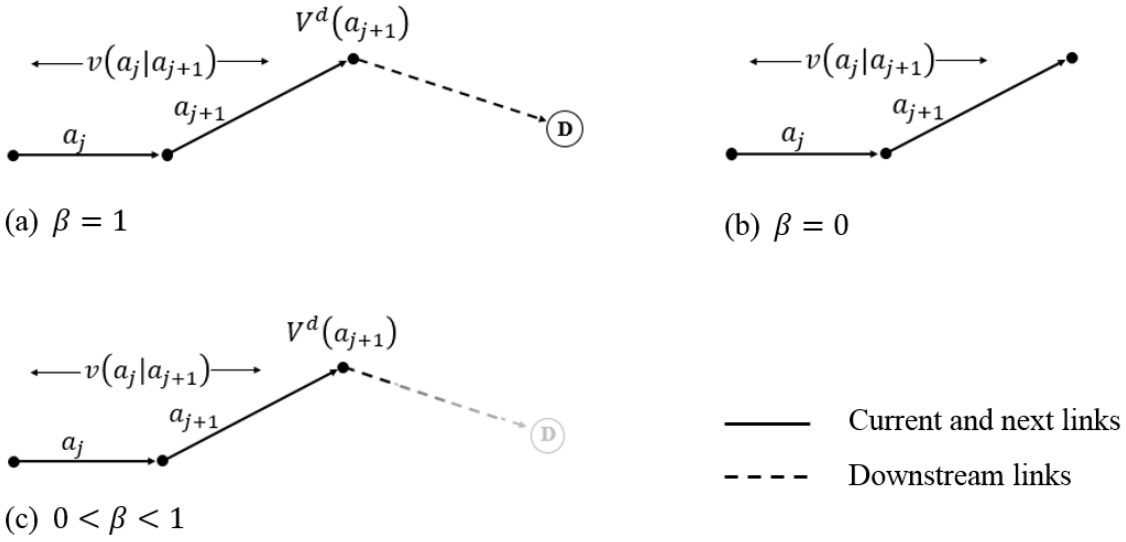

Figure 3.1 Graphical representation of different states of sequential time discount rate

When β equals to one, it is assumed that drivers are fully knowledgeable about the downstream conditions and hence they are able to evaluate the expected utility of forward

space V and the instanteneous utility of the next link v, with equal weights. Accordingly, the route choice behaviour depends on global decision over the network. In the case of β equals to zero as shown in Figure 3.1 (b), drivers are expected to unaware about the downstream link and their conditions. Hence, they are supposed to myopically choose the next link based only on instantaneous utility v.

In the intermediate state, which displayed in Figure 3.1 (c), drivers could evaluate the expected utility of forward space V up to a certain extent. In most of the normal traveling conditions, drivers don't have the perfect information on the downstream links but they are knowledgeable up to a certain percentage. Therefore, variability of the sequential time discount rate become crucial. Further, when it becomes a disastrous condition, the information which could drivers get become lesser and hence the sequential time discount rate is expected to be have a lower value.

For solving the Bellman equation, closer steps are carried out as stated in the solving process of RL model. Accordingly, the equation 3.9 is transformed by taking the logsum,

$$e^{\frac{V_n^d(a_j)}{\mu}} = \begin{cases} \sum_{a_{j+1}\in A} \delta(a_{j+1}|a_j) e^{\frac{1}{\mu}\{v_n(a_{j+1}|a_j)+\beta V_n^d(a_{j+1})\}}, & a_j \in A \\ 1, & a_j = d \end{cases} \tag{3.11}$$

Further, based on the RL model, defined the matrix $\mathbf{z}(|\tilde{A}| \times 1)$ and $\mathbf{M}(|\tilde{A}| \times |\tilde{A}|)$ with the entries in equation 3.6. Consequently, the value functions are the solutions to the following system of non-linear equations with the sequential time discount rate,

$$z_{a_j} = \begin{cases} \sum_{a_{j+1}\in A} M_{a_j a_{j+1}} \left(z_{a_{j+1}}\right)^{\beta}, & a_j \in A \\ 1, & a_j = d \end{cases} \tag{3.12}$$

This can be written in matrix notations,

$$\mathbf{z} = \mathbf{MX}(\mathbf{z}) + \mathbf{b} \tag{3.13}$$

where $\mathbf{X}(\mathbf{z})(|\tilde{A}| \times |\tilde{A}|)$ is the matrix with entries $X(z)_{a_j} = \left(z_{a_j}\right)^{\beta}$. The equation 3.13 is solved by iterative process until the value function reaches a fixed point (same method is found in Mai et al., 2015 (Mai, Fosgerau, & Frejinger, 2015)). First initialize the vector $\mathbf{z}^{(0)}$ and then update as $\mathbf{z}^{(1)} = \mathbf{MX}(\mathbf{z}^{(0)}) + \mathbf{b}$. When $\mathbf{z}$ converges, i.e., if it satisfies $|\mathbf{z}^{(n+1)} - \mathbf{z}^{(n)}| < \gamma$, where γ is the convergence tolerance, finish the iteration, otherwise update $\mathbf{z}$ in equation 3.12. It is known that, when $\beta < 1$, equation 3.13 reaches a contraction mapping (Rust, 1994) and the problem has a unique fixed-point solution. When $\beta = 1$, as stated in Fosgerau et al. (2013), it depends on the balance between the network structure and the size of the instantaneous utilities $v(a_{j+1}|a_j)$.

3.3 Sensitivity analysis of sequential time discount rate

As indicated in the previous section, sequential time discount ratio is changing based on the network condition. Hence, this property can be utilized to determine the network assignment in disastrous conditions. Therefore, in this section, it is expected to illustrate the sensitivity of sequential time discount rate based on a sample network under different scenarios. The considered sample network and its features are shown in Figure 3.2.

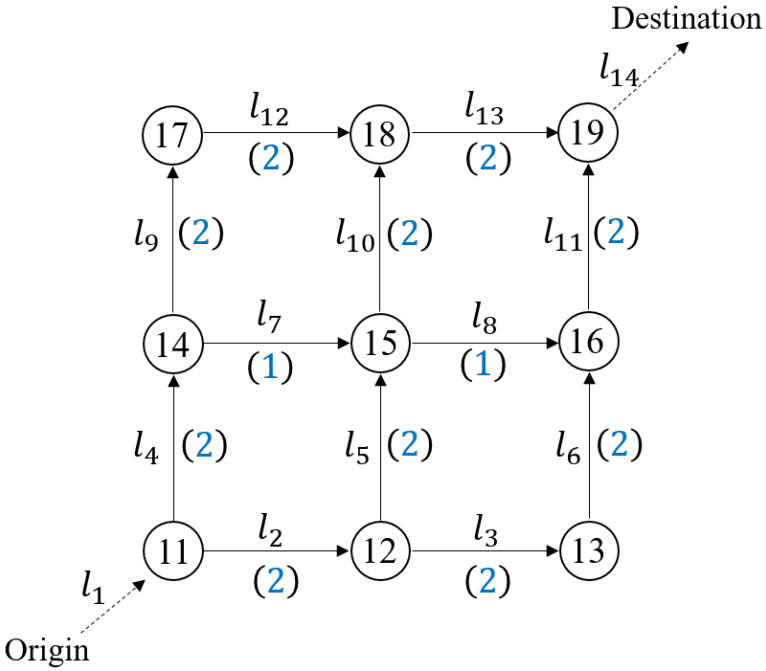

Figure 3.2 Original status of the considered sample network

In the Figure 3.2, the links are numbered from l_1 to l_{14} respectively from origin link to destination link. The cost of each link is indicated within the parenthesis. Only the distance was considered for the link utility and distance parameter was assumed as -1. Five scenarios as the original network conditions shown in Figure 3.2, introducing low cost links at the downstream, introducing high cost links at the downstream, introducing low cost links near the origin and introducing high cost links near the origin are examined in order to analyse the influence of sequential time discount rate on traveller's route choice decisions. Flow generation at the origin was hypothesised as 1000 vehicles for each case. All together six routes are available to reach the destination from the origin as route 1 $(l_1, l_2, l_3, l_6, l_{11}, l_{14})$, route 2 $(l_1, l_2, l_5, l_8, l_{11}, l_{14})$, route 3 $(l_1, l_2, l_5, l_{10}, l_{13}, l_{14})$, route 4 $(l_1, l_4, l_7, l_8, l_{11}, l_{14})$, route 5 $(l_1, l_4, l_7, l_{10}, l_{13}, l_{14})$ and route 6 $(l_1, l_4, l_9, l_{12}, l_{13}, l_{14})$.

3.3.1 Analysis of the original network condition

The sample network shown in Figure 3.2 was used to determine the assignment results based on three status of sequential time discount rate as, $\beta = 0$, $\beta = 0.5$, $\beta = 1$ under

the recursive logit framework. The results are shown in Figure 3.3. Arrow thicknesses were drawn proportional to the flow in each link.

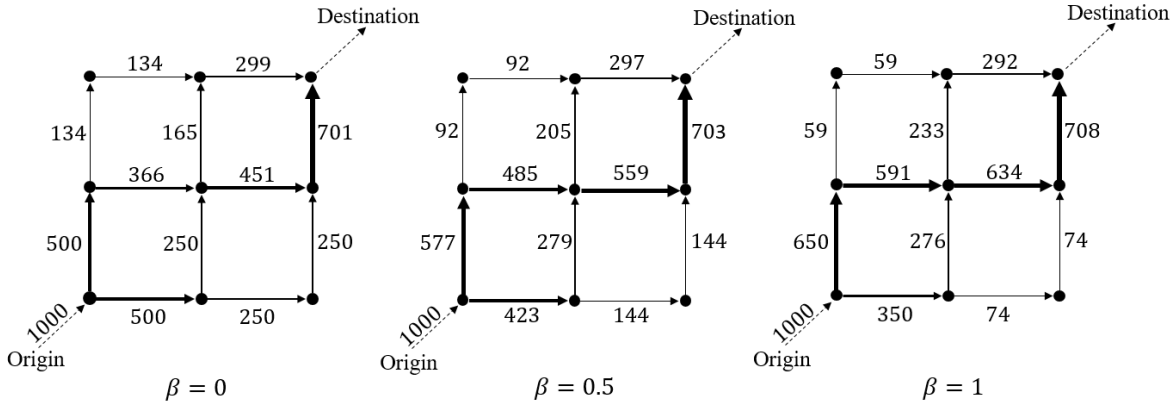

Figure 3.3 Assignment results for the original network condition

Under the prevailing network conditions, the total route costs and the route choice probabilities were calculated by using the link choice probabilities as explained in equation 2.19 in chapter 2 and tabulated in Table 3.1

Table 3.1 Route choice probabilities under different scenarios of sequential time discount rate for the hypothetical network

Route No.	Link connectivity	Route cost	$\beta = 0$	$\beta = 0.5$	$\beta = 1$
1	$l_1, l_2, l_3, l_6, l_{11}, l_{14}$	8	0.250	0.144	0.074
2	$l_1, l_2, l_5, l_8, l_{11}, l_{14}$	7	0.183	0.204	0.201
3	$l_1, l_2, l_5, l_{10}, l_{13}, l_{14}$	8	0.067	0.075	0.074
4	$l_1, l_4, l_7, l_8, l_{11}, l_{14}$	6	0.267	0.354	0.433
5	$l_1, l_4, l_7, l_{10}, l_{13}, l_{14}$	7	0.098	0.130	0.159
6	$l_1, l_4, l_9, l_{12}, l_{13}, l_{14}$	8	0.134	0.092	0.059

Hence, when travellers choose routes based on their cost, they should select route 4 since it is least costed. Correspondingly, when the sequential time discount rate equals to one, its probability become highest and accordingly, a major flow can be observed along the links connecting route 4. Meanwhile, travellers are supposed to made their route choices based on the myopic decisions when the sequential time discount rate is equal to zero. Accordingly, the assignment results under $\beta = 0$, indicates that travellers have chosen the next link based on the instantaneous utility without concerning the downstream link features. Further, the probability of choosing the least costed route has dropped considerably, while high cost route like route 1, has increased its choosing probability. In addition, the assignment results along with the route choosing probabilities under the

condition $\beta = 0.5$, show the intermediate status of route choosing and the low-cost links l_7, l_8 seems to be good links.

3.3.2 Analysis by introducing low cost links at downstream

Under this scenario, two low cost links were introduced at the downstream. Precisely, the cost of each links, link l_6 and l_{11} were set to 0.5. The revised network is shown in Figure 3.4.

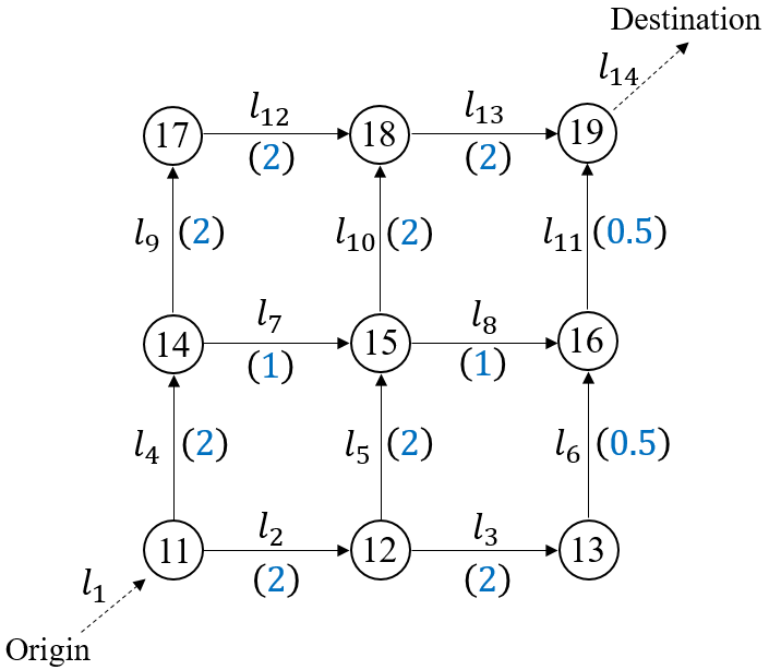

Figure 3.4 Revised network after introducing low cost links at downstream

Then the route costs, route choice probabilities and the network flows were determined under the aforementioned three stages of sequential time discount rate. The route costs, route choice probabilities are tabulated in Table 3.2 while the respective assignment results are shown in Figure 3.5

Table 3.2 Route choice probabilities under different scenarios of sequential time discount rate for the hypothetical network after adding low cost links at the downstream

Route No.	Link connectivity	Route cost	$\beta = 0$	$\beta = 0.5$	$\beta = 1$
1	$l_1, l_2, l_3, l_6, l_{11}, l_{14}$	5.0	0.250	0.221	0.191
2	$l_1, l_2, l_5, l_8, l_{11}, l_{14}$	5.5	0.183	0.172	0.147
3	$l_1, l_2, l_5, l_{10}, l_{13}, l_{14}$	8.0	0.067	0.030	0.012
4	$l_1, l_4, l_7, l_8, l_{11}, l_{14}$	4.5	0.267	0.413	0.547
5	$l_1, l_4, l_7, l_{10}, l_{13}, l_{14}$	7.0	0.098	0.072	0.045
6	$l_1, l_4, l_9, l_{12}, l_{13}, l_{14}$	8.0	0.134	0.092	0.059

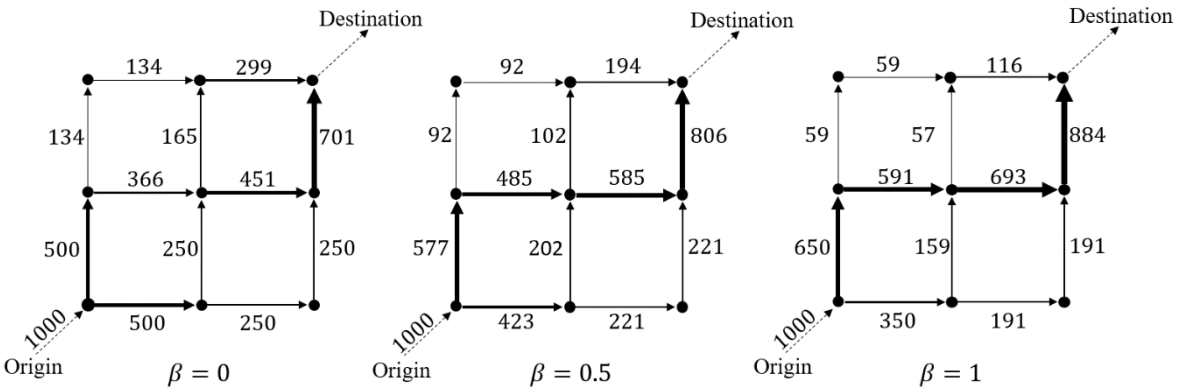

Figure 3.5 Assignment results after introducing low cost links at downstream

As stated in the previous section also, travelers choose the links based on separated link costs when the sequential time discount rate is equal to zero. Correspondingly, introducing low cost links at the downstream has made no influence to the route choice probabilities and assignment results under the condition $\beta = 0$. On the other hand, when they select the links based on route-based cost from origin to destination when the $\beta = 1$, high probability is being assigned and a major flow can be seen through the lowest cost route, which is route 4.

3.3.3 Analysis by introducing high cost links at downstream

Two high cost links were introduced at downstream, in order to examine the route choice probabilities and link flow variability under the different status of sequential time discount rate. Accordingly, the cost of each link l_{12} and l_{13} were doubled as their usual cost. The revised network is shown in Figure 3.6

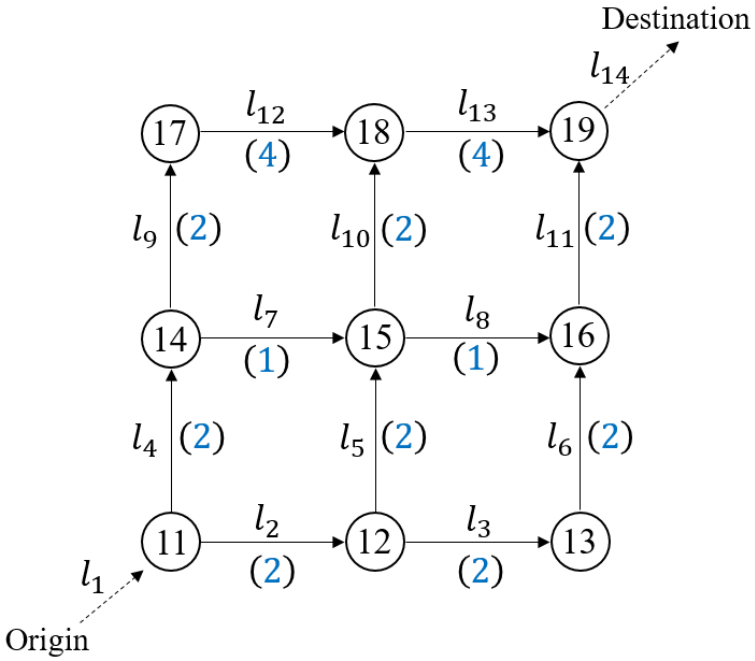

Figure 3.6 Revised network after introducing high cost links at downstream

Then the route costs, route choice probabilities and the network flows were determined under the aforementioned three stages of sequential time discount rate. The revised route costs and route choice probabilities are calculated and included in Table 3.3 while the respective assignment results are shown in Figure 3.7

Table 3.3 Route choice probabilities under different scenarios of sequential time discount rate for the hypothetical network after adding high cost links at the downstream

Route No.	Link connectivity	Route cost	$\beta = 0$	$\beta = 0.5$	$\beta = 1$
1	$l_1, l_2, l_3, l_6, l_{11}, l_{14}$	8	0.250	0.144	0.074
2	$l_1, l_2, l_5, l_8, l_{11}, l_{14}$	7	0.183	0.245	0.263
3	$l_1, l_2, l_5, l_{10}, l_{13}, l_{14}$	10	0.067	0.033	0.013
4	$l_1, l_4, l_7, l_8, l_{11}, l_{14}$	6	0.267	0.475	0.611
5	$l_1, l_4, l_7, l_{10}, l_{13}, l_{14}$	9	0.098	0.064	0.030
6	$l_1, l_4, l_9, l_{12}, l_{13}, l_{14}$	12	0.134	0.038	0.009

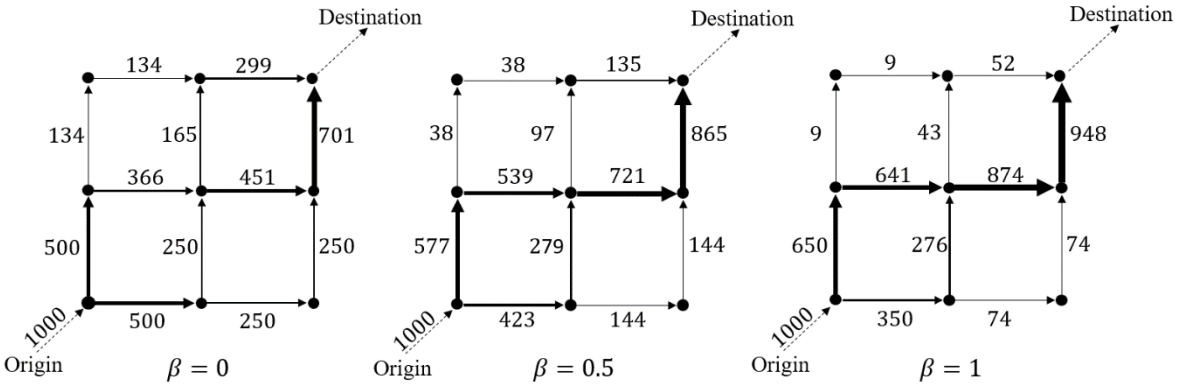

Figure 3.7 Assignment results after introducing high cost links at downstream

As seen in the previous condition, here also we cannot observe any difference in the route choice probabilities and assignment results under the condition of $\beta = 0$. But, it can be observed that a larger flow has being assigned to a high cost link. Precisely, the cost of l_{13} is largest under the condition but it has assigned a flow of 299. Hence, this indicated that myopic decisions can lead to a wrong route selection and the congestion of the high cost link could be further increased. Meanwhile, with the condition of $\beta = 1$, it can be seen that the link flow through the high cost links have kept under lower values and the lowest cost route has given the highest chosen probability.

3.3.4 Analysis by introducing low cost links near the origin

Having understand the influence on changes in downstream, here it is introduced two low cost links near the origin. Accordingly, the link cost of each link l_4 and l_9 were reduced to half of its original cost. The revised network is shown in Figure 3.8

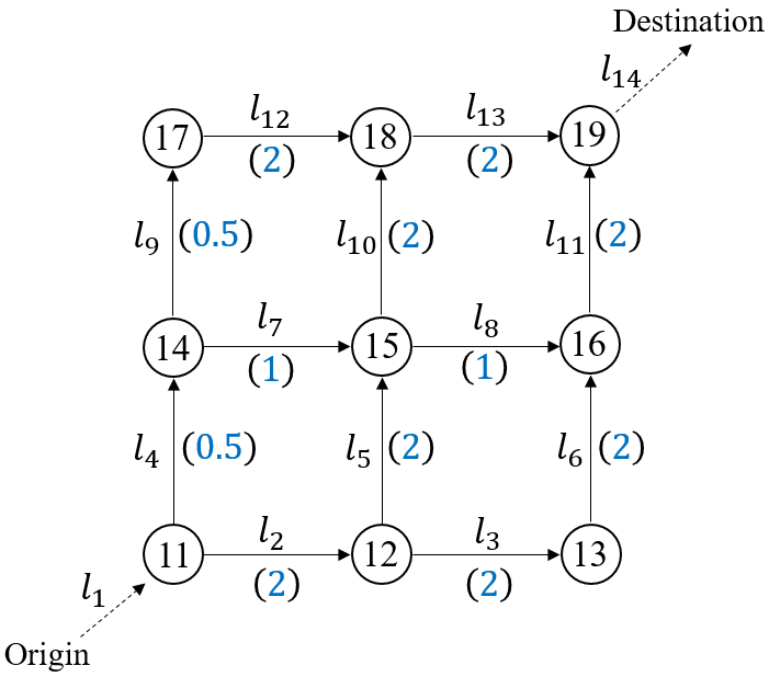

Figure 3.8 Revised network after introducing low cost links near the origin

Based on the new network, route costs and choice probabilities are included in Table 3.4 while calculated link flows under different conditions of sequential time discount rate are visualized in Figure 3.9

Table 3.4 Route choice probabilities under different scenarios of sequential time discount rate for the hypothetical network after adding low cost links near the origin

Route No.	Link connectivity	Route cost	$\beta = 0$	$\beta = 0.5$	$\beta = 1$
1	$l_1, l_2, l_3, l_6, l_{11}, l_{14}$	8.0	0.091	0.036	0.012
2	$l_1, l_2, l_5, l_8, l_{11}, l_{14}$	7.0	0.067	0.051	0.034
3	$l_1, l_2, l_5, l_{10}, l_{13}, l_{14}$	8.0	0.025	0.019	0.012
4	$l_1, l_4, l_7, l_8, l_{11}, l_{14}$	4.5	0.226	0.353	0.477
5	$l_1, l_4, l_7, l_{10}, l_{13}, l_{14}$	5.5	0.083	0.130	0.175
6	$l_1, l_4, l_9, l_{12}, l_{13}, l_{14}$	5.0	0.509	0.412	0.289

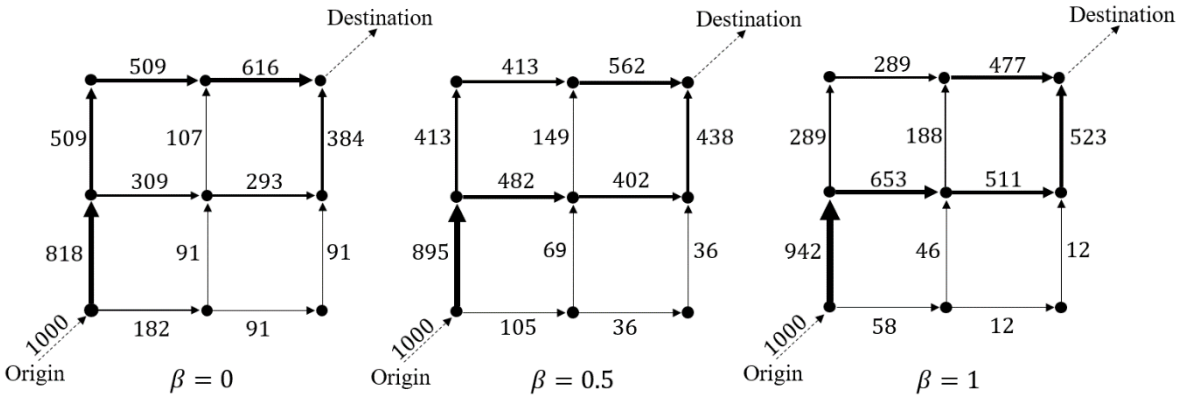

Figure 3.9 Assignment results after introducing low cost links near the origin

As per the Table 3.4 and Figure 3.9 indicates, travelers have unexploited the lowest cost route with myopic decisions under the condition of $\beta = 0$. Meanwhile, under the condition of $\beta = 1$, where the global decision is given the priority, travellers have avoided the high cost routes (route 1, 2 and 3) by giving them lesser probabilities. Further, a larger flow has assigned to the lowest link near the origin and it has captured the lowest cost route later.

3.3.5 Analysis by introducing high cost links near the origin

Under this section, two high cost links were introduced near the origin. Correspondingly, the cost of each link, l_2 and l_3 were revised as twice their original values. The amended network is shown in Figure 3.10

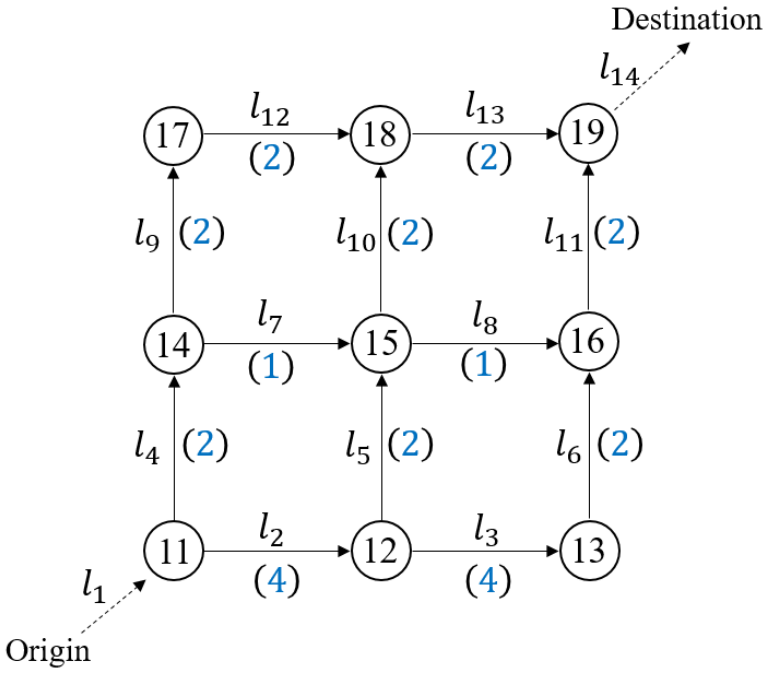

Figure 3.10 Revised network after introducing high cost links near the origin

As per the new network shown in Figure 3.10, route 1 becomes the highest cost route with a cost of 12 while route 4 is the lowest with a cost of 6 which is half of the longest route. The route costs and recursive logit link probabilities are shown in Table 3.5.

Table 3.5 Route choice probabilities under different scenarios of sequential time discount rate for the hypothetical network after adding high cost links near the origin

Route No.	Link connectivity	Route cost	$\beta = 0$	$\beta = 0.5$	$\beta = 1$
1	$l_1, l_2, l_3, l_6, l_{11}, l_{14}$	12	0.014	0.005	0.001
2	$l_1, l_2, l_5, l_8, l_{11}, l_{14}$	9	0.077	0.048	0.028
3	$l_1, l_2, l_5, l_{10}, l_{13}, l_{14}$	10	0.028	0.017	0.010
4	$l_1, l_4, l_7, l_8, l_{11}, l_{14}$	6	0.471	0.571	0.639
5	$l_1, l_4, l_7, l_{10}, l_{13}, l_{14}$	7	0.173	0.210	0.235
6	$l_1, l_4, l_9, l_{12}, l_{13}, l_{14}$	8	0.237	0.149	0.086

Then the assignment flows were calculated in recursive logit framework and illustrated in Figure 3.11

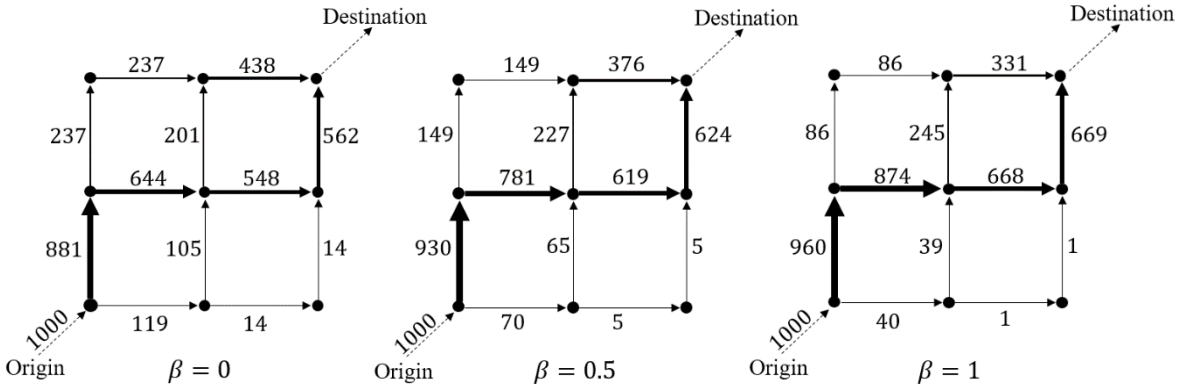

Figure 3.11 Assignment results after introducing high cost links near the origin

As seen in the previous scenarios, here also it is visualized that major flow has taken place through the lowest cost route under the route-based decision-making process, where $\beta = 1$ by assigning a higher route selection probability. Meanwhile, comparatively larger flows have assigned to high cost links under the myopic decisions with lesser β.

Having made a sensitivity analysis by incorporating different status of sequential time discount rate and various link cost combinations, it was visualized the importance or the impact of sequential time discount rate in determining network assignments. Hence, this feature can be utilized to predict network assignments in real networks in real time. Therefore, testing the stability (chapter 4), performance (chapter 5) of the sequential time discount rate under different network conditions and determine sequential time discount rate in disastrous networks (chapter 6) are essential.

3.4 Conclusions and discussions

In this chapter, theoretical framework of recursive logit model (Fosgerau, Frejinger, & Karlstrom, 2013) and $\beta -$ scaled recursive logit model (Oyama, Chikamatsu, Shoji, Hato, & Koga, 2016) were explained in detail. Then a sensitivity analysis was carried out over the $\beta -$ scaled recursive logit model. Three status of sequential time discount rate were used as $\beta = 0, \beta = 0.5\ and\ \beta = 1$ for understanding the link assignments under each condition. A sample network with changing link costs were utilized to succeed the aforementioned purpose.

A directed connected hypothetical network having six routes to reach the destination from the origin was considered for the analysis. Five scenarios as the original network conditions (Figure 3.2), introducing low cost links at the downstream, introducing high cost links at the downstream, introducing low cost links near the origin and introducing high cost links near the origin were used for the analysis. Route choice probabilities and link assignments under the recursive logit framework indicated that myopic decisions become crucial when the $\beta = 0$ and link choices being made based on the separated link costs. Further it clearly visualized the worst impacts of myopic decisions for route choosing by assigning larger flows to high costs links. This could lead to make heavy congestions in congested links. In addition, its further showed that making changes at downstream has no impact on the network assignments under the myopic decisions.

Meanwhile, higher values of sequential time discount rate always made the route choice decisions considering route-based decisions from origin to destination. Hence, it was clearly visualized that under the condition of $\beta = 1$, larger flows being assigned to low cost routes as they were given higher probabilities. As a conclusion, the analysis clearly showed the impact of sequential time discount rate on predicting link assignments under different circumstances. Therefore, having estimate sequential time discount rate for real networks become very important.

4 Comparison and stability analysis of sequential time discount rate

4.1 Introduction

Parameter stability is essential for drawing conclusions or making inference on estimation results. Basically, an econometric random utility model is described by its parameters and hence, model stability is equivalent to the parameter stability. Making predictions based on a stable model is indispensable especially in disastrous networks as they are expected to cause significant delays in traffic networks and cost human lives, in addition to, consume time, fuel and increase environmental pollution.

Model stability has been discussed in the literature based on various models e.g. (Lee, Heydecker, Kim, & Park, 2017; Huang, Liu, & H, 2010; Gao, Zhang, & Lou, 2016; Cantarella & Watling, 2016; Zhang & Nagurney, 1996) and model parameters (Zhuang, Fukuda, & Yai, 2007) as it is an essential criterion for practical usage of the model. Hence this chapter is basically focused on testing the stability of sequential time discount rate along with travel time and right turn dummy variable parameters of the β −SRL model, which has not done in the past. Then propose model limitations and stability for usage under different circumstances involve in route choice problems especially in unsteady travel conditions. Further, it is expected to identify the characteristics of sequential time discount rate under the different network conditions.

Parameter stability was initially tested under moving time and random sampling under different sampling rates. Then the random sampling technique was applied under the following criteria;

- In different time zones considering morning peak, day peak and evening peak
- In unsteady state by considering the cumulative link delay time of trips under the categories less than 5 minutes, between 5 – 10 minutes and over 10 minutes
- In different areas (networks) such as Toyosu where some events of the 2020 Olympic games will be conducted, city center of Tokyo basically in an area inside of ring road 8, and in suburbs or considering an area outside of the ring 8 road.

Set up of the stability analysis is shown in Figure 4.1 as a schematic diagram.

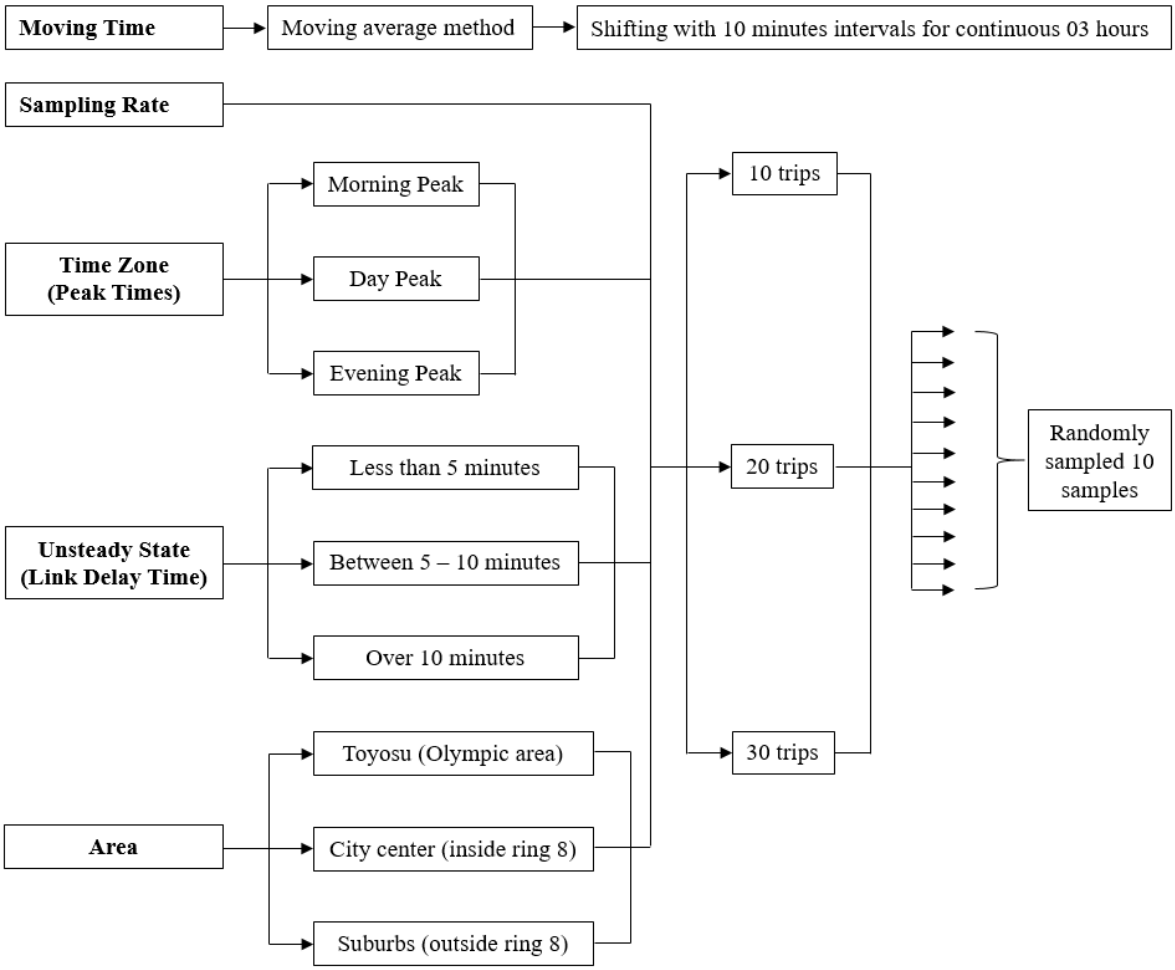

Figure 4.1 Set up of the stability analysis

4.2 Comparing and testing criteria

Initially, t-statistics and parameter signs of estimations are checked as a usual practice. Then distributions under each category shown in Figure 4.1 (10 trips, 20 trips and 30 trips) are visually compared by using graphs. Basically, the difference between minimum and maximum estimations and the mean were compared at this stage. Thereafter, the distributions are compared by using statistical parameters such as variance (VAR), standard deviation (SD), relative standard deviation (RSD), coefficient of variation (CV), standard error of the mean (SEM) and true value (μ) by using below mentioned relationships.

$VAR = \frac{\sum(x_i - \bar{x})^2}{n-1}$, $SD = \sqrt{\frac{\sum(x_i - \bar{x})^2}{n-1}}$, $RSD = \frac{SD}{\bar{x}}$, $CV = \frac{SD}{\bar{x}} \times 100\%$,

$SEM = \frac{SD}{\sqrt{n}}$, $\mu = \bar{x} \pm t\frac{SD}{\sqrt{n}}$

where $\bar{x}$ is the mean of the sample, n is the number of samples and t is the critical value which equals to 2.26 for 95% confidence (degree of freedom is 9 and two sided) (van Reeuwijk & Houba, 1998).

In addition, the asymptotic t test, which is usually carry out for checking the equality of individual coefficients between two market segments (Ben-Akiva & Lerman, 1985), was performed for examining the parameter equality within each sample. Market segmentation is basically used in the field of economics where they segment the consumers based on key demographics such as age, gender, income level, marital status and beyond to identify who share similar needs and wants. Since here we have segmented the samples, the technique can be adopted for comparison. Asymptotic t values were calculated based on equation 4.1 (Ben-Akiva & Lerman, 1985).

$$t = \frac{\beta_1 - \beta_2}{\sqrt{var(\beta_1) + var(\beta_2)}} \tag{4.1}$$

where β_i is an estimated parameter. It is possible that all the t values become insignificant indicating that there are no significant differences between the estimated parameters and it is the hypothesis too.

4.3 Comparison and stability analysis

4.3.1 Stability analysis by moving time

Sequential time discount rate together with travel time and right turn dummy variable parameter were estimated through the $\beta-$SRL model by using the probe taxi data collected in Tokyo on 11th March 2011 (an extended explanation on data is given in chapter 6 under the section 6.2 Data). The estimated area belongs to the regional mesh code 533946 which consisted 3653 nodes and 4776 links. The parameters are varying over the time as the network behavior is changed. Hence the objective here is to scrutinize the variability of model parameters over the shorter periods of time and test the parameter stability along with the model performance. In usual practice, we estimate model parameters on hourly basis and Figure 4.2 visualized the variation of sequential time discount rate for the period from 12:00 to 15:00 hours in JST.

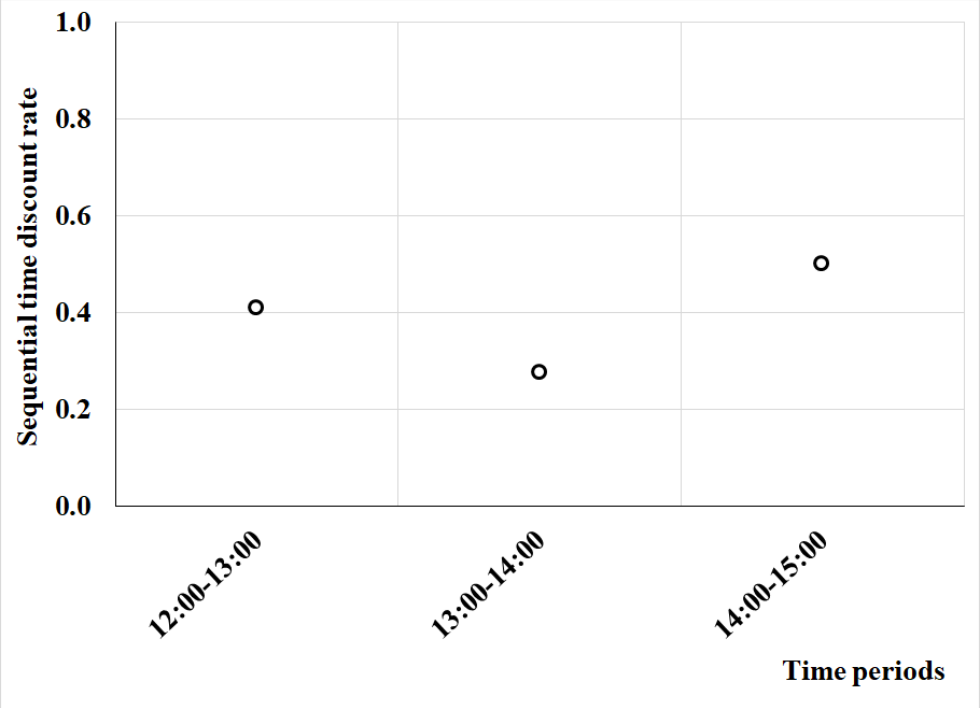

Figure 4.2 Variation of sequential time discount rate in each hour

Based on the Figure 4.2, it can be explained that sequential time discount rate has decreased from 13:00 to 14:00 indicating some congestion and released by next hour. Instead of this analysis, we could have a better explanation by estimating over moving time. Hence, the analysis with moving time is performed by slicing one-hour periods, shifting with 10 minute intervals between the consecutive samples for a continuous period of 03 hours. Precisely, 13 samples were simulated from 12:00 to 15:00 hrs., as starting first sample from 12:00 to 13:00, second sample from 12:10 to 13:10 etc. and finishing with 13th sample from 14:00 to 15:00 JST on 11th March 2011. Each sample consisted number of trips 15, 18, 19, 18, 19, 19, 20, 14, 17, 17, 15, 14, and 24 respectively. The resulted estimations are shown in Table 4.1

Table 4.1 Estimation results of β for different time periods

Sample No.	Sampling period	β	t-value	ρ^2
1	12:00 – 13:00	0.410	-2.236	0.19
2	12:10 – 13:10	0.424	-2.208	0.26
3	12:20 – 13:20	0.493	-1.831	0.39
4	12:30 – 13:30	0.502	-1.410	0.39
5	12:40 – 13:40	0.413	-1.825	0.24
6	12:50 – 13:50	0.433	-2.178	0.30
7	13:00 – 14:00	0.275	-2.509	0.15
8	13:10 – 14:10	0.400	-2.276	0.24
9	13:20 – 14:20	0.378	-2.676	0.25
10	13:30 – 14:30	0.276	-2.864	0.18
11	13:40 – 14:40	0.408	-2.381	0.29
12	13:50 – 14:50	0.409	-2.370	0.29
13	14:00 – 15:00	0.500	-2.348	0.53

The t-statistics are significant and likelihood ratio indices (ρ^2) are above 0.15 in most of the simulations. ρ^2 is an index which measure the goodness-of-fit informally as a fraction of an initial log likelihood value explained by the model. More precisely, it measures how well the model performs with its estimated parameters when compared with the model in which all the parameters are zero (Train, 2003). ρ^2 is calculated as;

$$\rho^2 = 1 - \frac{LL(\hat{\beta})}{LL(0)} \tag{4.2}$$

where $LL(0)$ is the value of the log likelihood function when all the parameters are zero and $LL(\hat{\beta})$ is the value of the log likelihood function when its maximum. ρ^2 is somewhat analogous to R^2 used in regression analysis but they are not same. Normally ρ^2 produces smaller values compare to the R^2 and values over 0.15 are considered as satisfactory. This is also known as the McFadden's pseudo-R squared (McFadden D. , 1974). Values will depend on the model which used for estimations and has more usage when it compared the estimations that used the exact same set of data. The variation of the respective estimations is plotted and showed in the Figure 4.3

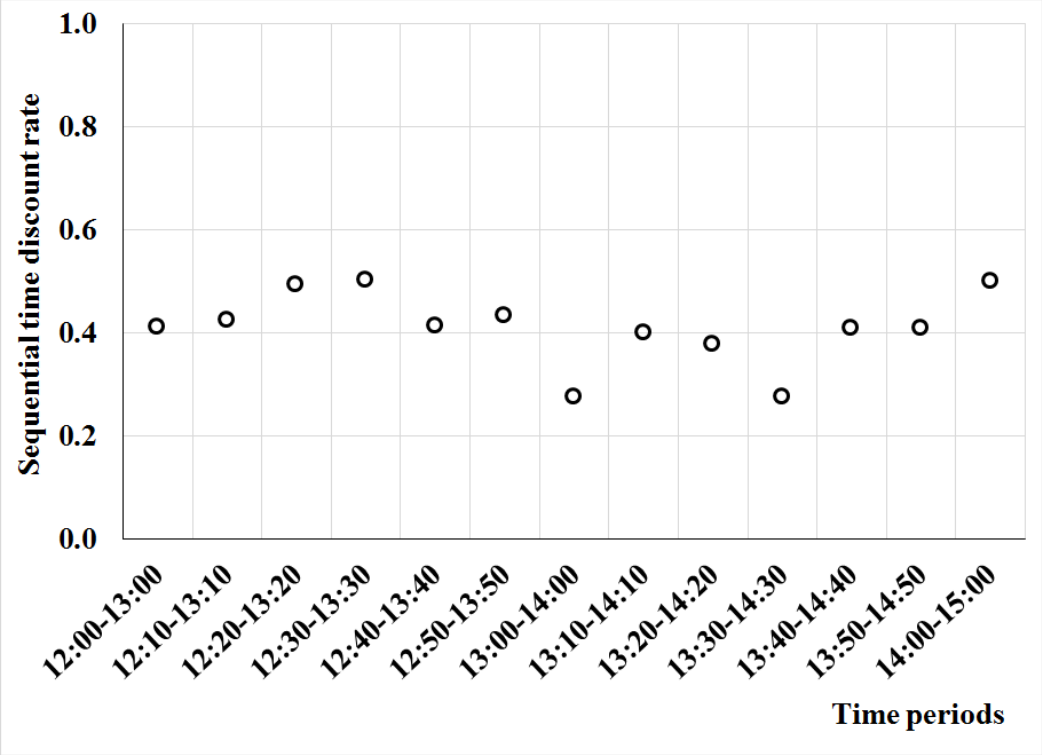

Figure 4.3 Variation of sequential time discount rate over the moving time

In comparison with Figure 4.2, the Figure 4.3 clearly visualized the variation of sequential time discount rate over the tiny periods of time. Precisely, it indicates increasing tendencies during the periods from 12:20 to 13:30 and 14:00 to 15:00. Further, it shows decreasing tendencies during the periods from 13:00 to 14:00 and 13:30 to 14:30. In addition, simulation results proved the model consistency of producing better estimations for sequential time discount rate over the moving time. The results indicate the variation of drivers' decision-making dynamics over the time.

More importantly, the stability of the sequential time discount rate was tested through the asymptotic t test. t values were calculated based on equation 4.1 and the respective results are tabulated in Table 4.2

Table 4.2 t values of asymptotic t test between estimations

Sample	1	2	3	4	5	6	7	8	9	10	11	12
1												
2	-0.02											
3	-0.10	-0.08										
4	-0.10	-0.08	-0.01									
5	0.00	0.01	0.09	0.09								
6	-0.03	-0.01	0.07	0.08	-0.02							
7	0.14	0.15	0.23	0.22	0.13	0.16						
8	0.01	0.03	0.11	0.11	0.01	0.04	-0.13					
9	0.04	0.06	0.15	0.14	0.04	0.07	-0.11	0.03				
10	0.15	0.16	0.24	0.23	0.14	0.17	0.00	0.13	0.12			
11	0.00	0.02	0.11	0.10	0.01	0.03	-0.14	-0.01	-0.04	-0.15		
12	0.00	0.02	0.10	0.10	0.00	0.03	-0.14	-0.01	-0.04	-0.15	0.00	
13	-0.12	-0.10	-0.01	0.00	-0.10	-0.09	-0.25	-0.13	-0.17	-0.28	-0.13	-0.13

Magnitudes of all the t values tabulated on Table 4.2 are less than 1.65 and hence, they all are insignificant. This indicates that there are no significant differences between the estimated sequential time discount rates in each sample. Precisely, the model estimations are stable.

Along with sequential time discount rate, two other parameters, travel time and right turn dummy variable were also estimated. The respective estimations are shown in Table 4.3

Table 4.3 Estimation results of travel time (TT) and right turn dummy (RT) parameter for different time periods

Sample No.	Sampling period	Travel time		Right turn dummy		ρ^2
		Estimate	t value	Estimate	t value	
1	12:00 – 13:00	-0.087	-1.836	-0.770	-3.407	0.19
2	12:10 – 13:10	-0.223	-3.374	-0.827	-3.244	0.26
3	12:20 – 13:20	-0.229	-3.123	-1.061	-3.753	0.39
4	12:30 – 13:30	-0.179	-2.497	-0.936	-2.957	0.39
5	12:40 – 13:40	-0.166	-2.564	-0.823	-2.861	0.24
6	12:50 – 13:50	-0.245	-3.624	-0.868	-3.432	0.30
7	13:00 – 14:00	-0.202	-3.552	-0.770	-3.261	0.15
8	13:10 – 14:10	-0.193	-3.554	-0.746	-3.146	0.24
9	13:20 – 14:20	-0.260	-4.483	-0.966	-3.977	0.25
10	13:30 – 14:30	-0.262	-4.466	-1.092	-4.240	0.18
11	13:40 – 14:40	-0.239	-3.946	-1.209	-4.221	0.29
12	13:50 – 14:50	-0.241	-3.929	-1.184	-4.126	0.29
13	14:00 – 15:00	-0.407	-4.903	-1.656	-4.988	0.53

As Table 4.3 indicates, both parameters, travel time and right turn dummy variable have achieved the expected sign which is minus. This indicates the peoples dislikeness to increase of travel time or make right turns. The t statistic values are significant for all the samples. All the ρ^2 values are equal or greater than 0.15 which indicates the goodness of fit of the data to the model. Then the temporal changes of the parameters were visualized as parameter ratios, travel time ratio [$\theta_{TT}/(\theta_{TT} + \theta_{RT})$] and right-turn ratio [$\theta_{RT}/(\theta_{TT} + \theta_{RT})$]. Since the utility function was formed including these two parameters or in other words, the link utility was calculated based on the link travel time and the right turns, it is not justifiable to compare them individually or independently. Hence the respective ratios were used for the comparison purpose and is shown in Figure 4.4

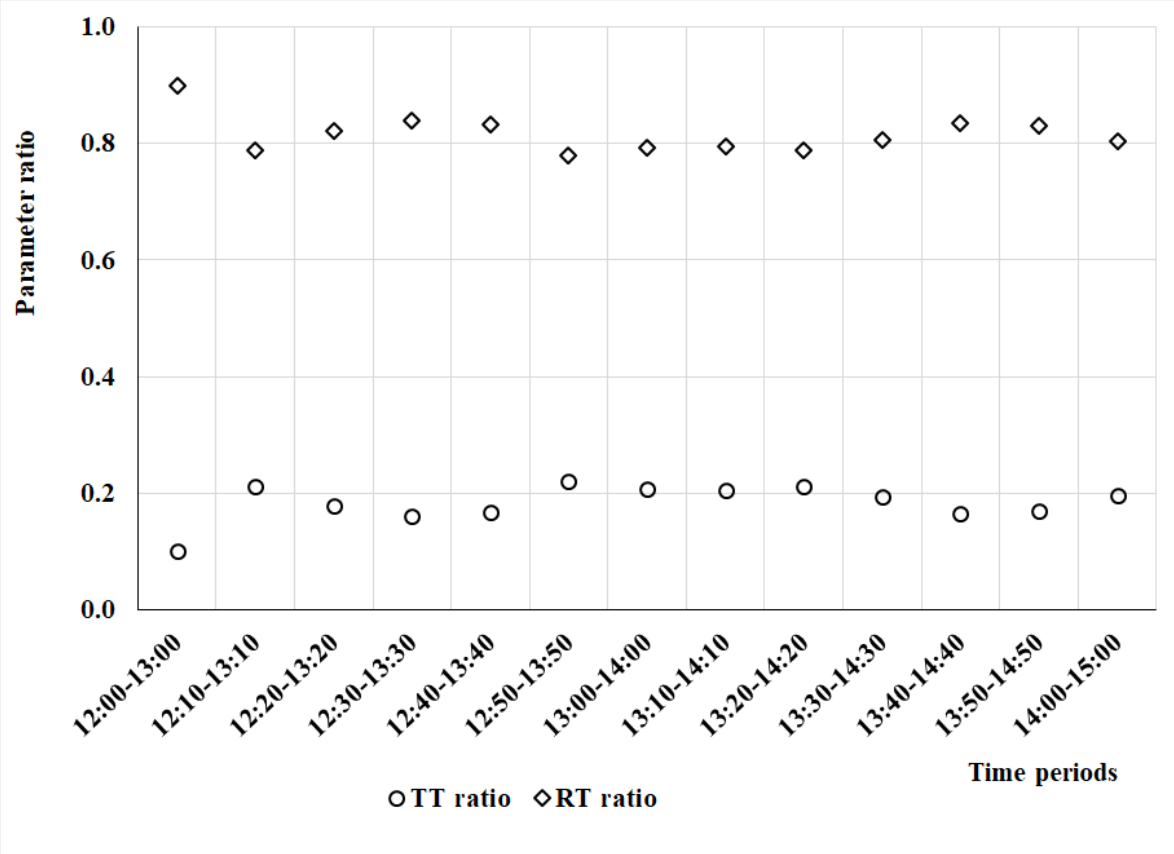

Figure 4.4 Variation of parameter ratios with moving time

As Figure 4.4 illustrates, there is no any significant fluctuation movement in both parameter ratio curves during the considered period of time. Along with, the results prove the model consistency of producing better estimations with the moving time. More importantly, they all are stable throughout the considered period. In summary, by using this analysis under moving time, it can be concluded that the results are able to figure out the tiny variations of each parameters and they all are stable throughout the considered period.

4.3.2 Stability analysis by sampling rate

Number of trips in a sample has a huge impact on the estimation time of sequential time discount rate. In general, with a personnel computer having 32 GB RAM, 3.60 GHz processor with Windows 10 operating system, randomly sampled 30 trips sample take about 25 – 35 hours for completing a simulation. This reduces to 15 – 25 and 10 – 15 for 20 trips and 10 trips samples respectively. Therefore, finding the minimum number of trips for a stable estimation is very important for saving the time and obtaining a better result. Hence, sampling rate is crucial and made under 03 categories as 10 trips, 20 trips and 30 trips. Randomly sampled 10 trips were included in each of the 10 samples under all three categories and estimated through β – SRL model. The sample formulation is visualized in Figure 4.5.

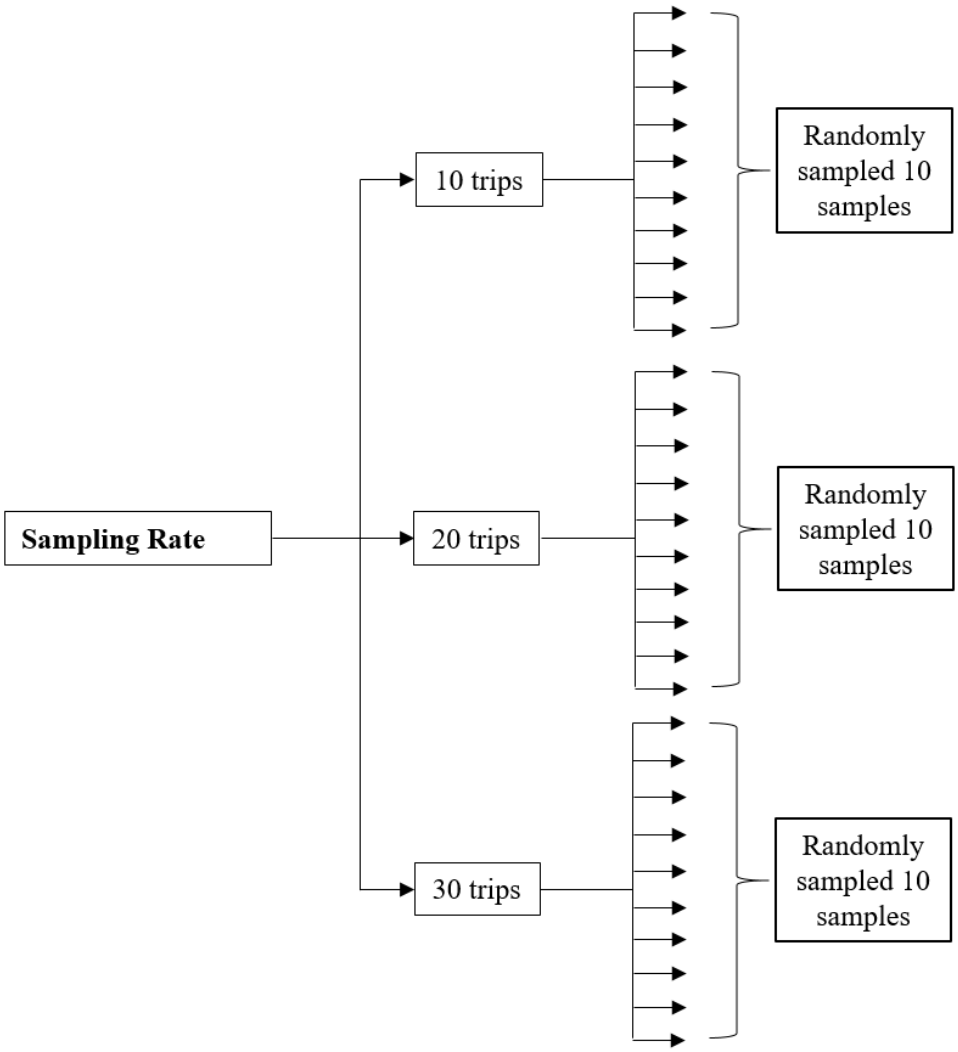

Figure 4.5 Formations of samples for simulating under sampling rate

The probe taxi data collected in Tokyo on 11th March 2011 from 15:00 to 17:00 hrs. JST was used for the analysis. The period was selected based on the availability of taxi trips and there were 49 trips in the main sample. Maximization of the log-likelihood function, within the estimation process, consume more time when the number of links in the network are high. Hence, network reduction is necessary in order to achieve a smooth estimation process. Accordingly, a reduced area which includes 2616 nodes and 3438 links was used for parameter estimation. Estimated results of sequential time discount rate for each of above categories are displayed respectively in Table 4.4. ρ^2 indicates the likelihood ratio index for each sample and is above 0.15 in most of the cases.

Table 4.4 Estimation results of β for random sampling of 10, 20 and 30 trips

Sample	10 trips			20 trips			30 trips		
	β	t-value	ρ^2	β	t-value	ρ^2	β	t-value	ρ^2
1	0.177	-2.401	0.16	0.337	-3.452	0.25	0.326	-4.951	0.22
2	0.249	-3.558	0.24	0.256	-3.540	0.19	0.159	-5.186	0.16
3	0.182	-2.770	0.20	0.249	-3.502	0.19	0.233	-4.857	0.16
4	0.106	-2.865	0.31	0.144	-3.516	0.17	0.187	-4.340	0.14
5	0.423	-1.809	0.28	0.258	-4.327	0.25	0.256	-4.412	0.19
6	0.186	-4.590	0.34	0.249	-3.999	0.22	0.122	-3.831	0.13
7	0.144	-4.106	0.29	0.111	-2.345	0.12	0.150	-5.052	0.18
8	0.345	-2.765	0.30	0.095	-3.405	0.22	0.223	-5.593	0.18
9	0.192	-3.021	0.18	0.177	-4.134	0.22	0.219	-5.937	0.18
10	0.178	-1.714	0.12	0.271	-3.959	0.19	0.133	-4.017	0.15

The t-statistics for all estimations are significant. Since all these samples are randomly sampled and independent from each other, for the easiness of visual observation, the estimated values of sequential time discount rate are sorted and plotted as shown in Figure 4.6. Hence the horizontal axis of the Figure 4.6 contains the sorted sample number for each category and it is not equal to the sample number appeared in the Table 4.4

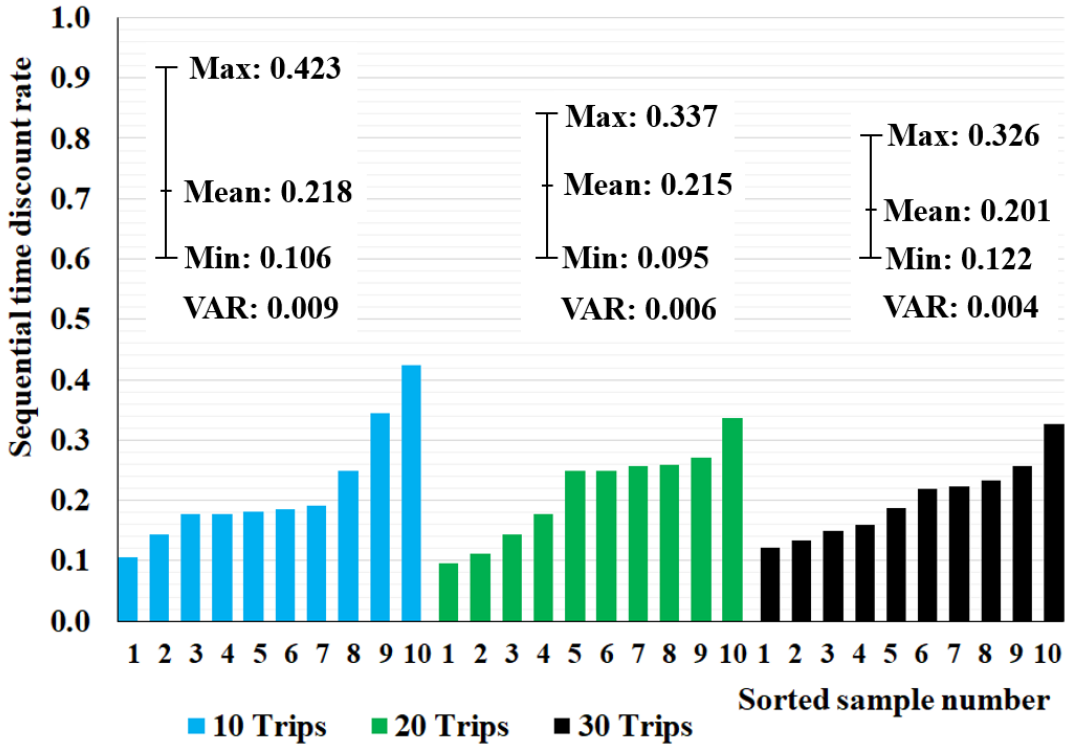

Figure 4.6 Variation of sequential time discount rate with random sampling

Sequential time discount rate varies between zero to one and hence, the vertical axis of the Figure 5.6 is kept under that limitations to illustrate the ranges where it varies. As data referred to a congested time after the occurrence of great east Japan earthquake, sequential time discount rate varies in a lower range where means for all three categories lies between 0.201 to 0.218. Therefore, drivers' decision-making behavior during the period is more rely on myopic decisions. The distance between the minimum and maximum estimations of each category is visualized in same scale for all three categories. As Figure 4.6 shows, the gap between the minimum and maximum estimations is comparatively high in the 10 trips samples and it indicates the possibility of larger deviation from the mean.

Then, the statistical parameters stated in section 4.2 were calculated and the resulted values are presented in Table 4.5

Table 4.5 Statistical parameters of the samples

Parameter	10 trips	20 trips	30 trips
Variance	0.009	0.006	0.004
Standard deviation	0.096	0.079	0.063
Relative standard deviation	0.441	0.366	0.315
Coefficient of variation (%)	44	37	31
Standard error of the mean	0.030	0.025	0.020
True value	0.218 ± 0.069	0.215 ± 0.056	0.201 ± 0.045

All the considered statistical parameters have decreased when the number of trips in a sample is increased from 10 to 20. From 20 to 30, they either decreased or remains same. The uncertainty of the estimations or possible fluctuations is expressed by the true value and its range get shortened when the number of trips in a sample is increased. All these indicates the lessening of the spread of estimations with the increase of number of trips within respective samples.

In addition, the asymptotic t test was also carried out based on equation 4.1 and the respective t values are included in Table 4.6, Table 4.7 and Table 4.8 respectively for samples with 10 trips, 20 trips and 30 trips.

Table 4.6 t values of asymptotic t test between estimations of 10 trips per sample

Sample	1	2	3	4	5	6	7	8	9
1									
2	-0.06								
3	0.00	0.06							
4	0.05	0.12	0.05						
5	-0.19	-0.19	-0.21	-0.24					
6	-0.01	0.08	0.00	-0.07	0.26				
7	0.03	0.12	0.03	-0.03	0.28	0.05			
8	-0.14	-0.11	-0.15	-0.19	0.08	-0.20	-0.22		
9	-0.01	0.06	-0.01	-0.06	0.21	-0.01	-0.05	0.15	
10	0.00	0.04	0.00	-0.04	0.15	0.01	-0.02	0.11	0.01

Table 4.7 t values of asymptotic t test between estimations of 20 trips per sample

Sample	1	2	3	4	5	6	7	8	9
1									
2	0.11								
3	0.11	0.01							
4	0.21	0.12	0.11						
5	0.12	0.00	-0.01	-0.12					
6	0.12	0.01	0.00	-0.11	0.01				
7	0.16	0.10	0.10	0.02	0.11	0.10			
8	0.23	0.14	0.14	0.04	0.15	0.14	0.01		
9	0.20	0.09	0.08	-0.03	0.10	0.09	-0.05	-0.07	
10	0.09	-0.02	-0.03	-0.14	-0.02	-0.03	-0.11	-0.16	-0.12

Table 4.8 t values of asymptotic t test between estimations of 30 trips per sample

Sample	1	2	3	4	5	6	7	8	9
1									
2	0.27								
3	0.16	-0.11							
4	0.21	-0.04	0.06						
5	0.12	-0.14	-0.04	-0.09					
6	0.24	0.04	0.12	0.07	0.15				
7	0.27	0.01	0.12	0.05	0.15	-0.03			
8	0.19	-0.10	0.02	-0.05	0.05	-0.12	-0.11		
9	0.21	-0.09	0.02	-0.05	0.06	-0.11	-0.10	0.01	
10	0.24	0.03	0.12	0.06	0.14	-0.01	0.02	0.11	0.11

All the t values tabulated on Table 4.6, Table 4.7 and Table 4.8 are insignificant. This indicates that there are no significant differences between the estimated sequential time discount rates in each category. Precisely, the model estimations are stable. Accordingly, considering the visual observations of Figure 4.6, statistical parameters in Table 4.5 and asymptotic t values, it can be concluded that the 20 trips and 30 trips samples have shown more stability compare to the 10 trips samples, while 10 trips samples also have produced stable results consistently.

In addition to the sequential time discount rate, the parameters, travel time and right turn dummy variable were also estimated. The resulted estimations are shown in Table 4.9, Table 4.10 and Table 4.11 respectively for 10 trips, 20 trips and 30 trips samples.

Table 4.9 Estimation results of travel time (TT) and right turn dummy (RT) parameter for 10 trips random sampling samples

Sample No.	Travel time		Right turn dummy		ρ^2
	Estimate	t value	Estimate	t value	
1	-0.151	-3.156	-1.545	-4.018	0.16
2	-0.190	-4.028	-1.925	-4.976	0.24
3	-0.132	-2.985	-1.994	-4.468	0.20
4	-0.281	-3.989	-3.113	-4.844	0.31
5	-0.105	-2.256	-1.133	-3.116	0.28
6	-0.281	-4.751	-3.031	-5.334	0.34
7	-0.237	-4.721	-3.090	-5.543	0.29
8	-0.227	-3.456	-1.623	-4.083	0.30
9	-0.145	-3.424	-2.001	-4.899	0.18
10	-0.096	-2.535	-1.217	-3.235	0.13

Table 4.10 Estimation results of travel time (TT) and right turn dummy (RT) parameter for 20 trips random sampling samples

Sample No.	Travel time		Right turn dummy		ρ^2
	Estimate	t value	Estimate	t value	
1	-0.120	-4.290	-1.766	-6.154	0.25
2	-0.109	-3.975	-1.933	-6.495	0.19
3	-0.138	-4.542	-1.773	-6.090	0.19
4	-0.152	-4.927	-1.837	-6.193	0.17
5	-0.190	-5.280	-2.134	-6.667	0.25
6	-0.135	-4.734	-2.244	-7.166	0.22
7	-0.098	-3.701	-1.459	-5.522	0.12
8	-0.178	-5.687	-2.473	-7.728	0.22
9	-0.170	-5.605	-2.280	-7.283	0.22
10	-0.104	-4.108	-1.728	-6.341	0.19

Table 4.11 Estimation results of travel time (TT) and right turn dummy (RT) parameter for 30 trips random sampling samples

Sample No.	Travel time		Right turn dummy		ρ^2
	Estimate	t value	Estimate	t value	
1	-0.110	-5.802	-1.747	-8.742	0.22
2	-0.144	-7.307	-1.816	-9.809	0.16
3	-0.106	-5.866	-1.713	-8.726	0.16
4	-0.106	-5.679	-1.601	-8.208	0.14
5	-0.104	-5.110	-1.832	-7.896	0.19
6	-0.097	-5.567	-1.727	-8.734	0.13
7	-0.148	-6.985	-2.031	-9.744	0.18
8	-0.138	-7.057	-1.806	-9.697	0.18
9	-0.156	-7.759	-1.764	-9.918	0.18
10	-0.099	-5.312	-1.891	-8.650	0.15

The t-statistics under all three categories are significant. The sign of the all estimated parameters are minus which is the expected sign. As under the case of sequential time discount rate, since all these are randomly sampled, and for the sake of painless understanding, the estimated values of parameters are sorted and plotted. The individual variations for travel time parameter ratio $[\theta_{TT}/(\theta_{TT}+\theta_{RT})]$ and right-turn dummy parameter ratio $[\theta_{RT}/(\theta_{TT}+\theta_{RT})$ are shown in Figure 4.7 and Figure 4.8 respectively. The horizontal axis of the Figure 4.7 and Figure 4.8 contains the sorted sample numbers which are not equal to the sample numbers in Table 4.9, Table 4.10 and Table 4.11

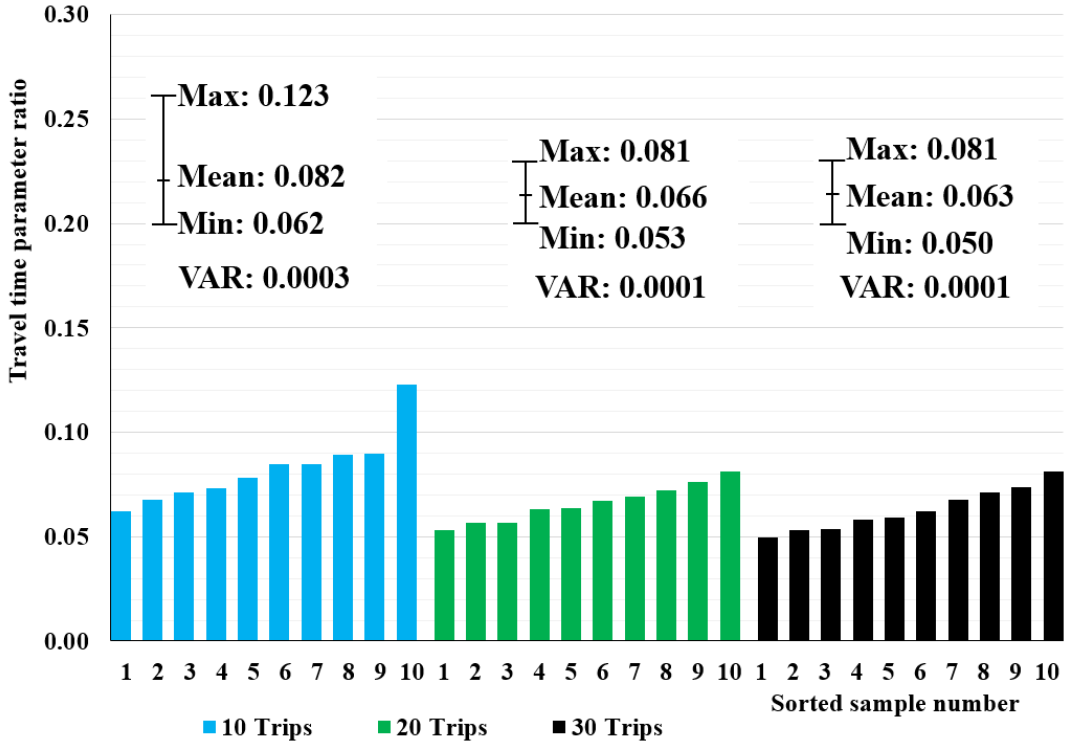

Figure 4.7 Variation of travel time parameter ratio under random sampling

Given the congestion of the network when about 2-3 hours after the occurrence of great east Japan earthquake, the estimation results show very lower values under the all three categories. Precisely, the means of the ratios are 0.082, 0.066 and 0.063 for the categories 10 trips, 20 trips and 30 trips respectively. This illustrates the difficulty for travelers to evaluate the travel time under the so called congested circumstances. Conclusions under the explanations of sequential time discount rate are further being supported by these variations as 20 trips and 30 trips samples shown much consistency where the variation under the 10 trips showed marginal deviation from others. But in overall, the model has produced good estimations under all three categories as the variances of those results are very small as 0.0003, 0.0001 and 0.0001 respectively for 10 trips, 20 trips and 30 trips samples.

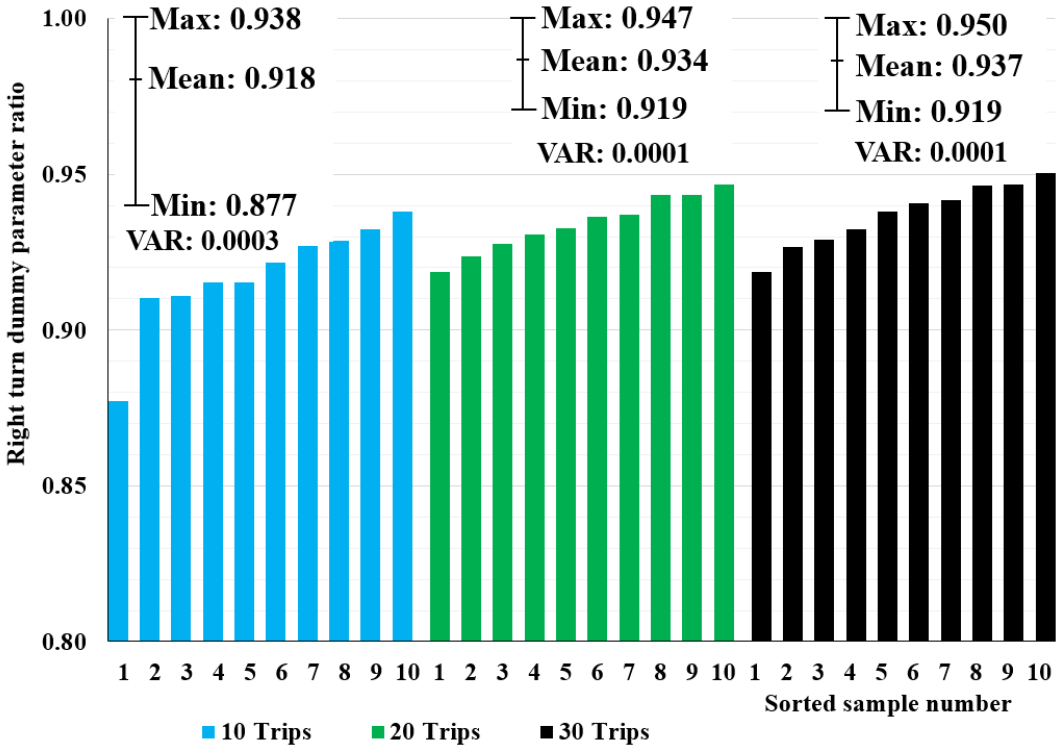

Figure 4.8 Variation of right turn dummy parameter ratio under random sampling

As discussed under the Figure 4.7, because of the congestion occurred by the time of which the estimations or the data are referred, values of right turn dummy parameter ratio stays in high values under the all three sampling techniques. The means are 0.918, 0.934 and 0.937 for 10 trips, 20 trips and 30 trips samples respectively. This illustrates the difficulty of making right turns in a congested environment. Further, Figure 4.8 also support the fact that 20 trips and 30 trips samples have made better estimations than the 10 trips samples as 10 trips estimations contain some deviating results. When it comes to the sample variances, they show a much similar pattern the previous parameter ratio. Precisely, 0.0003, 0.0001 and 0.0001 for 10 trips, 20 trips and 30 trips samples respectively, which indicate the overall quality of the model estimations. Hence, based on the variations of all three parameters under the described categories, it can be recommended to use 20 trips per sample as a threshold value in order to achieve better estimations through the β −SRL model.

4.3.3 Stability analysis during the peak time periods

Peak hour traffic congestion has been identified as a key problem for transport planners in many populated cities around the world e.g. (Holyoak & Taylor, 2006; Zhu & Long, 2016; Noordegraaf & Annema, 2012). Transport infrastructure struggles to handling continuously rising demands and hence it is important to carryout studies on behavior analysis during these periods. The situation can be further worse when a disaster also occurred. Therefore, in this section, it is expected to illustrate the travel behavior analysis by using sequential time discount rate along with travel time and right turn dummy

parameter through β −SRL model at Tokyo based on the probe taxi data collected on 11th March 2011. The selected area belongs to the secondary mesh code 533946 of the region mesh. The average link speed of the selected area was plotted and showed in Figure 4.9

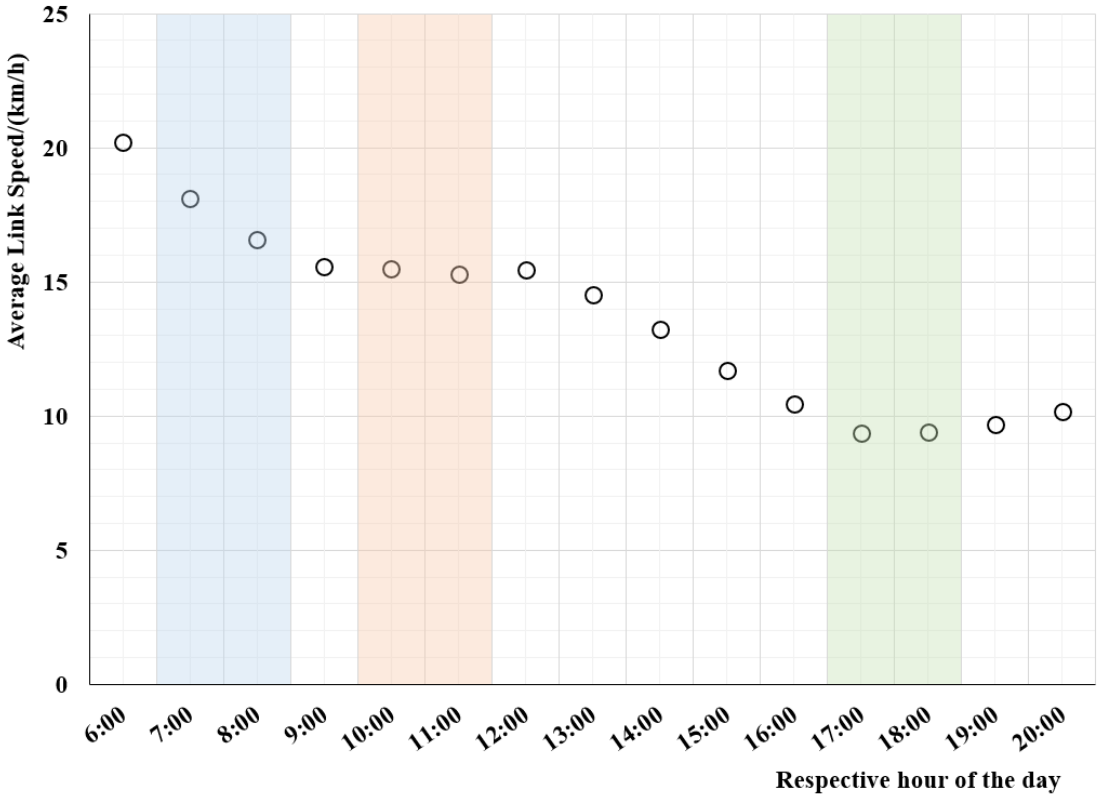

Figure 4.9 Variability of average link speed

The peak times are selected as 7:00 to 9:00 hrs. the morning peak, 10:00 to 11:00 hrs. the day peak and 17:00 to 19:00 hrs. the evening peak as highlighted in the Figure 5.9 in light blue, orange and green colors respectively. It is a common practice to use a plot of number of departures during each hour when analyzing peak hours but since here in this study I'm using probe taxi data, it is more suitable for presenting an average link speed plot. Because, congestion might have occurred due to all the vehicles running in the network including taxies but taxi percentage may less compare to all the vehicles present in the network in respective times.

As per the Figure 4.9 shows, link speed decreases during the morning peak. Then it is little stable from 9:00 to 10:00 but again a marginal decreasing is observed during the day peak. In the afternoon, the great east Japan earthquake was occurred and link speed was continuously decreasing due to the occurred congestion. Evening peak is the time where the average link speed is lowest for the day where it drops less than 10 km/h. The stability analysis is carried out based on three categories as 10 trips, 20 trips and 30 trips samples where 10 randomly sampled trips are included in each sample. A schematic diagram of sampling is shown in Figure 4.10

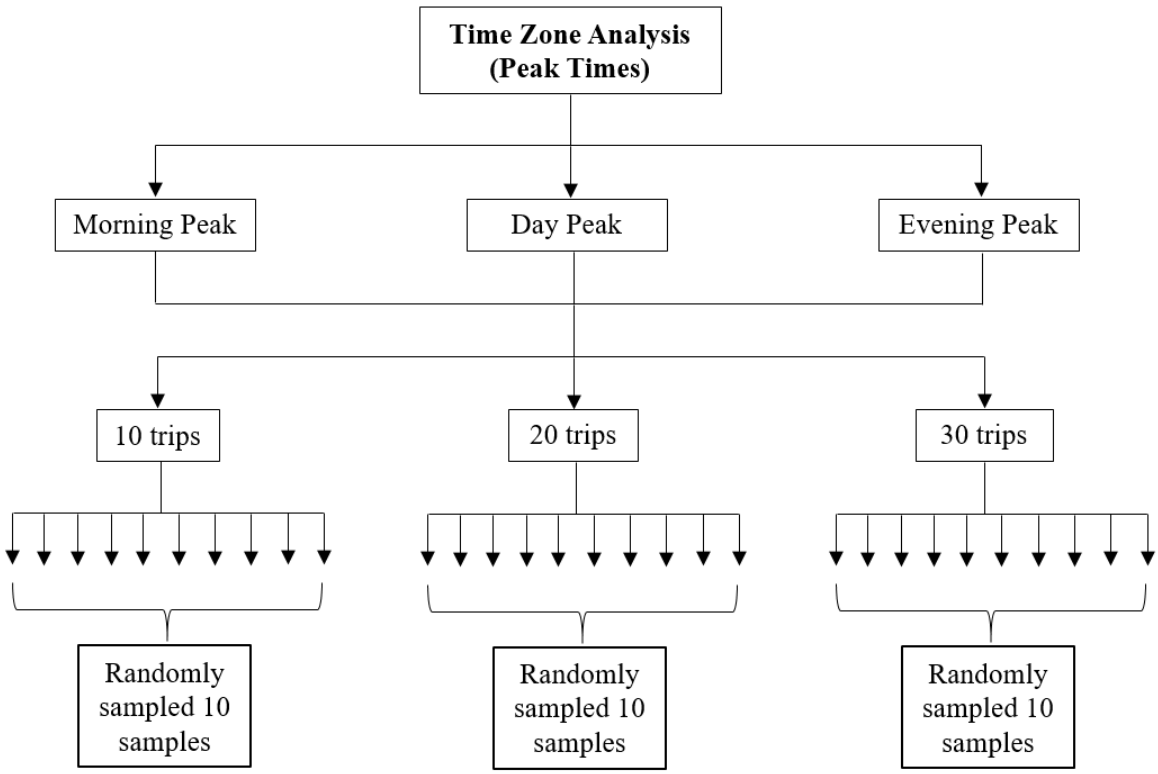

Figure 4.10 Schematic diagram of sampling under time zone analysis

4.3.3.1 Stability analysis during morning peak

Parameter estimations were done based on above sampling at a reduced network in aforementioned area where it contains 4556 links and 2967 nodes. The respective results for sequential time discount rate under the categories of 10 trips, 20 trips and 30 trips per sample are tabulated in Table 4.12. ρ^2 indicates the likelihood ratio index for each sample.

Table 4.12 Estimation results of β for random sampling of 10, 20 and 30 trips during the morning peak time

Sample	10 trips			20 trips			30 trips		
	β	t-value	ρ^2	β	t-value	ρ^2	β	t-value	ρ^2
1	0.362	-2.80	0.33	0.320	-4.00	0.28	0.478	-2.75	0.47
2	0.357	-2.19	0.28	0.284	-4.30	0.28	0.400	-3.91	0.36
3	0.478	-2.10	0.49	0.299	-3.76	0.29	0.511	-2.80	0.57
4	0.362	-2.95	0.33	0.475	-2.80	0.49	0.377	-4.09	0.35
5	0.442	-1.87	0.39	0.376	-3.43	0.29	0.295	-4.52	0.27
6	0.342	-2.77	0.29	0.338	-3.43	0.30	0.406	-3.92	0.38
7	0.399	-2.66	0.35	0.355	-3.25	0.32	0.315	-4.24	0.30
8	0.520	-1.85	0.55	0.313	-3.87	0.28	0.412	-3.56	0.39
9	0.351	-2.88	0.28	0.353	-3.36	0.30	0.407	-3.83	0.36
10	0.189	-2.72	0.27	0.445	-2.83	0.45	0.379	-4.28	0.34

As the Table 4.12 shows, the t-statistics are significant for all estimations. ρ^2 is greater than 0.25 in all samples. Since all these are randomly sampled, and for the easiness of visual observation, the estimated values of sequential time discount rate are sorted and plotted as shown in Figure 4.12. Hence the horizontal axis of the Figure 4.12 contains the sorted sample which is not equal to the sample number appeared in the Table 4.12

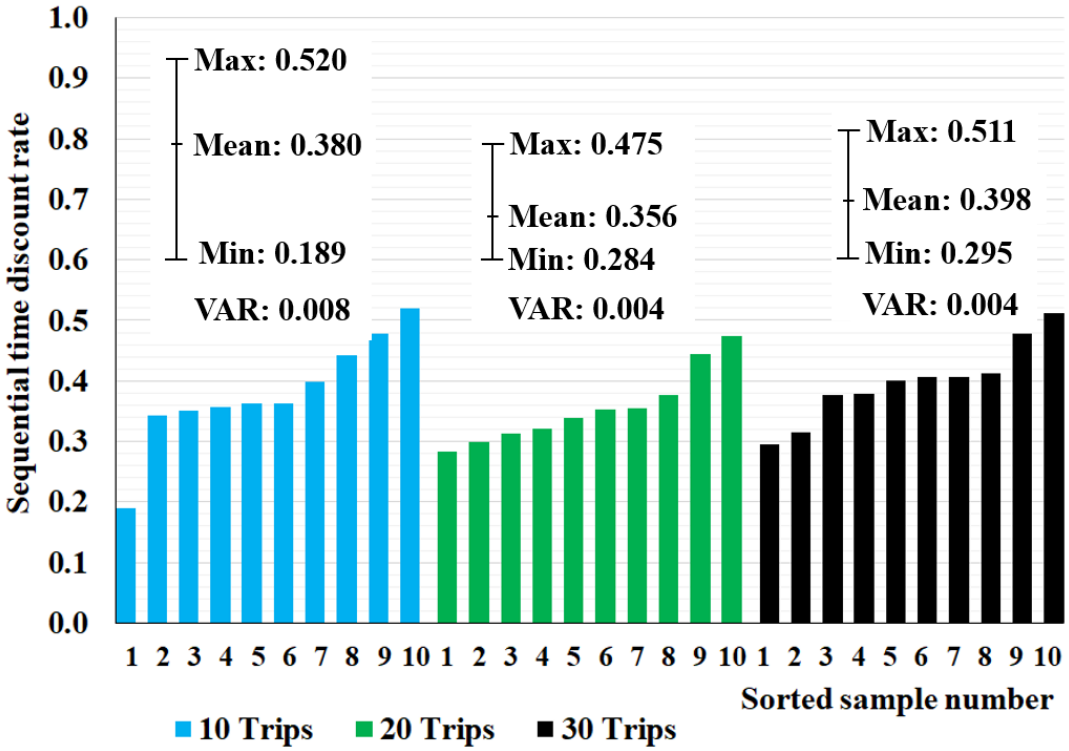

Figure 4.11 Variation of sequential time discount rate with random sampling during morning peak

Morning peak is the time where many trips are started and accordingly the network get congested. As the Figure 4.9 indicates, average link speed is dropping from twenties to fifteen range and correspondingly the estimations of sequential time discount rate vary in a lower range. Precisely, the means are 0.380, 0.356 and 0.398 for 10 trips, 20 trips and 30 trips samples respectively. Therefore, drivers' decision-making behavior during the period is more rely on myopic decisions than the global decisions. The estimations in each category have varied in similar fashion except one 10 trips samples, which showed relatively a lower value. The difference between maximum and minimum estimations is comparatively higher in 10 trips sample while 20 and 30 trips categories showed a much closer and stable variability. Then, the statistical parameters stated in section 4.2 were calculated and the resulted values are presented in Table 4.13

Table 4.13 Statistical parameters of estimated β for samples during morning peak time

Parameter	10 trips	20 trips	30 trips
Variance	0.008	0.004	0.004
Standard deviation	0.09	0.06	0.06
Relative standard deviation	0.24	0.17	0.16
Coefficient of variation (%)	24	17	16
Standard error of the mean	0.029	0.020	0.020
True value	0.380 ± 0.065	0.356 ± 0.044	0.398 ± 0.046

Considering the statistical parameters tabulated in Table 4.13, it is clear that 20 trips and 30 trips samples have produced better results compare to the 10 trips samples. In addition to these parameters, asymptotic t test also carried out for testing the similarity of the estimations. The values indicate that there are no significant differences between the estimated sequential time discount rates in each category and hence, the model estimations are stable. The resulted t values are included in the appendix A.

4.3.3.2 Stability analysis during day peak

Day peak time was considered as from 10:00 to 12:00 hours and it is the period where the lowest average link speed shown in the Figure 4.9 for the first half of the day. Sequential time discount rate was estimated based on the same area considered under the morning peak analysis and same sampling technique were applied. The respective results are inserted in Table 4.14

Table 4.14 Estimation results of β for random sampling of 10, 20 and 30 trips during the day peak time

Sample	10 trips			20 trips			30 trips		
	β	t-value	ρ^2	β	t-value	ρ^2	β	t-value	ρ^2
1	0.175	-2.26	0.15	0.251	-4.03	0.17	0.201	-4.31	0.18
2	0.108	-1.77	0.15	0.255	-3.52	0.21	0.256	-4.44	0.21
3	0.511	-1.72	0.57	0.134	-3.29	0.16	0.341	-4.34	0.30
4	0.165	-2.60	0.25	0.239	-3.57	0.18	0.325	-4.55	0.26
5	0.051	-1.22	0.16	0.376	-3.80	0.32	0.388	-3.92	0.32
6	0.151	-2.35	0.22	0.298	-3.97	0.23	0.393	-4.00	0.32
7	0.286	-2.78	0.21	0.320	-3.57	0.25	0.272	-4.50	0.21
8	0.229	-2.48	0.19	0.378	-3.21	0.34	0.270	-4.74	0.21
9	0.318	-2.29	0.21	0.243	-3.81	0.21	0.254	-4.13	0.21
10	0.150	-2.17	0.18	0.312	-3.71	0.22	0.210	-4.61	0.21

According to the results shown in Table 4.14, all the t statistics are significant except one sample under the 10 trips category. Likelihood ratio indices shown by ρ^2 are greater than or equal to 0.15 for all the samples. The respective variations are then plotted as column chart by sorting the estimated values in each category for the convenience of visual observation and shown in Figure 4.12. As the samples are sorted, the sample numbers in the Figure 4.12 are not exactly same to the sample number appearing in the Table 4.14

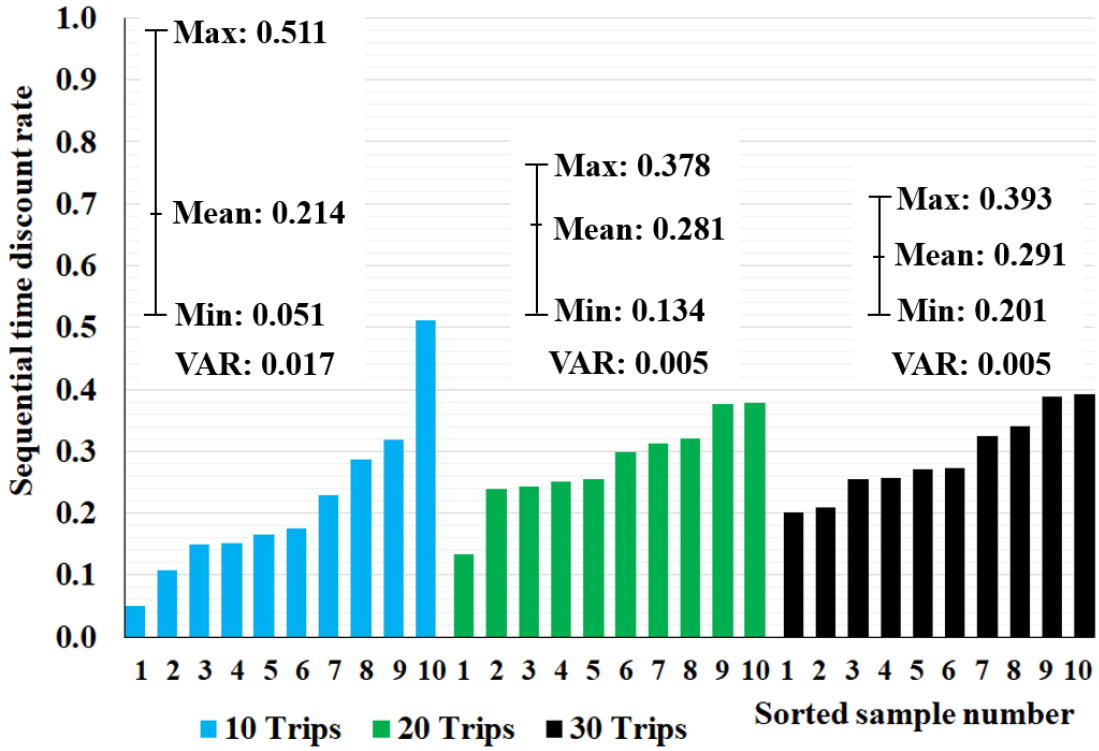

Figure 4.12 Variation of sequential time discount rate with random sampling during day peak

Day peak time is basically congested due to the work-related trips, shopping trips, recreational trips and beyond. As Figure 4.12 illustrates 20 trips and 30 trips samples have produced better estimations in comparison with 10 trips samples. Estimations of 10 trips samples showed higher variability in comparison with 20 and 30 trips samples. Since, it is a congested time and accordingly sequential time discount rate showed lower values and drivers more rely on their myopic decisions. For further analyzing of the estimations, statistical parameters were checked as in the case of the morning peak and the respective results are indicated in Table 4.15

Table 4.15 Statistical parameters of the samples during the day peak time

Parameter	10 trips	20 trips	30 trips
Variance	0.017	0.005	0.005
Standard deviation	0.13	0.07	0.07
Relative standard deviation	0.61	0.26	0.23
Coefficient of variation (%)	61	26	23
Standard error of the mean	0.041	0.023	0.021
True value	0.214 ± 0.094	0.281 ± 0.052	0.291 ± 0.049

As per values of statistical parameters tabulated in Table 4.15, it is certain that 20 trips and 30 trips samples have produced more stable results compare to the 10 trips samples. Further, asymptotic t test also carried out for testing the similarity of the estimations. The resulted t values are insignificant and it indicates that there are no significant differences between the estimated sequential time discount rates in each category. Precisely, the model estimations are stable during the period. The resulted t values are included in the appendix B.

4.3.3.3 Stability analysis during evening peak

In comparison with both morning peak and day peak, evening peak is the most congested period. It is the case for normal traffic network is concerned, but here even has worst due to the occurrence of the great east Japan earthquake. Due to the highly congested network, link flows are unsteady and it is very important to analyze the travel behavior. The same sampling technique was applied and the same area as in the morning peak and the day peak was used. The respective estimations for sequential time discount rate are shown in Table 4.16

Table 4.16 Estimation results of β for random sampling of 10, 20 and 30 trips during the evening peak time

Sample	10 trips			20 trips			30 trips		
	β	t-value	ρ^2	β	t-value	ρ^2	β	t-value	ρ^2
1	0.038	-0.93	0.09	0.111	-2.40	0.07	0.146	-3.44	0.12
2	0.450	-1.73	0.42	0.161	-3.66	0.16	0.407	-3.74	0.31
3	0.141	-2.39	0.09	0.133	-2.85	0.09	0.168	-3.95	0.14
4	0.281	-2.24	0.18	0.367	-2.85	0.20	0.100	-2.73	0.06
5	0.247	-2.70	0.17	0.340	-3.40	0.22	0.205	-3.99	0.14
6	0.229	-2.31	0.20	0.025	-0.89	0.07	0.108	-4.32	0.18
7	0.439	-2.16	0.44	0.275	-2.51	0.15	0.279	-4.32	0.20
8	0.343	-2.73	0.35	0.182	-3.14	0.09	0.032	-1.30	0.06
9	0.456	-1.81	0.38	0.107	-2.35	0.06	0.317	-4.39	0.22
10	0.100	-1.95	0.15	0.220	-3.17	0.13	0.167	-3.34	0.10

According to the results shown in Table 4.16, the t statistics are significant in most of the samples under all three categories, precisely one sample has become insignificant in each category. Since it is highly congested, the values are expected to be lower than the aforementioned two cases, morning peak and day peak. The respective variations are then plotted as column charts by sorting the values in each category for the easiness of visual observation and shown in Figure 4.13

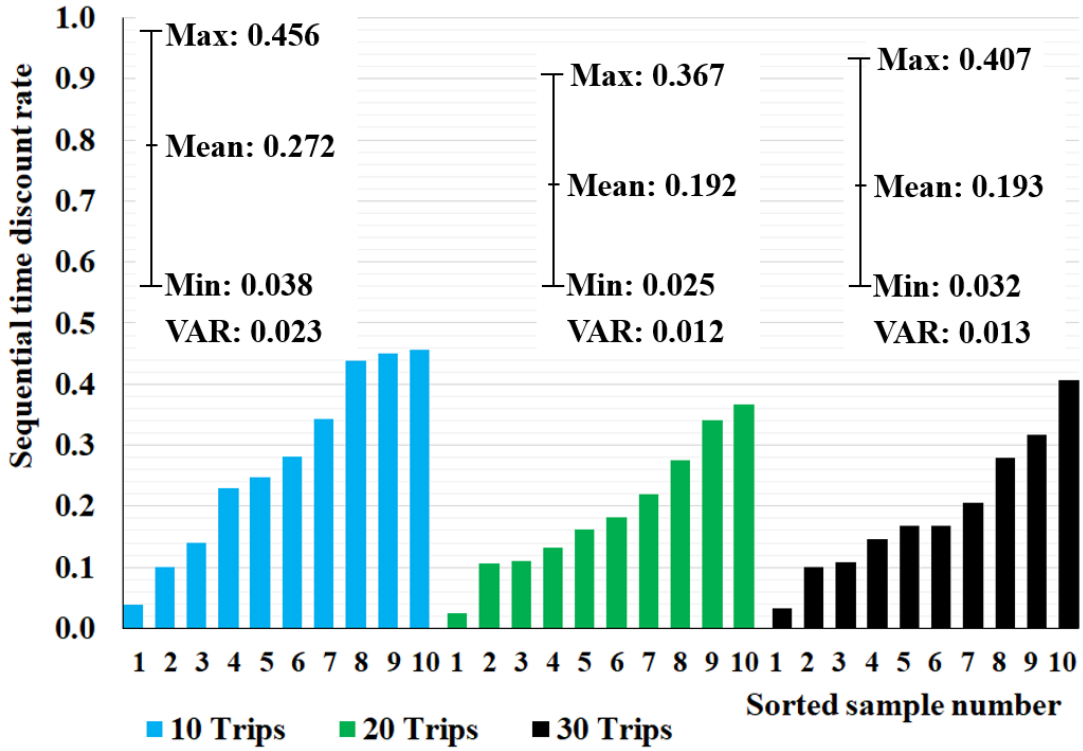

Figure 4.13 Variation of sequential time discount rate with random sampling during evening peak time

As expected, the estimations of sequential time discount rate vary in lesser values, with respect to the occurred congestion. Corresponding to the Figure 4.13, 20 trips and 30 trips samples have produced quite similar results for all randomly sampled ten samples. Meanwhile 10 trips samples have predicted little bit higher values comparatively. Here also, it is clear that drivers' decision-making behavior is more rely on the myopic decisions. In addition to visual observations, spreads of the estimations were tested through the statistical parameters and the respective results are indicated in Table 4.17

Table 4.17 Statistical parameters of the samples during the evening peak time

Parameter	10 trips	20 trips	30 trips
Variance	0.023	0.012	0.013
Standard deviation	0.15	0.11	0.11
Relative standard deviation	0.55	0.57	0.58
Coefficient of variation (%)	55	57	58
Standard error of the mean	0.047	0.034	0.036
True value	0.272 ± 0.107	0.192 ± 0.078	0.193 ± 0.080

According to the visual observations of Figure 4.13 and the statistical parameters of Table 4.17, it can be concluded that 20 trips and 30 trips samples have produced more reliable and stable results. Moreover, the asymptotic t test also carried out for testing the

similarity of the estimations. The resulted t values are insignificant and it indicates that there are no significant differences between the estimated sequential time discount rates in each category. Precisely, the model estimations are stable during the period. The resulted t values are included in the appendix C.

In addition, the estimation results of sequential time discount rate under the all three peak times, satisfies the congestions at each time visualized in the average link speed diagram (Figure 4.9). Precisely, the mean sequential time discount rates for 20 trips and 30 trips samples are 0.356 and 0.398, 0.281 and 0.291, 0.192 and 0.193 respectively for morning peak, day peak and evening peak. Hence, it indicates that the drivers' decision-making behavior movement towards the myopic decisions as the network congestion get severed.

4.3.4 Stability analysis in unsteady state

Taxi trips play an important role in urban public transportation to meet the demands of people who travel from door to door, and high percentage of them become short distance trips (Si, Weng, Chen, & Wang, 2014). Hence, link delay time become a critical factor when people make route choices in congested networks. More importantly from the travelers' perspective, the summation of each link's delay time of entire trip which gives the total trip delay time with respect to the free flow condition is more vital. The traffic network around Tokyo was heavily congested after the occurrence of great east Japan earthquake (explained in detail at chapter 6) and it is sensible to hypothesize that taxi passengers are in hurry to reach their destinations. Correspondingly, in the area which belongs to the secondary mesh code 533946 of the region mesh that considered for this analysis, most of the taxi trips are shorter distance trips. Majority of them are less than 5 km and hence trip delay time about 10 minutes, 5 minutes or even less become very crucial as it could save some lives given the havoc condition. Variation of the taxi trip distances is illustrated by plotting number of trips against their distances and shown in Figure 4.14 below.

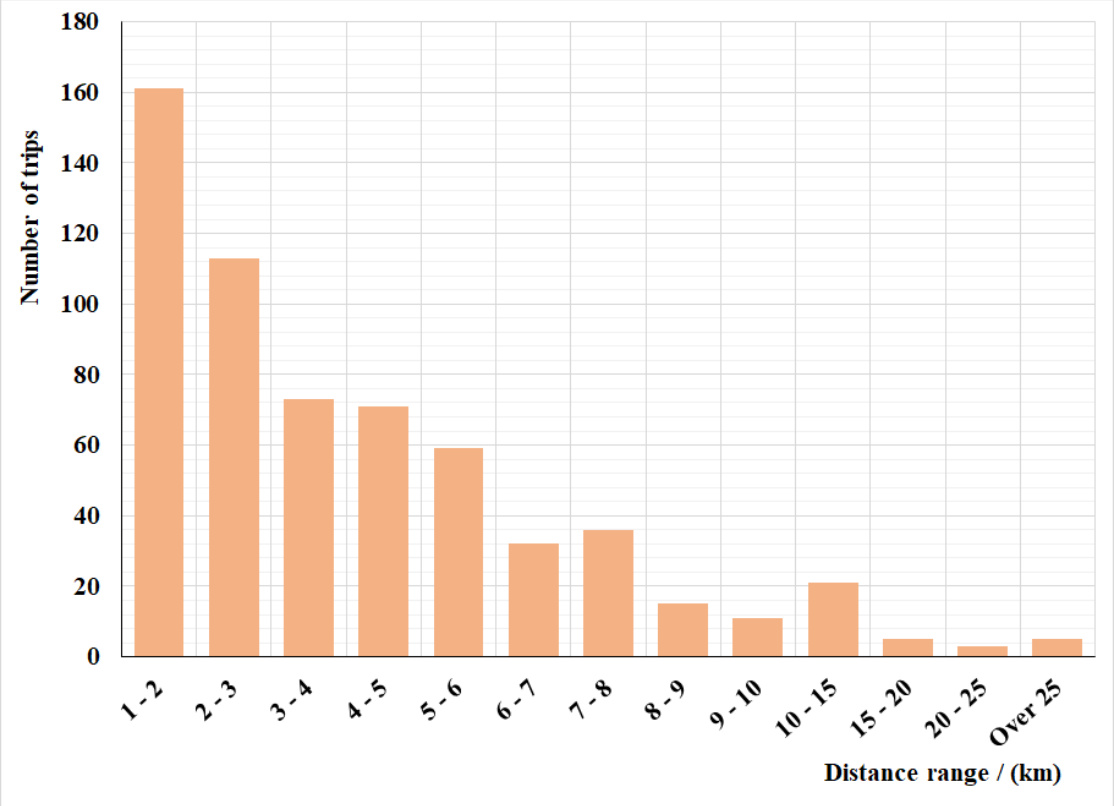

Figure 4.14 Variation of number of trips against their trip distances

Figure 4.14 is drawn based on the probe taxi data belongs to the area of secondary mesh code 533946 of the regional mesh collected on 11th March 2011. The period is from 16:00 to 17:00 hours. As it shows, majority of the taxi trips are shorter distance trips. Precisely, for this period and sample, 70% of the trips are less than 5 km. Therefore, delay in 5 or 10 minutes is become a huge hold back. For a simple example, if a traveler travels at a 30 km/h speed, he/she will reach 5 km by 10 minutes. If his/her trip is delayed by 10 minutes, it will cost him twice as the normal time. Hence, understanding travel behavior in such a situation where the flow is unsteady and testing the parameter stability is very important.

For this purpose, link delay time was calculated as the difference between the time taken under free flow speed and the time taken under the congested speed.

$$Link\ delay\ time = \left(\frac{Link\ length}{Congested\ speed}\right) - \left(\frac{Link\ length}{Free\ flow\ speed}\right) \quad (4.3)$$

Since here I'm using taxi data and, respective trips use many types of road sections such as expressways, highways, local roads, prefectural roads etc. in the Tokyo network, it is necessary to define a common free flow speed. As a solution, 85th percentile of the cumulative frequency of link's speed under the undisturbed condition (data of exactly one week after the occurrence of great east Japan earthquake) was used as the free flow speed. 85th percentile of the observed speed distributions is more frequently used as measure of the operating speed which vehicles are observed operating under free flow

conditions (Donnell, Hines, Mahoney, & Porter, 2009; Hou, Sun, & Edara, 2012; Rawson, 2015; Dinh & Kubota, 2013; Hashim, 2011).

A reduced area within the aforementioned grid which consisted of 4556 links and 2967 nodes was selected for the parameter estimation. Link delay time was calculated as above equation 4.3 and total delay time was plotted against the number of trips available in the sample. Resulted plot is shown in Figure 4.15

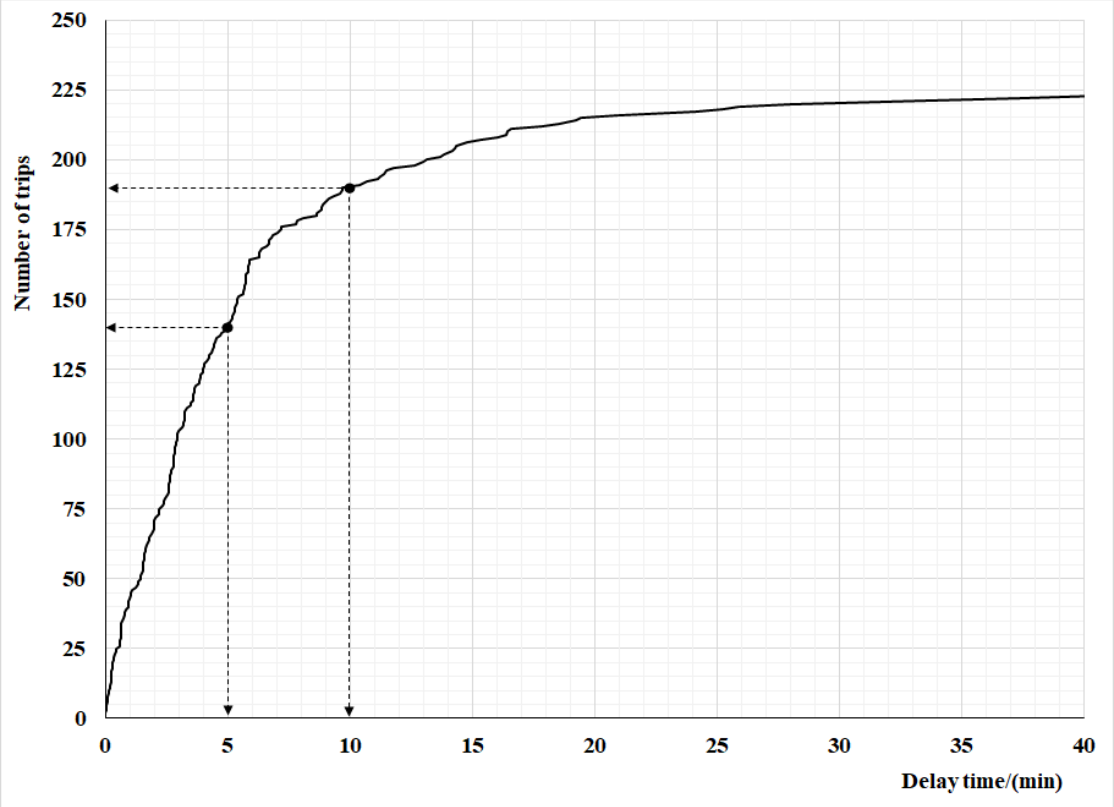

Figure 4.15 Distribution of number of trips against their delay time

As marked in Figure 4.15, three zones were identified based on trip delay time as less than 5 minutes, between 5 to 10 minutes and more than 10 minutes, in order to estimate the parameters through β −SRL model. The sampling was made randomly under the three categories as 10 trips, 20 trips and 30 trips per sample. A schematic flow of sampling is shown in Figure 4.16

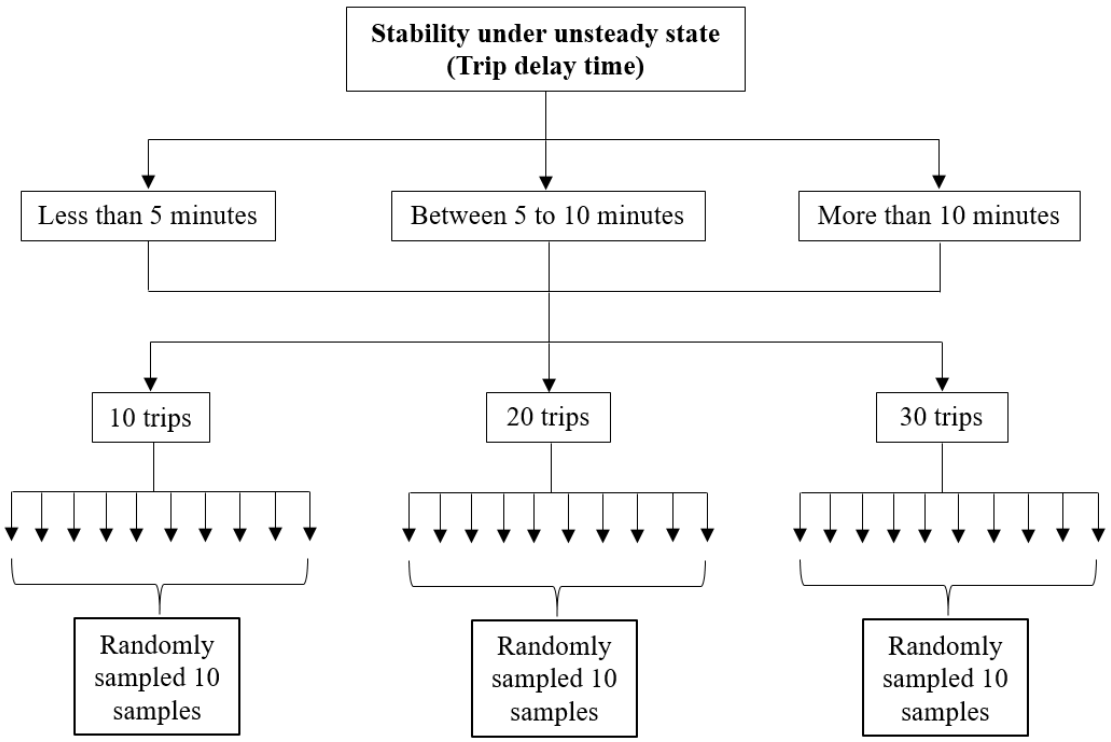

Figure 4.16 Schematic diagram of sampling under unsteady state analysis

4.3.4.1 Stability analysis for trips with delay time less than five minutes

As mentioned early, the trip delay time was calculated as a cumulative value of each individual link's delay time. Hence, obviously, lesser delay time trips are shorter trips. The average number of links per trip is about 20 links under all three categories 10 trips, 20 trips and 30 trips. The model estimations were done by using the β −SRL model and the respective estimations for sequential time discount rate are shown in Table 4.16

Table 4.18 Estimation results of β for random sampling of 10, 20 and 30 trips for the trips having delay time less than 5 minutes

Sample	10 trips			20 trips			30 trips		
	β	t-value	ρ^2	β	t-value	ρ^2	β	t-value	ρ^2
1	0.199	-1.60	0.15	0.311	-3.03	0.25	0.239	-3.17	0.16
2	0.314	-2.17	0.27	0.365	-2.90	0.37	0.293	-3.35	0.23
3	0.226	-2.12	0.19	0.539	-2.89	0.17	0.221	-3.11	0.15
4	0.342	-1.58	0.25	0.519	-3.04	0.21	0.278	-3.46	0.22
5	0.332	-1.84	0.22	0.274	-2.85	0.33	0.416	-3.14	0.43
6	0.281	-1.84	0.20	0.268	-2.60	0.40	0.336	-3.34	0.25
7	0.278	-1.78	0.19	0.316	-2.33	0.36	0.385	-2.87	0.31
8	0.049	-0.91	0.11	0.403	-2.48	0.26	0.309	-3.45	0.22
9	0.241	-2.07	0.22	0.522	-3.01	0.20	0.322	-3.41	0.28
10	0.355	-1.67	0.27	0.502	-2.87	0.20	0.366	-3.32	0.33

As per the results tabulated in Table 4.18, the t statistics are significant in all the samples under 20 trips and 30 trips categories while 10 trips category contains some insignificant samples. Likelihood ratio index also higher than 0.15 in most of the samples. In order to see the variability of sequential time discount rate graphically, column charts were made by sorting the values in each category for the easiness of visual observation and shown in Figure 4.17

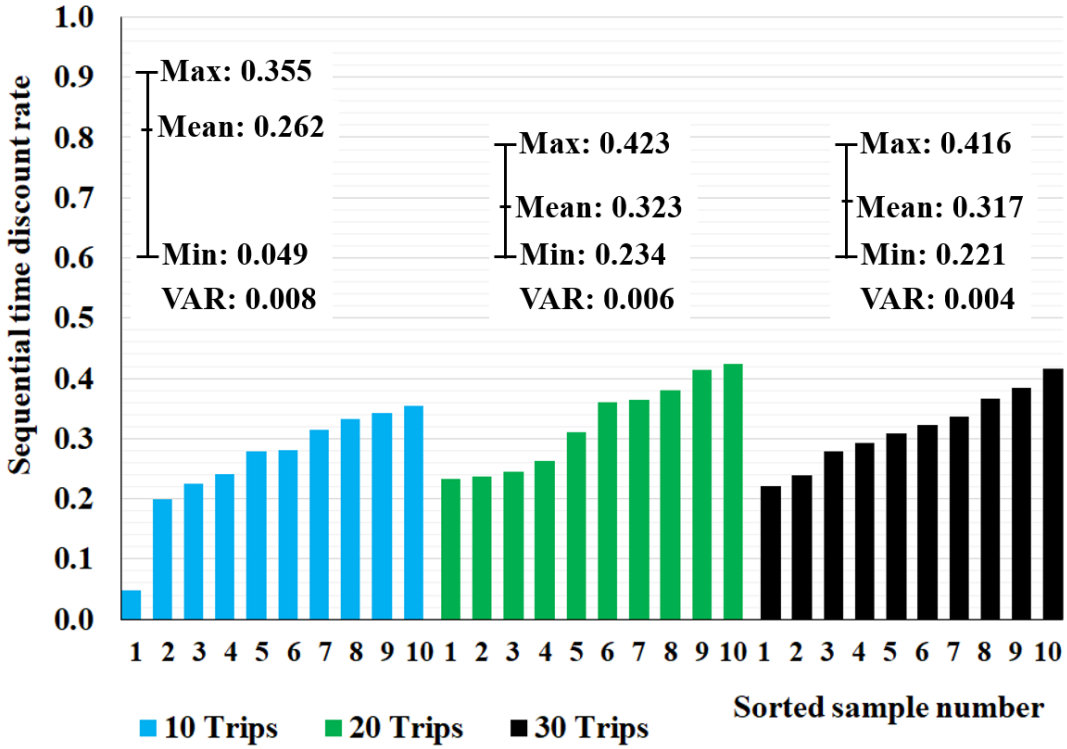

Figure 4.17 Variation of sequential time discount rate with random sampling for the trips having delay time less than 5 minutes

As visualized in the previous analysis, here also the difference between minimum and maximum estimations are comparatively lower in 20 trips and 30 trips samples. Variation also have lesser values when the number of trips in the sample are increased. Further the estimated values of sequential time discount rates under 20 trips and 30 trips samples have produced much similar results. In addition, spreads of the estimations were tested through the statistical parameters and the respective results are indicated in Table 4.19

Table 4.19 Statistical parameters of the samples with total trip delay time less than 5 minutes

Parameter	10 trips	20 trips	30 trips
Variance	0.008	0.006	0.004
Standard deviation	0.09	0.08	0.06
Relative standard deviation	0.35	0.23	0.20
Coefficient of variation (%)	35	23	20
Standard error of the mean	0.029	0.024	0.020
True value	0.262 ± 0.065	0.323 ± 0.053	0.317 ± 0.044

Statistical parameters in Table 4.19 and visual observations of Figure 4.17 indicate that 20 trips and 30 trips samples have produced much similar results. 10 trips samples also have produced some better results, except one sample which has produced a lower value

for sequential time discount rate. In addition, the asymptotic t test also carried out for testing the similarity of the estimation results. The resulted t values are insignificant for all categories and all samples which indicates that there are no significant differences between the estimated sequential time discount rates in each category. Precisely, the model estimations are stable during the period. The resulted t values are included in the appendix D.

4.3.4.2 Stability analysis for trips with delay time between five to ten minutes

In this section, stability of the sequential time discount rate was tested by considering little lengthier trips than in the previous section. Precisely, the average length of a trip under the previous section was about 1 km while here it is about 1.5 km, considering the trips in 30 trips samples. The estimated results of sequential time discount rate are shown in Table 4.20

Table 4.20 Estimation results of β for random sampling of 10, 20 and 30 trips for the trips having delay time between 5 to 10 minutes

Sample	10 trips			20 trips			30 trips		
	β	t-value	ρ^2	β	t-value	ρ^2	β	t-value	ρ^2
1	0.118	-1.78	0.13	0.224	-3.53	0.17	0.178	-3.70	0.16
2	0.110	-1.52	0.10	0.090	-2.09	0.11	0.054	-1.97	0.11
3	0.010	-0.31	0.14	0.107	-2.63	0.15	0.070	-2.39	0.13
4	0.068	-1.47	0.15	0.269	-3.48	0.19	0.212	-3.92	0.14
5	0.465	-2.25	0.47	0.256	-3.34	0.19	0.038	-1.59	0.12
6	0.081	-1.80	0.19	0.070	-1.99	0.12	0.060	-1.99	0.09
7	0.251	-2.51	0.17	0.328	-3.51	0.23	0.159	-3.47	0.14
8	0.185	-2.10	0.17	0.025	-0.84	0.07	0.046	-1.79	0.12
9	0.396	-2.29	0.30	0.047	-1.50	0.11	0.032	-1.40	0.12
10	0.095	-1.83	0.11	0.193	-3.25	0.17	0.034	-1.45	0.13

According to the results shown in Table 4.20, t statistics are significant in most of the samples under all three categories. Then the estimations are plotted in bar charts and are shown in Figure 4.18

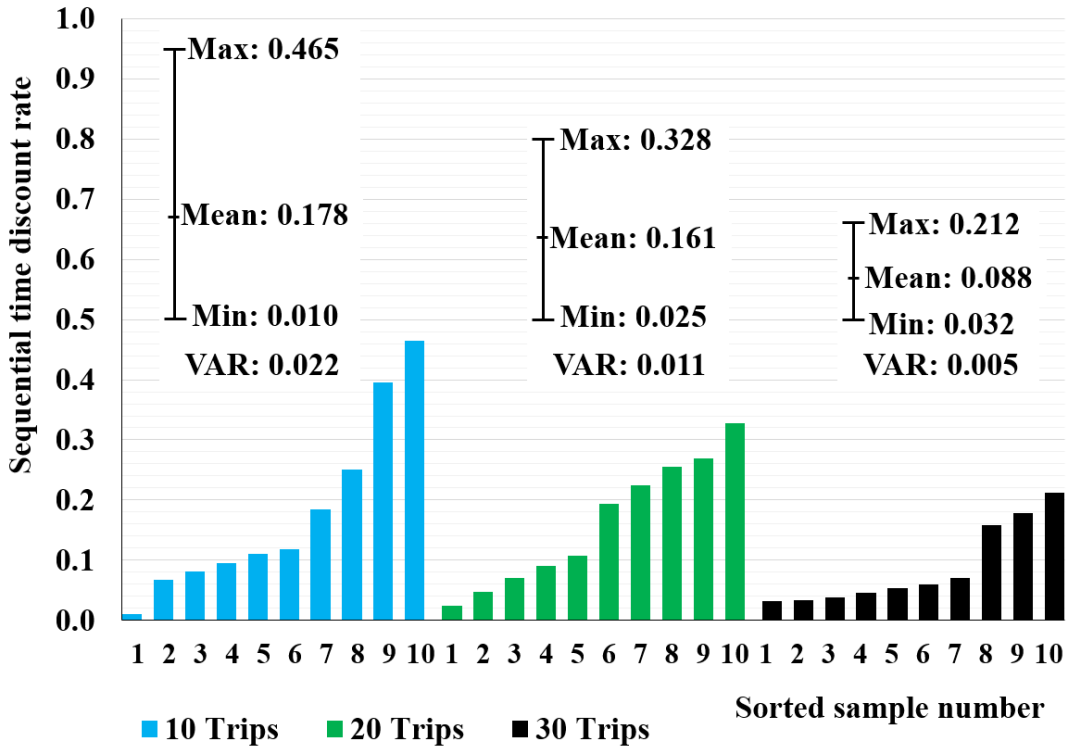

Figure 4.18 Variation of sequential time discount rate with random sampling for the trips having delay between 5 to 10 minutes

According to the Figure 4.18, 10 trips samples have spread through a larger range comparatively. Then it has reduced when it increases the number of trips in the sample. Variation is also lower in the 30 trips samples. Further, the aforementioned statistical parameters were also calculated to see the spread of estimations in detail. The results are indicated in Table 4.21

Table 4.21 Statistical parameters of the samples with total trip delay time between 5 to 10 minutes

Parameter	10 trips	20 trips	30 trips
Variance	0.022	0.011	0.005
Standard deviation	0.15	0.11	0.07
Relative standard deviation	0.84	0.66	0.76
Coefficient of variation (%)	84	66	76
Standard error of the mean	0.047	0.034	0.021
True value	0.178 ± 0.107	0.161 ± 0.106	0.088 ± 0.048

As visualized in Figure 4.18 and based on the statistical parameters tabulated in Table 4.21, 30 trips per sample category has produced the more stable results. In addition, its spread also less compares to the other two categories. Further, as in the early analysis, the asymptotic t test also carried out to see the similarity between the estimations. All the

t statistics across all three sampling categories are insignificant. Hence, the model estimations are stable during the considered period. The resulted t values are shown in appendix E.

4.3.4.3 Stability analysis for trips with delay time over ten minutes

Taxi trips having cumulative delay time of the links is greater than 10 minutes were considered in below analysis. Correspondingly, longer trips, averagely 3 km were considered for the estimation of sequential time discount rate. Sampling were performed in similar way to the previous cases and estimated the parameters. The respective results for 10 trips, 20 trips and 30 trips samples are tabulated in Table 4.22

Table 4.22 Estimation results of β for random sampling of 10, 20 and 30 trips for the trips having delay time over 10 minutes

Sample	10 trips			20 trips			30 trips		
	β	t-value	ρ^2	β	t-value	ρ^2	β	t-value	ρ^2
1	0.068	-1.80	0.05	0.405	-3.91	0.31	0.262	-5.54	0.16
2	0.478	-2.03	0.43	0.204	-4.46	0.12	0.326	-5.46	0.22
3	0.421	-3.10	0.41	0.137	-3.81	0.11	0.229	-5.21	0.13
4	0.381	-3.31	0.29	0.272	-4.75	0.16	0.238	-5.33	0.14
5	0.367	-3.48	0.33	0.212	-4.51	0.14	0.275	-5.44	0.17
6	0.024	-0.93	0.06	0.462	-3.37	0.41	0.200	-5.16	0.11
7	0.494	-2.17	0.52	0.472	-3.26	0.45	0.288	-5.41	0.18
8	0.359	-2.46	0.20	0.100	-3.03	0.08	0.259	-5.65	0.15
9	0.478	-2.16	0.44	0.315	-4.24	0.23	0.275	-5.67	0.17
10	0.386	-3.10	0.28	0.484	-3.38	0.49	0.370	-5.18	0.28

According to the tabulated results in Table 4.22, all the t statistics under the categories of 20 trips and 30 trips samples are significant. Under the 10 trips samples, t statistics are significant in nine out of ten samples. Then the resulted estimations are plotted in bar charts and illustrated in Figure 4.19. For sake of easy observation, the random samples are sorted in the bar charts. Hence the sample number shown in Table 4.22 is not the same appeared in the horizontal axis of Figure 4.19

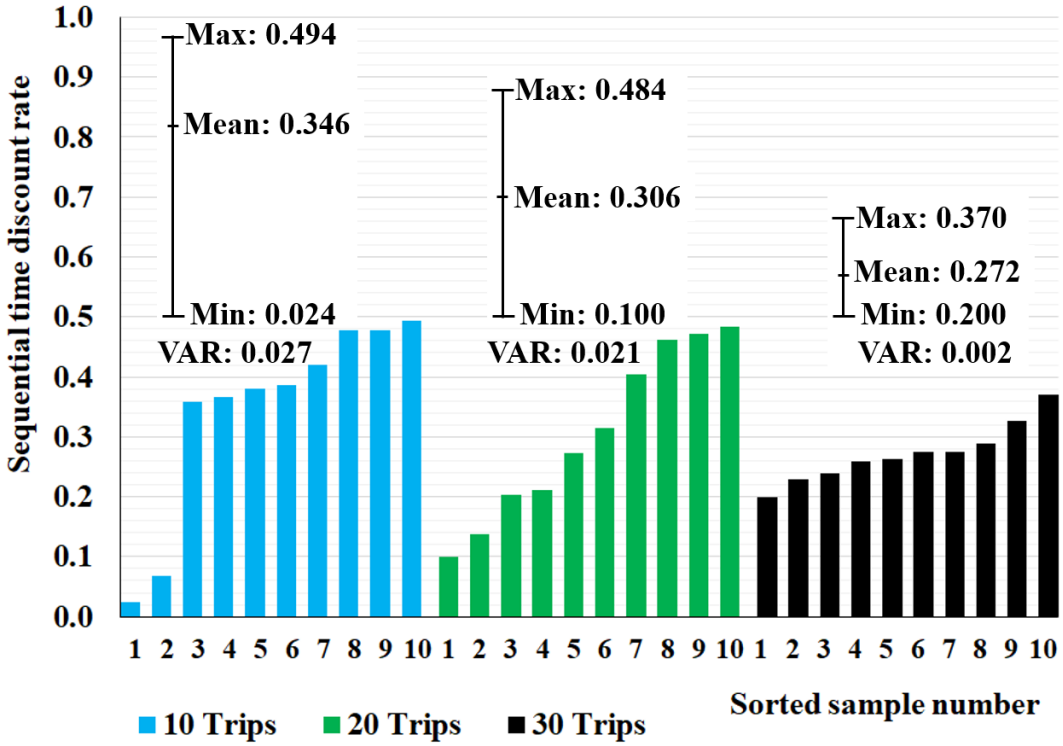

Figure 4.19 Variation of sequential time discount rate with random sampling for the trips having delay over 10 minutes

As shown in Figure 4.19, 10 trips samples have produced some higher results as well as lower results too. Also their difference is comparatively high. Meanwhile 30 trips have produced less fluctuated stable results. Further, the statistical parameters were also calculated to see the spread of estimations in detail. The results are indicated in Table 4.23

Table 4.23 Statistical parameters of the samples with total trip delay time over 10 minutes

Parameter	10 trips	20 trips	30 trips
Variance	0.027	0.021	0.002
Standard deviation	0.17	0.14	0.05
Relative standard deviation	0.48	0.47	0.18
Coefficient of variation (%)	48	47	18
Standard error of the mean	0.052	0.045	0.015
True value	0.346 ± 0.118	0.306 ± 0.102	0.272 ± 0.035

In comparison with the results tabulated in Table 4.23 and the visual observations on Figure 4.19, 30 trips per sample category has produced the better results. Its variance is low as well the spread of the estimations. These trips are longer trips in comparison with previous two analyses. Averagely a trip distance was about 3 km consisting about 60 links per trip. Since the estimated results of sequential time discount rate has a strong

relationship with trip distance, results in this section hints the necessity of network normalization for further comparisons. Further, as in the early analysis, the asymptotic t test also carried out to see the similarity between the estimations. All the t statistics across all three sampling categories are insignificant. Hence, the model estimations are stable during the considered period. The resulted t values are shown in appendix F.

4.3.5 Stability analysis in different networks

Stability analysis of the sequential time discount rate was tested under different networks under this section. Toyosu area where some of the 2020 Tokyo Olympic games will be held was selected as one area. Then another area outside of the ring 8 road was considered as the suburbs area. The area closer to the cities Akihabara and Ryogoku was selected as an area in the Tokyo city center. The selected areas are shown in Figure 4.20

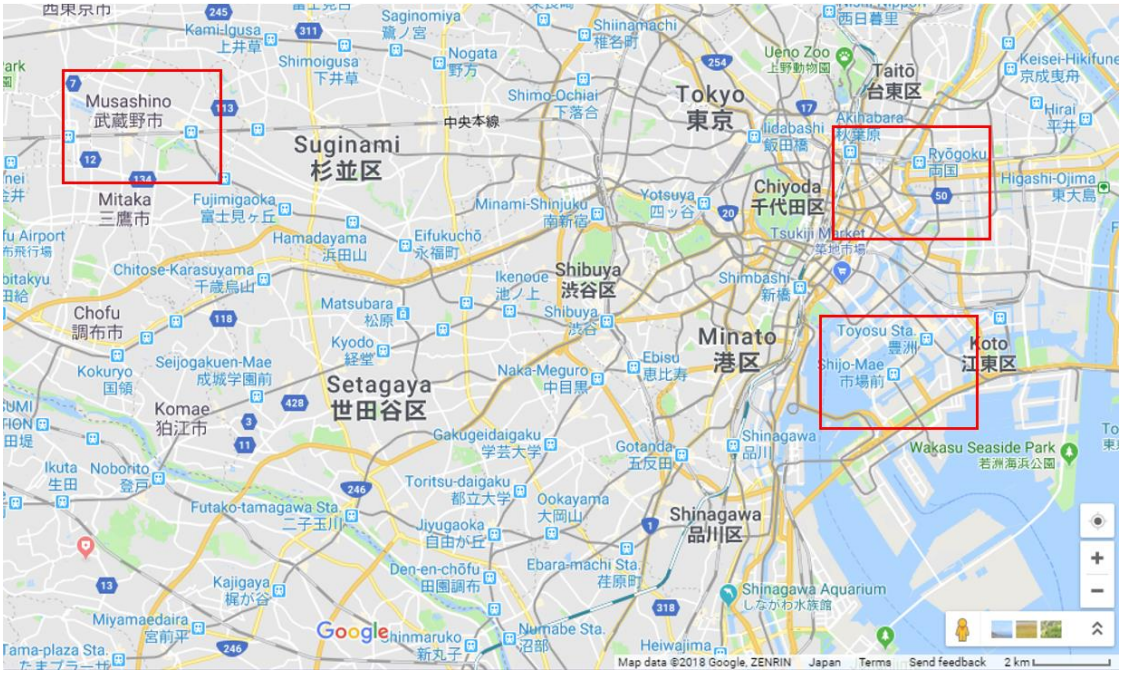

Figure 4.20 Different areas considered for the analysis

4.3.5.1 Stability analysis based on the taxi trips in Toyosu area

As illustrated in chapter 3, sequential time discount rate has great influence in network assignment. On the other hand, knowing sequential discount rate would be benefited to calculate accurate flows on links under congestions. Hence, with the upcoming 2020 Olympics, many foreigners will attract to the Toyosu area. Since, Japan is an earthquake prone country, knowing sequential time discount rate in the area would be an additional advantage. Considered area contained 4312 links and 2734 nodes. Similar sampling technique was applied as 10 trips, 20 trips and 30 trips per sample and sequential time discount rate was estimated by using β −SRL model. The respective results are tabulated in Table 4.24

Table 4.24 Estimation results of β for random sampling of 10, 20 and 30 trips at the Toyosu area

Sample	10 trips			20 trips			30 trips		
	β	t-value	ρ^2	β	t-value	ρ^2	β	t-value	ρ^2
1	0.265	-3.05	0.26	0.245	-3.74	0.26	0.268	-4.64	0.29
2	0.132	-2.16	0.22	0.289	-4.09	0.30	0.359	-3.96	0.37
3	0.475	-2.06	0.52	0.311	-4.05	0.31	0.287	-4.62	0.28
4	0.457	-2.02	0.48	0.265	-4.52	0.29	0.316	-4.50	0.32
5	0.318	-2.54	0.27	0.233	-4.36	0.25	0.360	-4.41	0.37
6	0.411	-2.18	0.41	0.220	-4.67	0.29	0.292	-4.91	0.29
7	0.582	-1.06	0.73	0.245	-4.55	0.27	0.355	-4.17	0.36
8	0.548	-1.18	0.61	0.266	-4.28	0.26	0.275	-5.34	0.32
9	0.296	-3.08	0.28	0.254	-4.23	0.32	0.371	-4.03	0.36
10	0.301	-2.78	0.31	0.291	-4.19	0.29	0.330	-4.82	0.33

Estimated results tabulated in Table 4.24 evidenced that the t statistics for all the samples under 10 trips and 20 trips samples are significant. In addition, many of them are significant under 10 trips samples too. Likelihood ratio index also shows higher values for all samples. Then, for the visual observation of the spread of the estimated results, they were plotted in bar charts and shown in Figure 4.21. For the easiness of the visual observation, the random samples are sorted and plotted. Hence, the sample numbers appeared in the Table 4.24 are not exactly same to the sorted sample numbers in the Figure 4.21

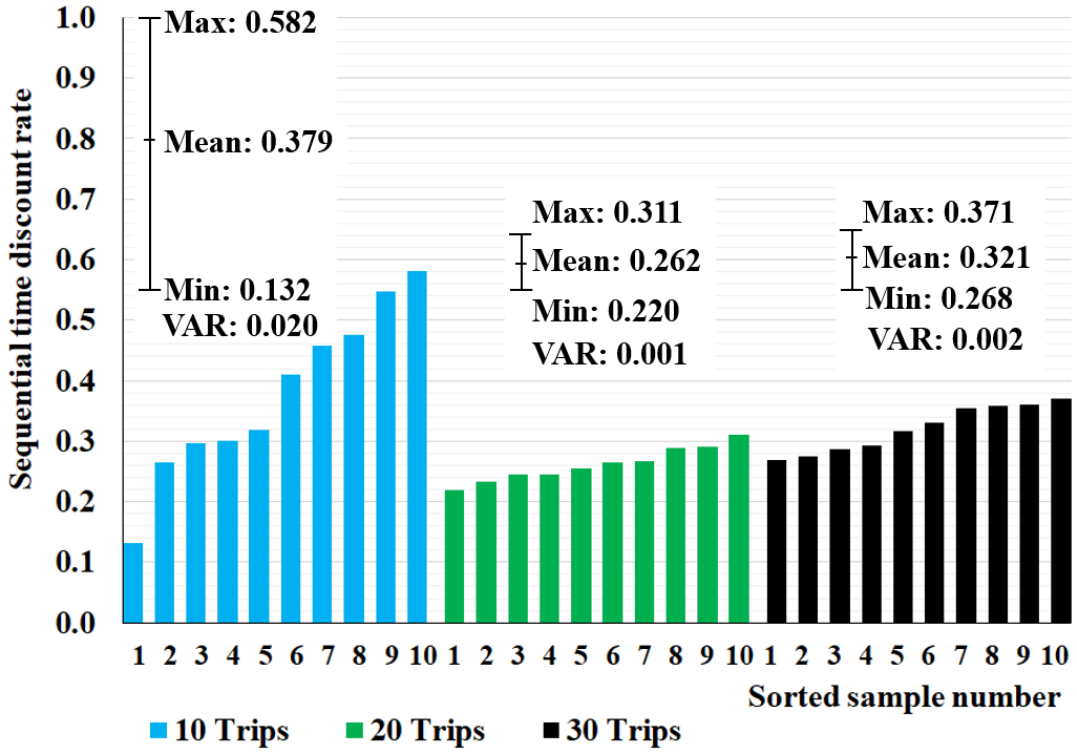

Figure 4.21 Variation of sequential time discount rate with random sampling for the trips at Toyosu area

According to the Figure 4.21 illustrates, the estimation results under the 10 trips samples have varied over larger range. Meanwhile, 20 trips and 30 trips samples have produced better and stable estimations with lesser spread through the samples for sequential time discount rate. In addition, their variation also low. Further, the statistical parameters, similarly as used in the previous sections were also calculated to see the spread of estimations in detail. The results are indicated in Table 4.25

Table 4.25 Statistical parameters of the estimated samples at Toyosu area

Parameter	10 trips	20 trips	30 trips
Variance	0.020	0.001	0.002
Standard deviation	0.14	0.03	0.04
Relative standard deviation	0.37	0.11	0.12
Coefficient of variation (%)	37	11	12
Standard error of the mean	0.044	0.009	0.012
True value	0.379 ± 0.100	0.262 ± 0.020	0.321 ± 0.028

According to the visual observations of Figure 4.21 and based on the statistical parameters tabulated in Table 4.25, 20 trips and 30 trips per sample categories have produced the more stable results in comparison with 10 trips samples. In addition, their spread also less compares to the 10 trips sample results. Further, as in the early analyses,

the asymptotic t test also carried out to see the similarity between the estimations. All the t statistics across all three sampling categories are insignificant. Hence, the model estimations are stable during the considered period. The resulted t values are shown in appendix G.

4.3.5.2 Stability analysis based on the taxi trips in Musashino area

Musashino area is considered as a suburb area since it is located out of the ring 8 road. It is hypothesized that the network behavior will be different from the Toyosu area as it is suburbs. The selected area for the parameter estimation consisted 3766 links and 3268 nodes. Number of links are little less than compare to the Toyosu area while number of nodes are little high. Parameter estimations were conducted based on the same sampling technique as 10 trips, 20 trips and 30 trips samples and estimated through the $\beta -$ SRL model. The respective results are tabulated in Table 4.26

Table 4.26 Estimation results of β for random sampling of 10, 20 and 30 trips at the Musashino area

Sample	10 trips			20 trips			30 trips		
	β	t-value	ρ^2	β	t-value	ρ^2	β	t-value	ρ^2
1	0.314	-1.34	0.05	0.219	-2.01	0.05	0.195	-2.35	0.04
2	0.150	-1.41	0.04	0.140	-1.69	0.04	0.045	-0.94	0.01
3	0.125	-1.06	0.02	0.193	-1.83	0.03	0.175	-2.21	0.03
4	0.131	-1.12	0.01	0.109	-1.48	0.01	0.081	-1.52	0.04
5	0.121	-1.06	0.01	0.105	-1.37	0.02	0.184	-2.35	0.04
6	0.180	-1.42	0.02	0.150	-1.01	0.05	0.109	-1.76	0.04
7	0.053	-0.66	0.01	0.169	-1.78	0.03	0.070	-1.31	0.01
8	0.455	-0.93	0.14	0.208	-1.75	0.03	0.177	-2.15	0.04
9	0.062	-0.81	0.05	0.070	-1.02	0.03	0.050	-1.13	0.04
10	0.065	-0.70	0.01	0.064	-1.12	0.03	0.103	-1.62	0.02

According to the estimation results tabulated in Table 4.26, the t statistics are all insignificant under the 10 trips sample while only five and six samples have significant t statistics under the 20 trips and 30 trips categories. This could be happening due to some network features. Since estimated value of the sequential time discount rate has a strong relationship with the link length, average link length under each sample were compared with the Toyosu area based on the 10 trips sample. The results are plotted in a bar chart and shown in Figure 4.22

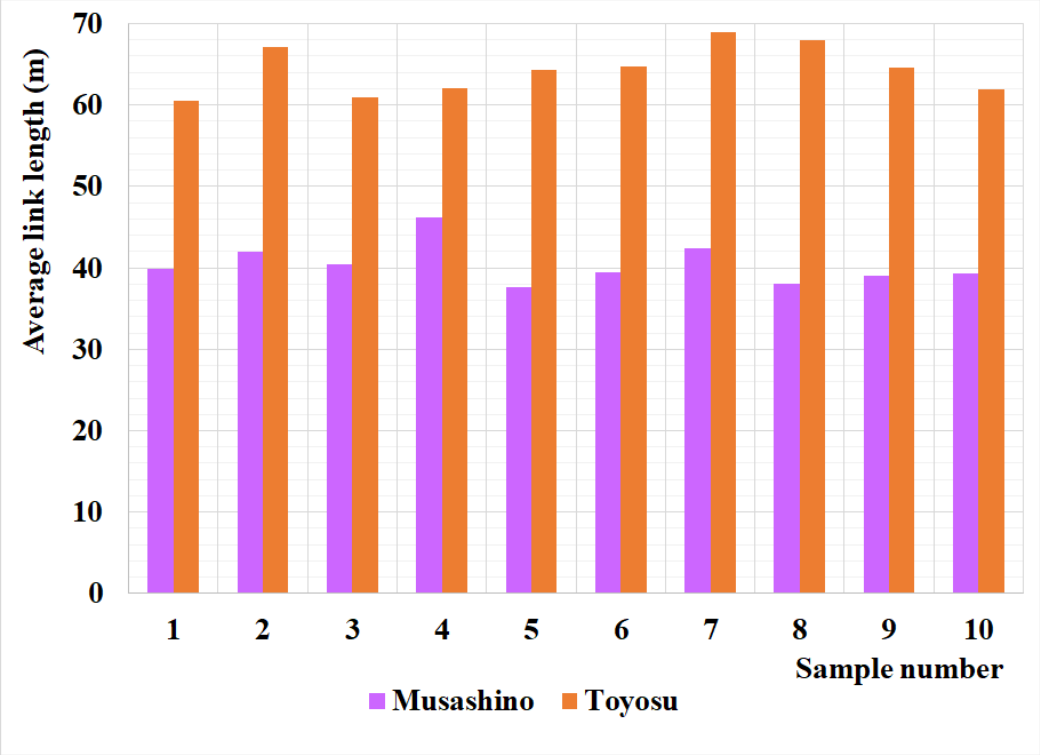

Figure 4.22 Comparison of average link size between Musashino and Toyosu areas

As the Figure 4.22 shows, average link size is considerably low in the Musashino area. Precisely, average link size of Musashino area is about 40 m while it is about 65 m in Toyosu area. Hence, this finding highlights the necessity of the network normalization. (Network normalization will be discussed in detail in Chapter 5). Thereafter, for the purpose of pattern comparison, the estimated results are plotted and shown in Figure 4.23. In order to compare, the random samples are sorted and plotted. Hence, the sample numbers appeared in the Table 4.26 are not exactly same to the sorted sample numbers in the Figure 4.23

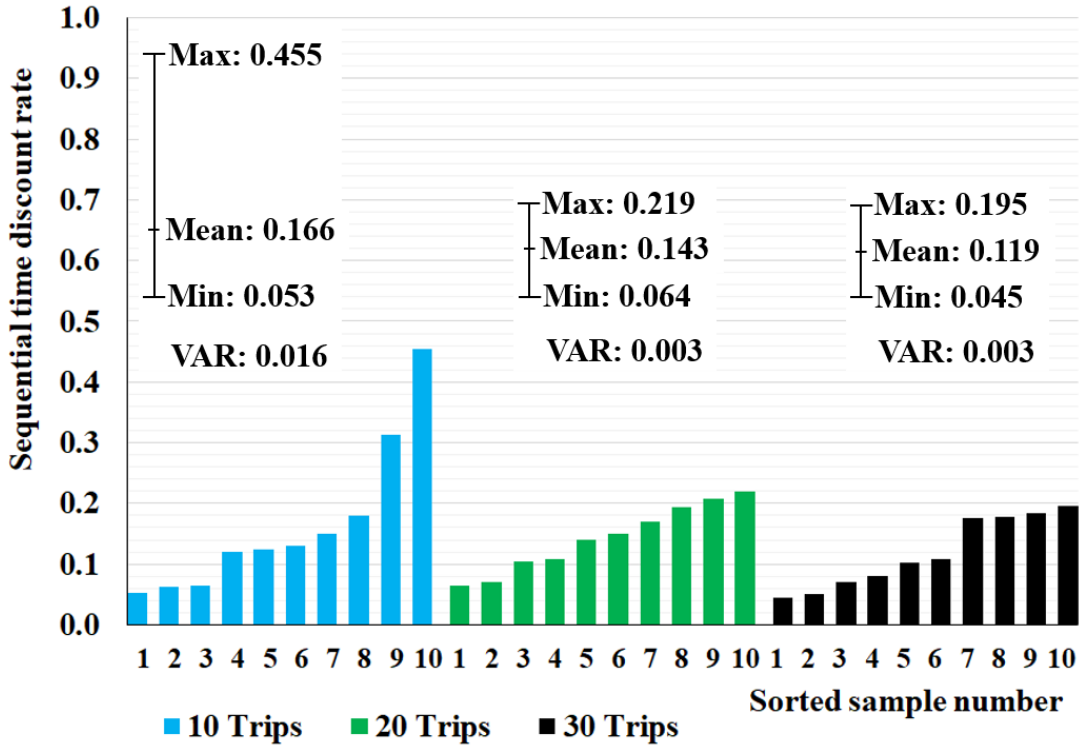

Figure 4.23 Variation of sequential time discount rate with random sampling for the trips at Musashino area

As visualized in Figure 4.23, same pattern which observed in many of the above analyses continues here too. The 20 trips and 30 trips samples have produced similar results and their variances are also comparatively low. Meanwhile, estimated sequential time discount rates under the 10 trips samples vary over larger range. Additionally, the statistical parameters, that considered in the previous sections were also calculated to see the spread of estimations in detail. The results are indicated in Table 4.27

Table 4.27 Statistical parameters of the estimated samples at Musashino area

Parameter	10 trips	20 trips	30 trips
Variance	0.016	0.003	0.003
Standard deviation	0.13	0.06	0.06
Relative standard deviation	0.77	0.39	0.49
Coefficient of variation (%)	77	39	49
Standard error of the mean	0.040	0.017	0.019
True value	0.166 ± 0.091	0.143 ± 0.039	0.119 ± 0.042

As per the visual observations of Figure 4.23 and based on the statistical parameters tabulated in Table 4.27, 20 trips and 30 trips per sample categories have produced the more stable results in comparison with 10 trips samples. In addition, their spread also less compares to the 10 trips sample results. Further, as in the early analyses, the asymptotic

t test also carried out to see the similarity between the estimations. All the t statistics across all three sampling categories are insignificant. Hence, the model estimations are stable during the considered period. The resulted t values are shown in appendix H.

4.3.5.3 Stability analysis based on the taxi trips in Akihabara area

The area covering cities like Akihabara and Ryogoku was considered as an area within Tokyo city center. The area is congested even under the normal circumstances as many people doing shopping and other recreational activities there. Hence, knowing sequential time discount rate on those areas are important as well as testing the parameter stability. The considered area is consisted with 3827 links and 2456 nodes. The parameter estimations were similar to the previous sections and the resulted estimations are tabulated in Table 4.28

Table 4.28 Estimation results of β for random sampling of 10, 20 and 30 trips at the Akihabara area

Sample	10 trips			20 trips			30 trips		
	β	t-value	ρ^2	β	t-value	ρ^2	β	t-value	ρ^2
1	0.420	-1.94	0.32	0.140	-2.79	0.07	0.365	-3.47	0.24
2	0.376	-1.96	0.29	0.275	-3.07	0.13	0.352	-3.79	0.23
3	0.231	-2.05	0.12	0.361	-2.99	0.24	0.242	-3.98	0.13
4	0.507	-1.17	0.46	0.378	-3.05	0.25	0.215	-3.98	0.11
5	0.147	-2.03	0.10	0.224	-3.13	0.12	0.207	-3.86	0.10
6	0.381	-2.09	0.29	0.144	-2.44	0.09	0.339	-3.64	0.22
7	0.286	-2.27	0.20	0.528	-1.80	0.52	0.351	-3.85	0.23
8	0.132	-1.53	0.06	0.317	-3.19	0.18	0.165	-3.61	0.08
9	0.021	-0.64	0.05	0.203	-3.27	0.09	0.238	-3.94	0.12
10	0.343	-2.47	0.19	0.070	-1.96	0.07	0.178	-3.64	0.09

According to the results presented in Table 4.28, all the t statistics under the 20 trips and 30 trips samples are well significant. Meanwhile, most of the t statistics of 10 trips samples are also significant. The likelihood ratio indices also high in many samples. Then, for the visual observation of the spread of the estimated results, they were plotted in bar charts and presented in Figure 4.24. For the easiness of the comparison, the random samples are sorted and plotted. Hence, the sample numbers appeared in the Table 4.28 are not exactly same to the sorted sample numbers in the Figure 4.24

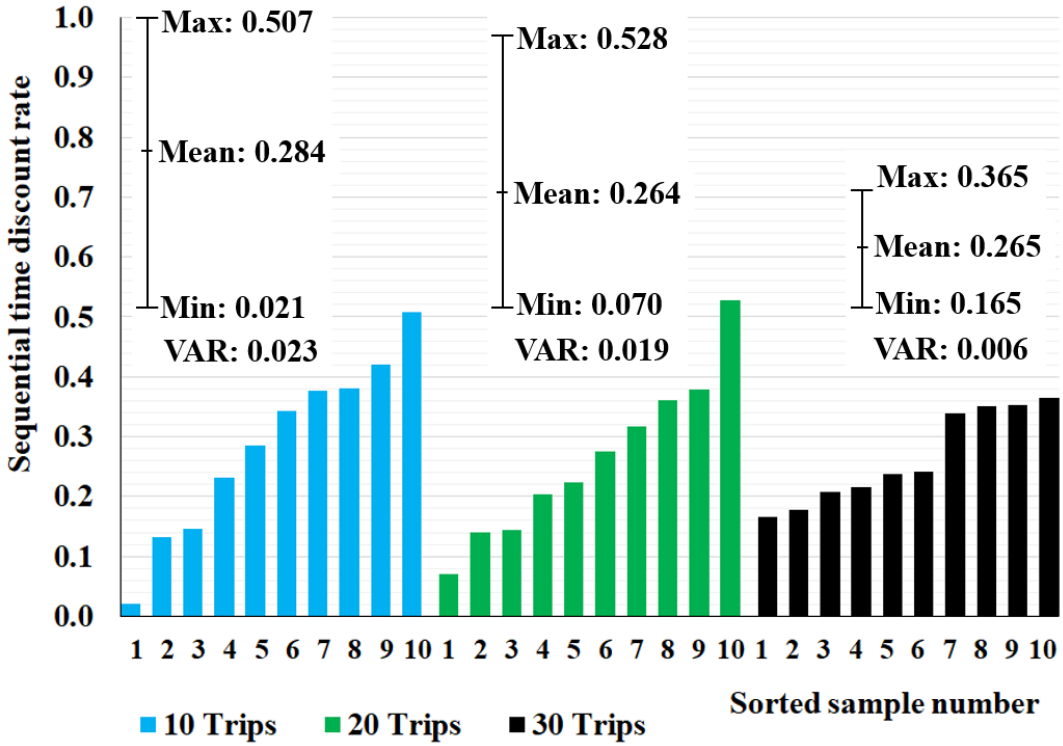

Figure 4.24 Variation of sequential time discount rate with random sampling for the trips at Akihabara area

As Figure 4.24 shows, 30 trips samples have produced better and stable results for the sequential time discount rate. Further, it visualized that 10 trips and 20 trips sample results are much closer. But individual value comparisons indicated that 6 of the 10 samples of 20 trips are much closer to the estimates of 30 trips. In addition, the statistical parameters which considered in all other sections too, used to compare the spread of the results. The results are indicated in Table 4.25

Table 4.29 Statistical parameters of the estimated samples at Akihabara area

Parameter	10 trips	20 trips	30 trips
Variance	0.023	0.019	0.006
Standard deviation	0.15	0.14	0.08
Relative standard deviation	0.53	0.52	0.30
Coefficient of variation (%)	53	52	30
Standard error of the mean	0.048	0.043	0.025
True value	0.284 ± 0.107	0.264 ± 0.098	0.265 ± 0.056

As seen in the Figure 4.24 and according to the presented results in Table 4.29, 30 trips samples have produced better results. Further, as in the early analyses, the asymptotic t test also carried out to see the similarity between the estimations. All the t statistics across

all three sampling categories are insignificant. Hence, the model estimations are stable during the considered period. The resulted t values are shown in appendix I.

4.4 Conclusions and discussions

Parameter stability is essential for drawing conclusions or making inference on estimation results. Hence, chapter 4 was designed focusing on testing the stability of the sequential time discount rate under different network conditions. As a usual practice, parameter estimations are done hourly basis. Therefore, network changes within an hour may not be captured. For an example network, if the estimations are done from 12:00 to 13:00 and 13:00 to 14:00, the variation from 12:30 to 13:00 may not be correctly presented. Hence, it is important to test the model ability to estimate sequential time discount rate under moving time. Accordingly, the analysis with moving time is performed by slicing one hour periods, shifting with 10 minute intervals between the consecutive samples for a continuous period of 03 hours. The results showed, that the β −SRL model is capable of estimating stable and reliable values for sequential time discount rate for the entire considered period of time.

The time consumed for parameter estimation in β −SRL model depends on the network size used at the time of estimation. The size of the network depends on the spread of the trips, which are selected for estimation. Correspondingly, less number of trips will provide a small network and hence, the estimation time will reduce. Therefore, finding the adequate minimum number of trips for stable estimation is always important for time saving. Accordingly, the study was carried out under 03 categories as 10 trips, 20 trips and 30 trips. Randomly sampled 10 trips were included in each of the sample and 10 samples under each category were estimated through β – SRL model. The results were checked through t statistics, log likelihood ratios at the beginning before plotting them for the visual observation. Visual observations together with statistical parameters such as variance, standard deviation, true value and so forth illustrated that the 20 trips and 30 trips samples produced more stable results comparatively to the 10 trips samples. Besides, the asymptotic t test, which is usually carry out for checking the equality of individual coefficients between two market segments, was performed for examining the parameter equality within each sample. The resulted t values were insignificant for all the considered samples and this indicated that there are no significant differences between the estimated sequential time discount rates in each category. Precisely, the model estimations are stable.

Having understood the results under the above sampling rate, 09 travelling conditions were selected based on 03 major categories for testing the stability of sequential time discount rate. Accordingly, different time zones as morning peak, day peak and evening peak, different important networks (areas) as Toyosu area (where the 2020 Olympic games will hold), Akihabara area (covering Tokyo city center as an area inside of the ring 8 road) and Musashino area (as a suburb area outside of the ring 8 road), different size of trips considering total trip delay time less than 5 minutes, between 5 to 10 minutes and

over 10 minutes were used for estimating and testing the stability of sequential time discount rate. Overall results showed that β – SRL model estimate better results under all 03 categories while 20 trips and 30 trips samples always provide stable and reliable results compare to the 10 trips samples. Further, the improvements of the results from 10 trips samples to 20 trips samples was larger in comparison with the improvements from the 20 trips samples to 30 trips samples.

5 Mathematical characteristics and performance analysis

5.1 Introduction

Mathematical formulation of the recursive logit model has briefly discussed in Fosgerau, Frejinger, & Karlstrom, 2013 and Zimmermann, Mai, & Frejinger, 2017 while the same on the β −Scaled recursive logit model has discussed in Oyama, Chikamatsu, Shoji, Hato, & Koga, 2016. But in the literature, it has not discussed the mathematical formulation in elementary stages of the matrices. Hence, in order to have a better understanding of the β −SRL model and the characteristics of the sequential time discount rate in different network settings, it is necessary to reach the element stage of the value function matrices. At the beginning of this chapter, unde the section 5.2, we discussed the elementary changes in value function in its solving stage.

Then the performance of the β − SRL model and characteristics of sequential time discount rate were discussed under different network settings as they were not discussed by the previous studies. As discussed in previous chapter, sequential time discount rate produced lower values when the network is having shorter distance links. Hence, identifying the model performance under normalized networks and different settings of link length are important. Normalized network was created by introducing additional links and nodes to the existing network in such a way that all the links in the network becomes links with a same link cost. Variations of the route choice probabilities under the different scenarios of sequential time discount rate and the changes in the mathematical formulations of deterministic utility and the value function are discussed in details by using a hypothetical network under real and normalized network conditions. Further, the variability of sequential time discount rate, log likelihood ratio index and model simulation speed were described by using a case study data in real world in comparison with real network and normalized network conditions.

Later part of the chapter is used to analyze model performances with different network settings. Scaled network was created by scaling the links length of the network and variability of the sequential time discount rate along with other usual entities were tested. The results satisfied the respective theoretical explanations. Further, the model was tested with the extended link length. Unlike in the scaled condition, in this case, link utility is changing in different percentages and the variability of model parameters were studied. At the end of the chapter, the influence of the number of links per path was analyzed by using three different categories. Randomly sampled samples were used for the analyses as trips having number of links less than 25 per trip, trips consisting number of links from 25 to 50 per trip and trips having number of links over 50 per trip are estimated and compared. The results indicated that trips having number of links over 50 per trip produces better and stable estimations. Further, the model performances also become more stable when the number of links per trip is increased.

5.2 Mathematical characteristics

Mathematical characteristics in the contest of solving value function of the $\beta-$SRL model is explained in this section. The model formulation is discussed in chapter 3 under the sections 3.1 and 3.2. As it has stated there, the value functions with respect to each link of the considered network can be determined by solving the system of non-liner equations with the sequential time discount rate. For the sake of smooth connectivity, restate the equation 3.11 and equation 3.12;

$$z_{a_j} = \begin{cases} \sum_{a_{j+1} \in A} M_{a_j a_{j+1}} \left(z_{a_{j+1}}\right)^{\beta}, & a_j \in A \\ 1, & a_j = d \end{cases} \tag{3.11}$$

This can be written in matrix notations,

$$\mathbf{z} = \mathbf{M}\mathbf{X}(\mathbf{z}) + \mathbf{b} \tag{3.12}$$

Matrix **z** represents the value functions while matrix **M** represents the components related to link utility. $\mathbf{X}(\mathbf{z})\left(\left|\tilde{A}\right| \times \left|\tilde{A}\right|\right)$ is the matrix with entries $X(z)_{a_j} = \left(z_{a_j}\right)^{\beta}$. **b** is a single column vector with number of rows equal to the number of links. The values of the elements are zero except for the destination, where it is equal to one.

Let's consider a hypothetical network in order to have a detail explanation about the aforementioned matrices.

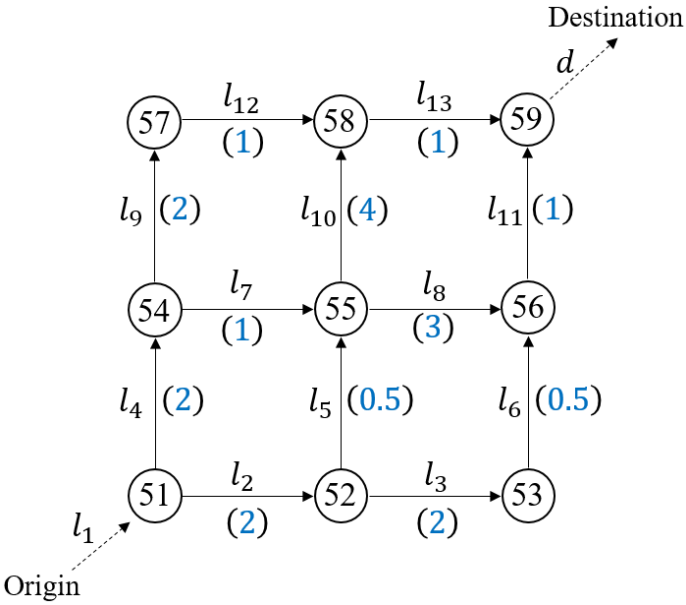

Figure 5.1 A hypothetical network

The hypothetical network shown in Figure 5.1 consists of 9 nodes numbered from 51 to 59. It also have 12 node to node connecting links and two dummy links representing the origin (l_1) and the destination (d). The cost for each link is shown within the parentheses. The all links are directed and connected. The network contains 6 different paths which

connect the origin and the destination. The paths and their total link costs are stated below;

a) $l_1 -> l_4 -> l_9 -> l_{12} -> l_{13} -> d$; $cost = 6.0$
b) $l_1 -> l_4 -> l_7 -> l_{10} -> l_{13} -> d$; $cost = 8.0$
c) $l_1 -> l_4 -> l_7 -> l_8 -> l_{11} -> d$; $cost = 7.0$
d) $l_1 -> l_2 -> l_5 -> l_{10} -> l_{13} -> d$; $cost = 7.5$
e) $l_1 -> l_2 -> l_5 -> l_8 -> l_{11} -> d$; $cost = 6.5$
f) $l_1 -> l_2 -> l_3 -> l_6 -> l_{11} -> d$; $cost = 5.5$

Accordingly, each path has a different total link cost while path f) having the minimum cost and path b) costs the maximum. Then the value functions were derived based on the matrices format illustrated in the equation 3.12 and shown Figure 5.2.

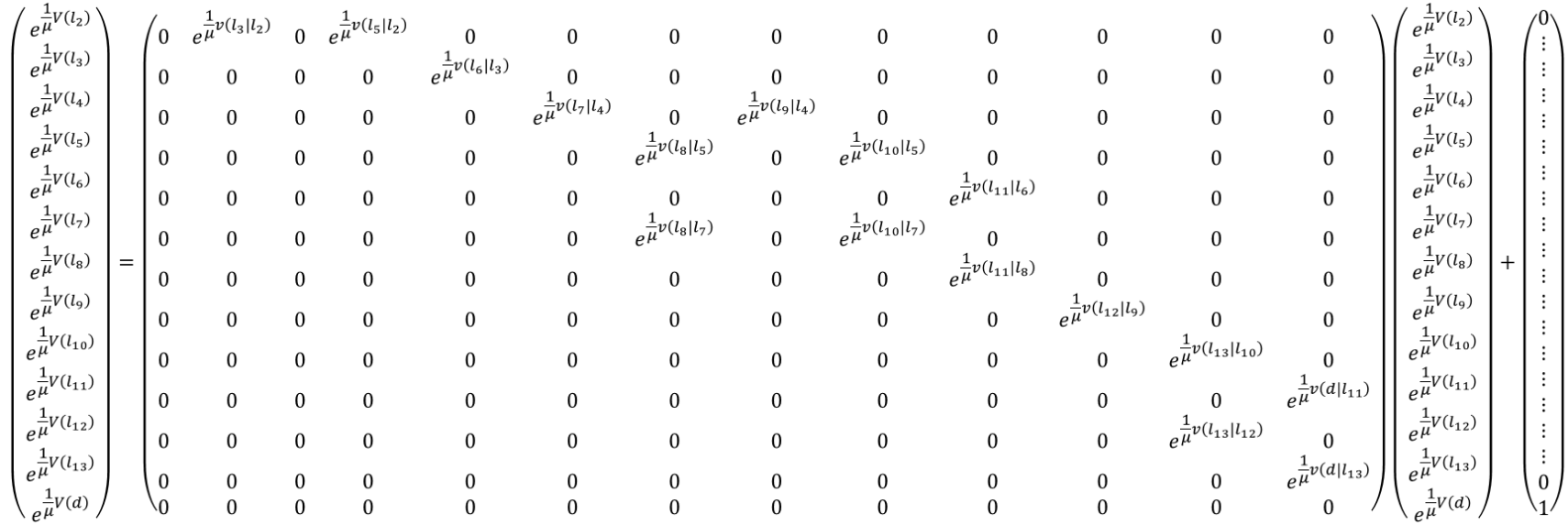

Figure 5.2 Initial step of the value function matrices

Value functions with respect to each link is represented in the matrix appears in the left side of the equal sign. Then followed by the matrix with the link utilities, matrix including value functions representing downstream utilities and matrix b respectively. β represents the sequential time discount rate. Denoting the link cost parameter by θ and considering the cost of each link, the elements of each matrices are substituted. The resulted matrices combination is shown in Figure 5.3.

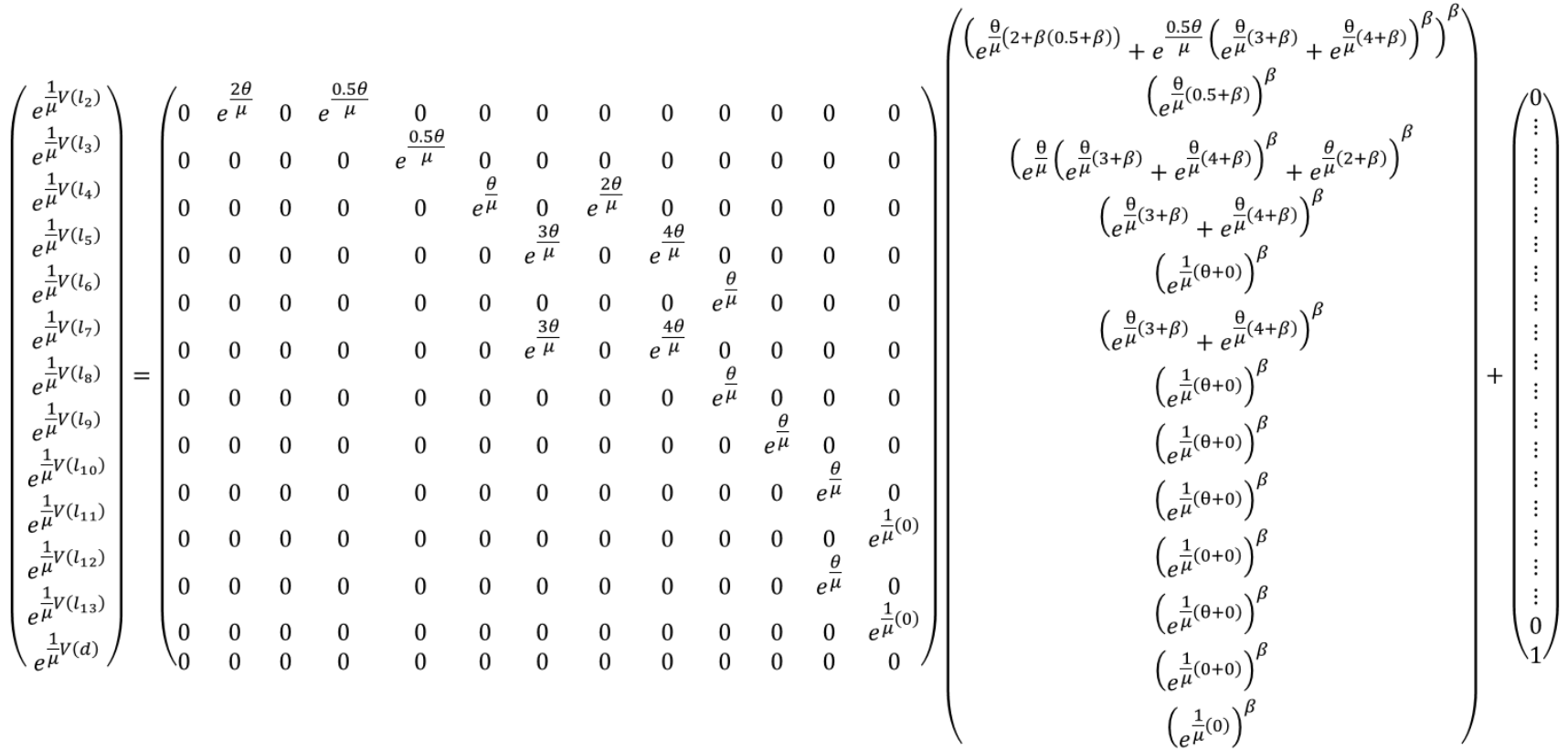

Figure 5.3 Second step of the value function matrices

In Figure 5.3, the value functions are expanded by introducing the parameters for the illustration purpose. Corresponding to the hypothetical network shown in Figure 5.1, the travelers who are coming through the links l_2, l_4, l_5 *and* l_7 have to make a decision on choosing a links from the two alternative links available at their sinking nodes while other links are straight moving connections.

Accordingly, the respective value functions have get complexed. Further, the links $l_2\ and\ l_4$ are connected to the links $l_5\ and\ l_7$ where they themselves again connecting to a node where they have alternative choices. Correspondingly, the value functions respective to the links $l_2\ and\ l_4$ have become more complicated. Therefore, in the real networks where many alternative links exist in number of nodes, the calculation process get more complexed and time consumed. Finally, as mentioned in the equation 3.8, the system has a solution if $(\boldsymbol{I}-\boldsymbol{M})$ is invertible and it is visualized in Figure 5.4.

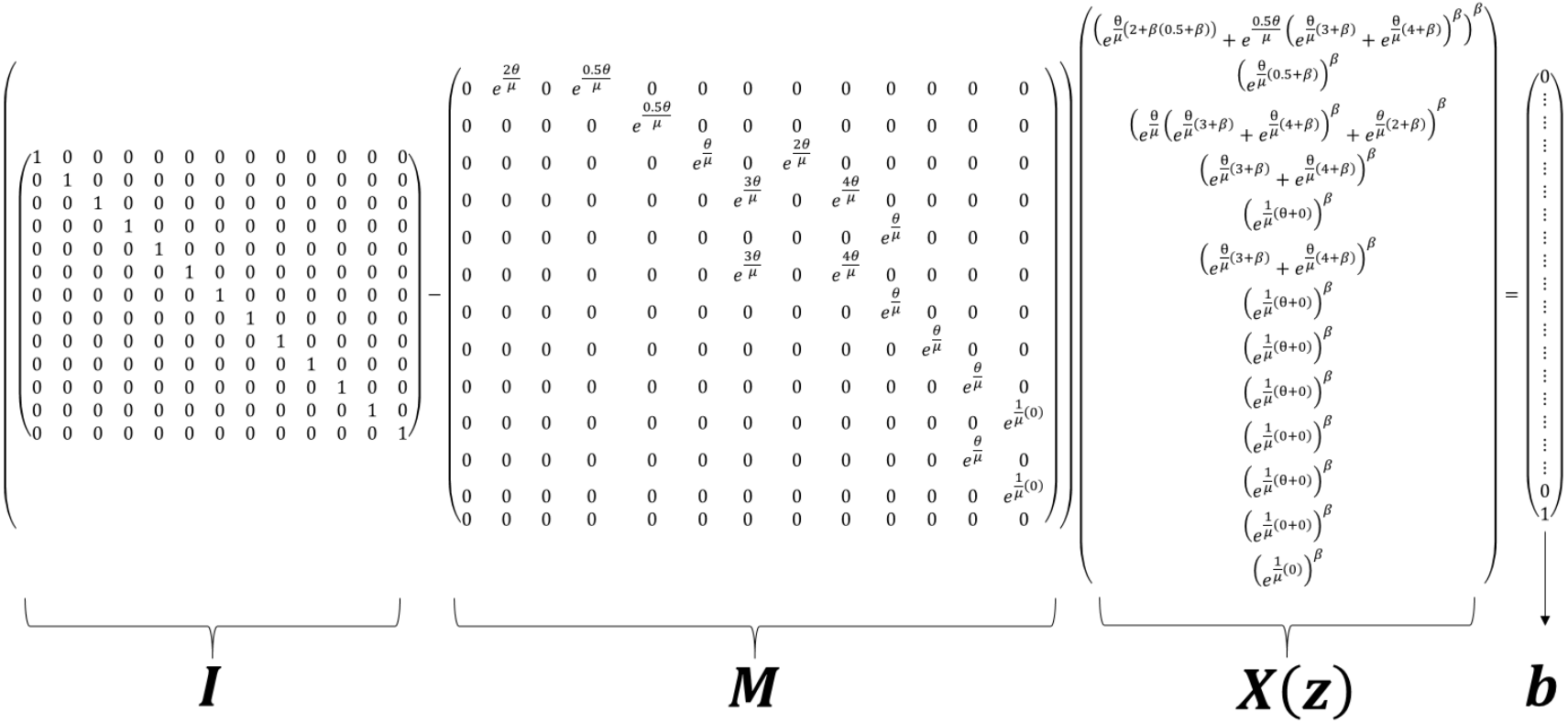

Figure 5.4 The system of matrices for solving value functions

5.3 Performance analysis

Understanding the performance of β −SRL model and characteristics of sequential time discount rate is very important in analyzing the existing results and generating future networks. Hence, this section provides a network performance analyses in a normalized network in comparison with a real network by including real and hypothetical networks, in scaled networks, in extended networks and based on the number of links in trips.

5.3.1 Performance based on normalized network

5.3.1.1 Based on a hypothetical network

Performance of the β −SRL model is analyzed and compared in between a real network and a normalized network. A hypothetical network consisting 9 nodes and 14 links (including dummy links for origin and destination) was used as the original network as a real case. The considered network is shown in Figure 5.5 below.

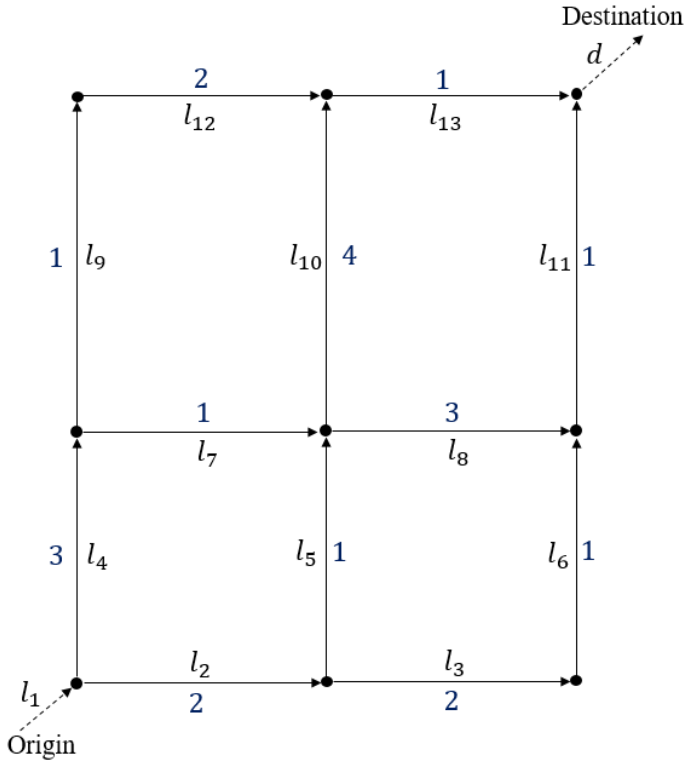

Figure 5.5 Network settings of the hypothetical real network

Since the link cost of the immediate links to the origin have a considerable influence on the link choice probability in recursive logit approach, they were set unequally. Six routes are available to reach the destination link from the defined origin link. The links costs were set in such a way one route is having minimum cost while another one having the maximum cost. The other four routes having total route cost in between and two of them are similar to each other separately. The route choice probabilities of the hypothetical network under the different scenarios of sequential time discount rate were calculated and tabulated with total route costs in Table 5.2 below.

Table 5.1 Route choice probabilities under different scenarios of sequential time discount rate for the hypothetical network

Route No.	Link connectivity	Route cost	$\beta = 0$	$\beta = 0.5$	$\beta = 1$
1	$l_1, l_4, l_9, l_{12}, l_{13}, d$	7	0.134	0.180	0.233
2	$l_1, l_4, l_7, l_{10}, l_{13}, d$	9	0.036	0.034	0.031
3	$l_1, l_4, l_7, l_8, l_{11}, d$	8	0.098	0.093	0.086
4	$l_1, l_2, l_5, l_{10}, l_{13}, d$	8	0.144	0.100	0.059
5	$l_1, l_2, l_5, l_8, l_{11}, d$	7	0.391	0.273	0.159
6	$l_1, l_2, l_3, l_6, l_{11}, d$	6	0.197	0.319	0.433

As Table 5.1 indicated, under the myopic decisions when the sequential time discount rate is equal to zero, travelers have unable to capture the lowest costed route. On the other hand, when the sequential time discount rate is given values, high probabilities are allocated the lowest costed roads. Thereafter, in order to visualize the flow in each link, the network flows were generated assuming 1000 travelers traveling from same origin to the same destination. The respective link flows under the real network condition is shown in Figure 5.6.

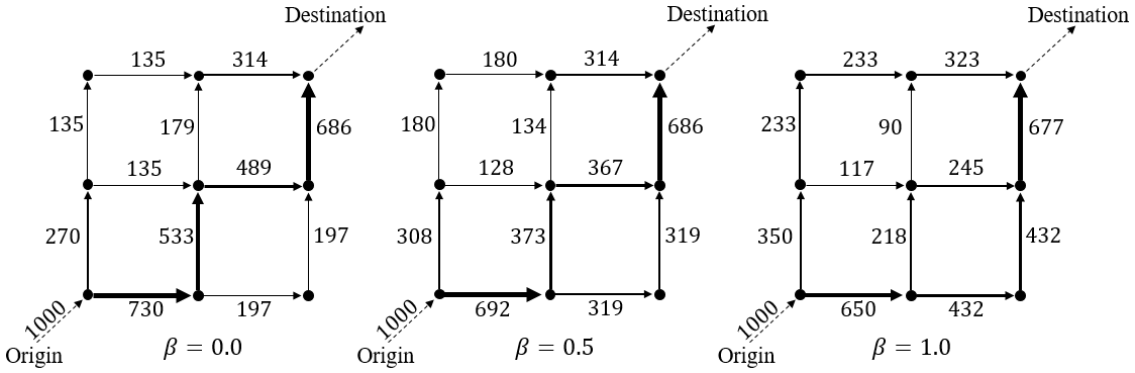

Figure 5.6 Assignment results for the hypothetical real network

As the Figure 5.6 illustrated, lesser flow can be seen in the lowest costed route under the condition of $\beta = 0$. Meanwhile, its opposite phenomena can be seen in link 8 and 10 where they are carrying relatively a larger flow even though they are having high link cost. Hence this reveals that myopic decisions can cause problems in congested networks.

When it moves to the situation where $\beta = 1$, given the knowledge on the downstream links, traffic on low cost links have improved. Precisely the three low cost paths, route 1, route 5 and route 6 are carrying the higher traffic with higher probabilities. Meanwhile, the route selection probability on high cost routes have significantly reduced (route 2, route 3 and route 4). Having observed the link traffic variation on the real network, the aforementioned hypothetical network was normalized. The network is normalized in such

a way that the cost of each link is 1. Additional nodes and links were introduced for succeeding the aforementioned purpose and the network revision is visualized in Figure 5.7 below.

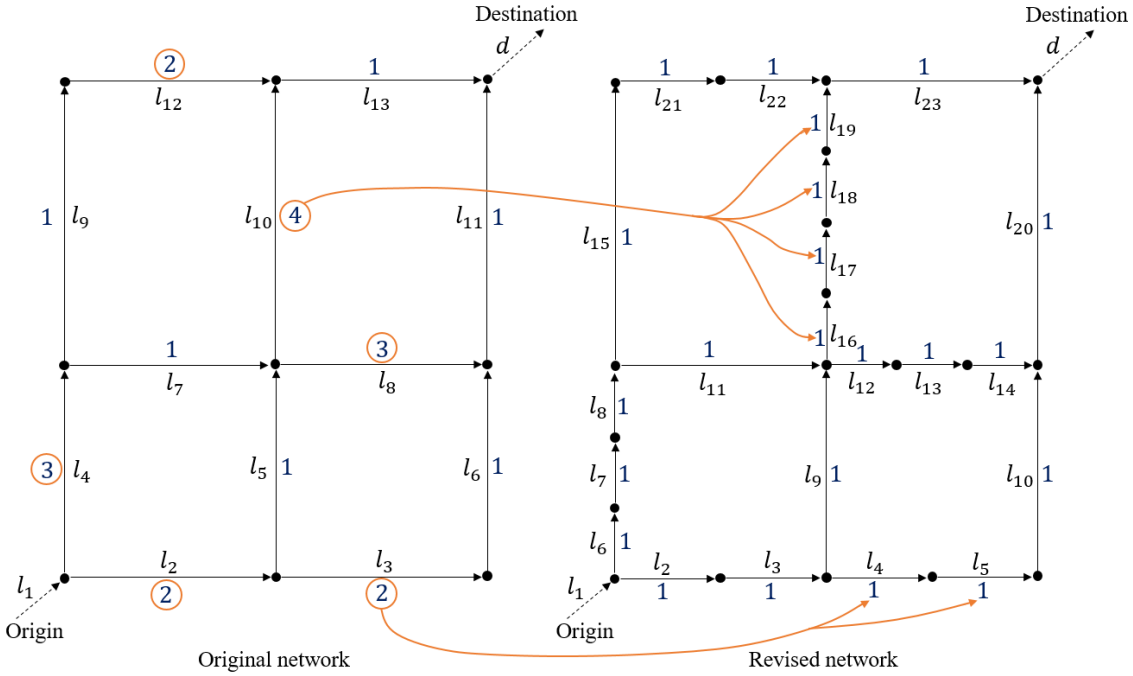

Figure 5.7 Conversion of the original network to the normalized network

As shown in the Figure 5.7, the revised hypothetical network contains 24 links including dummy links for origin and destination. Further it has 19 nodes. As shown by the arrows, all the high costed links were divided in to equal costed links in order to set all the links to a same cost. Same routes as mentioned in Table 5.1 were considered even though currently they are having different link numbers. But the total route cost for each and every route remains same as in the original network. Then the route choice probabilities were calculated under the β −scaled recursive logit framework and they are tabulated in Table 5.2 with the route cost with revised link combinations.

Table 5.2 Route choice probabilities under different scenarios of sequential time discount rate for the normalized hypothetical network

Route No.	Link connectivity	Route cost	$\beta = 0$	$\beta = 0.5$	$\beta = 1$
1	$l_1, l_6, l_7, l_8, l_{15}, l_{21}, l_{22}, l_{23}, d$	7	0.250	0.207	0.167
2	$l_1, l_6, l_7, l_8, l_{11}, l_{16}, l_{17}, l_{18}, l_{19}, l_{23}, d$	9	0.125	0.146	0.167
3	$l_1, l_6, l_7, l_8, l_{11}, l_{12}, l_{13}, l_{14}, l_{20}, d$	8	0.125	0.146	0.167
4	$l_1, l_2, l_3, l_9, l_{16}, l_{17}, l_{18}, l_{19}, l_{23}, d$	8	0.125	0.146	0.167
5	$l_1, l_2, l_3, l_9, l_{12}, l_{13}, l_{14}, l_{20}, d$	7	0.125	0.146	0.167
6	$l_1, l_2, l_3, l_4, l_5, l_{10}, l_{20}, d$	6	0.250	0.207	0.167

As shown in Table 5.2, route choice probabilities have changed remarkably even though their total link costs were unchanged. Under the myopic decisions where sequential time discount rate is zero, link is chosen based on the cost of the immediate links that are connected to the respective source node. Since all the links are having same cost in the normalized network, it is allocated same probability at for each alternative link. Hence when two alternative links are available, the model allocated 0.5 probability for choosing each link. Since, route 2, 3, 4 and 5 passing through two decision making points, their path choice probability is multiplied by 0.5 an additional time than the route 1 and 6.

Then the link flows were determined assuming 1000 travelers travelling from same origin to same destination as in the case of original network. The Figure 5.8 (a), (b) and (c) show the link flow variations respectively for the cases where sequential time discount rate equals to 0, 0.5 and 1.

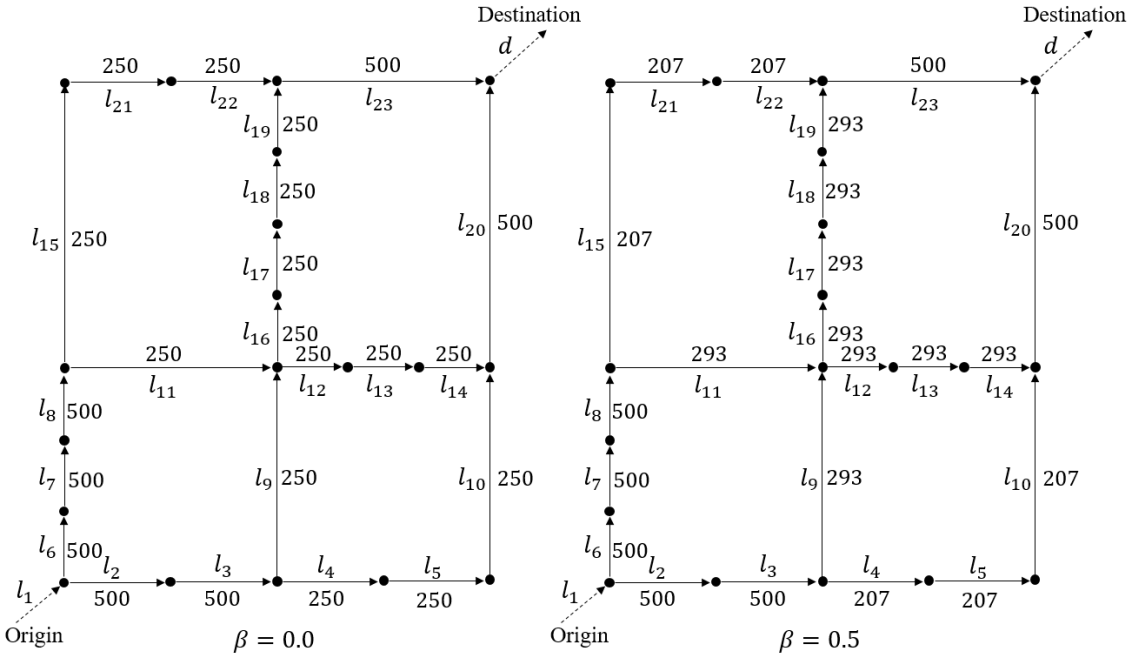

(a) (b)

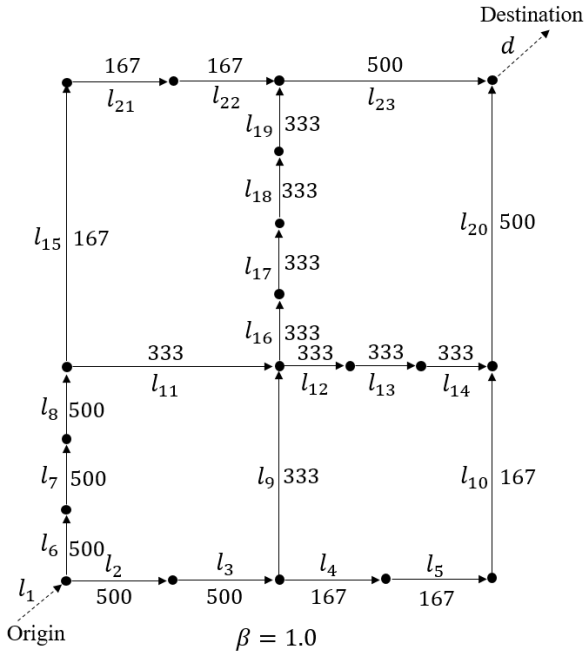

(c)

Figure 5.8 Assignment results for the hypothetical normalized network under the different scenarios of sequential time discount rate

As shown in part (a) of the Figure 5.8, link flow has divided to half at each decision-making node when the sequential time discount is zero. When the sequential time discount rate is increased, it can be observed that the route choice probabilities are also normalizing among the routes. At the peak of sequential time discount rate where it is equal to one, it can be noticed that all the routes are given equal selection probability irrespective of their initial total route costs. This happens, at the normalized stage, as the network reduces to a smaller network where it only considered the decision making links. According to the above concerned network, all routes become combinations of 4 links (excluding origin and destination links), where total route cost become 4 for all routes. Hence, under the condition of route-based decisions, model allocates same probability for all routes. Therefore, this clearly stressed that the calculation of the sequential time discount rate is highly correlated with the link costs.

In the aforementioned analysis, only the link length was the difference between the real network and the normalized network as the speed was kept unchanged. If the link speed of the normalized network was adjusted in such a way that it would produce the same link travel time as in the real network, the model is expected to produce the same sequential time discount rate.

5.3.1.2 Based on an actual network

As far as an actual network is concerned, it is extremely difficult to normalize and set up the network for simulation purpose. Precisely, the link length varies in a larger range and

accordingly, normalizing become a real headache. As an example, the lowest link length of the below considered network is 1 m while the maximum link length is 1079 m. Hence, as a reasonable approach, the normalized network is generated by adopting the average link length of the entire network to the all links in the network. The chosen routes are kept same for all the analyses while same parameters are considered in the utility function. Precisely, the only difference between the networks is the link length, as real network keeps the original link lengths while the normalized network having the network average link length. The analyses were done based on the probe taxi data collected in Tokyo on 11th March 2011 from 15:00 to 17:00 hrs. JST. The used network contained 2616 nodes and 3438 links. Randomly sampled 20 trips were included in samples which were used for the analyses. The respective estimation results are shown in Table 5.3

Table 5.3 Estimation results of real and normalized networks

Real Network						
	Sample 1	Sample 2	Sample 3	Sample 4	Sample 5	Sample 6
β	0.337	0.256	0.249	0.177	0.111	0.249
t – value	-3.45	-3.54	-4.00	-4.13	-2.34	-3.50
ρ^2	0.24	0.19	0.22	0.22	0.12	0.19
Lc	-292.4	-280.3	-262.8	-313.2	-245.0	-317.2
LL	-220.1	-228.1	-211.9	-245.3	-216.6	-248.3
Simulation time (hrs.)	12.8	10.4	10.1	10.8	15.1	9.70
Normalized Network						
	Sample 1	Sample 2	Sample 3	Sample 4	Sample 5	Sample 6
β	0.131	0.028	0.042	0.025	0.021	0.075
t – value	-3.11	-1.32	-1.68	-1.36	-0.078	-2.25
ρ^2	0.27	0.25	0.30	0.30	0.18	0.28
Lc	-264.2	-266.7	-250.0	-303.1	-242.1	-303.0
LL	-194.0	-199.2	-180.4	-211.7	-199.6	-210.9
Simulation time (hrs.)	10.1	8.9	8.5	9.5	11.4	9.3

LL is the value of log-likelihood function at the estimated parameters and Lc is its value when all the parameters are equal to zero. Sequential time discount rate, rho-squared value (likelihood ratio index) and simulation time were then compared among six samples by using bar charts. These samples are independent samples and hence there is no connectivity among themselves.

(a) Comparison of sequential time discount rate

As mentioned, sequential time discount rate was estimated by using six samples for a real network and a normalized network. The comparison of the sequential time discount rate is shown as bar charts in Figure 5.9.

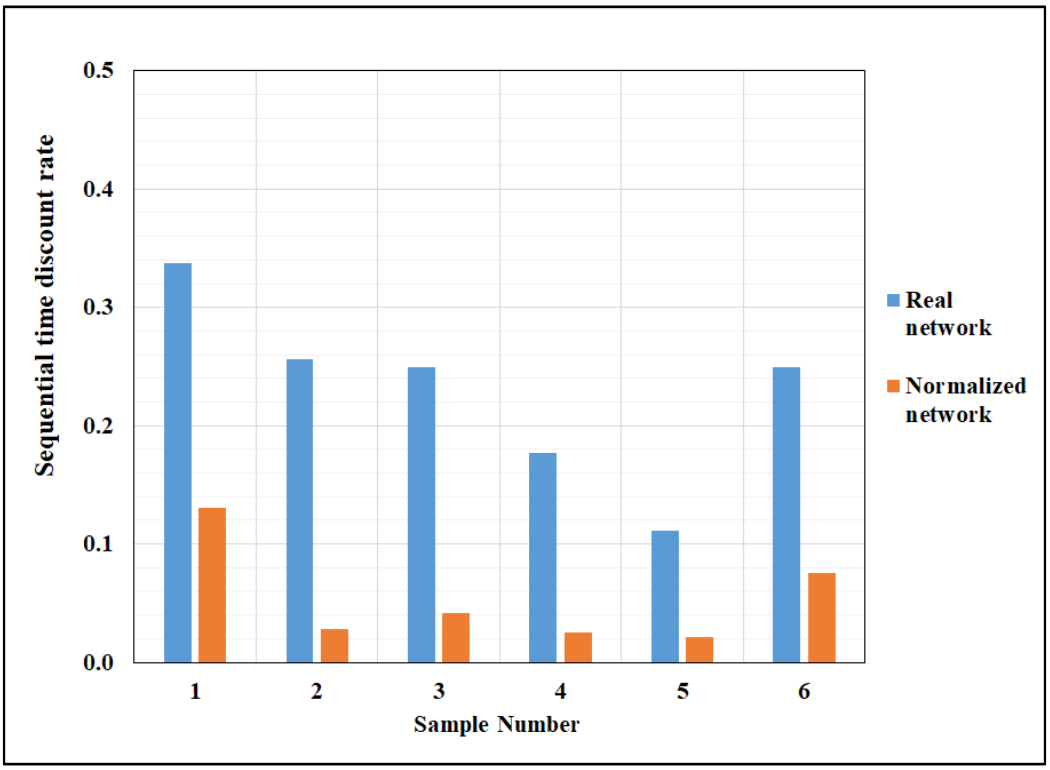

Figure 5.9 Comparison of sequential time discount rate between real and normalized network

As per the Figure 5.5 illustrates, the estimated sequential time discount rates for normalized networks show smaller values in comparison with the same of the real network. Sequential time discount rate under the real network situation has determined according to the actually chosen routes. The same route choices were kept unchanged in the normalized situation and it reduces the usage of travelers' knowledge on downstream links when they are choosing the links of normalized network. Correspondingly, the sequential time discount rate shows smaller values than the real network situation.

(b) Comparison of rho-squared value

Rho-squared values of the aforementioned samples are compared here. The respective variations are illustrated as bar chart in Figure 5.10 below.

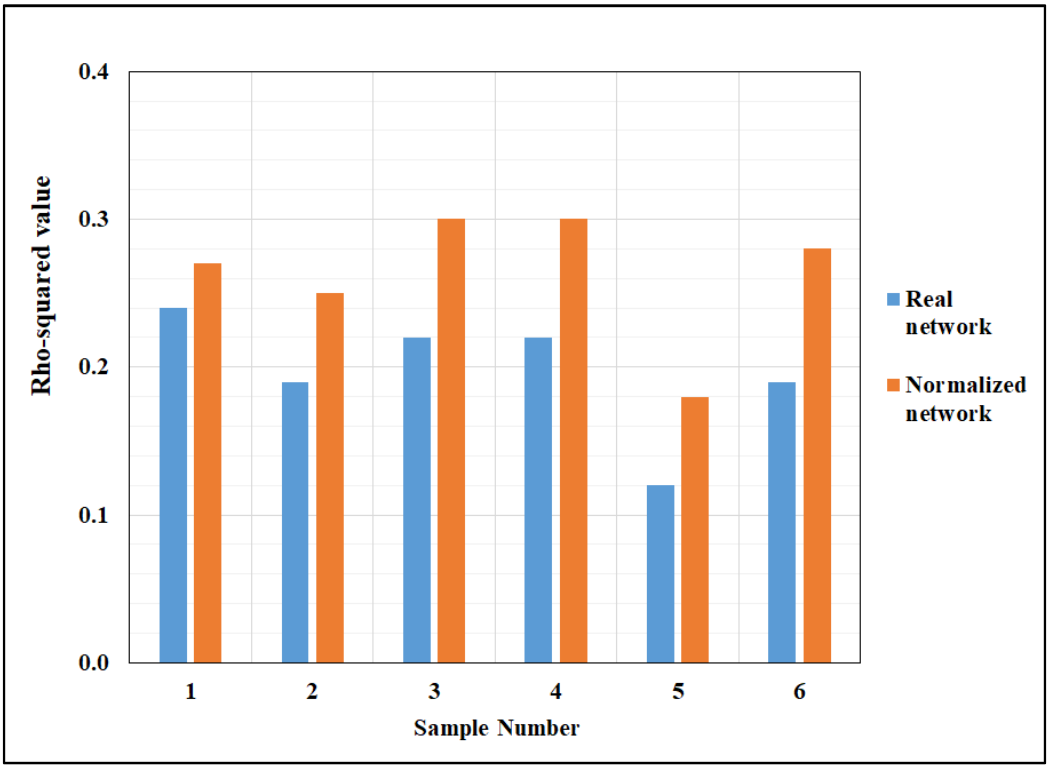

Figure 5.10 Comparison of rho-squared value between real and normalized network

According the Figure 5.10, rho-squared values have improved with the normalized network in all tested samples. As stated in the previous chapter (chapter 4), rho-squared value is calculated by deducting the ratio between the value of the log likelihood function when its maximum and the value of the log likelihood function when all the parameters are zero (no model condition), from 1.

As a result of normalizing the network and keeping the same route choices as in the actual network, the magnitude value of the log-likelihood function at the estimated parameters and when all the parameters are equal to one, is stayed at lower values in all the samples (Table 5.3). Hence the ratio between the log-likelihood function at the estimated parameters and when all the parameters are equal to one is calculated as a lower value in comparison with the real network values. Therefore, the respective rho-squared values stay in higher for all the estimated samples.

(c) Comparison of calculation speed

When considering the model performance, calculation speed becomes a crucial factor. Hence calculation speed of the β −SRL model was compared between a real network and a normalized network by utilizing the simulation time of the aforementioned samples. The respective elapsed time periods were plotted as column charts and shown in Figure 5.11 below.

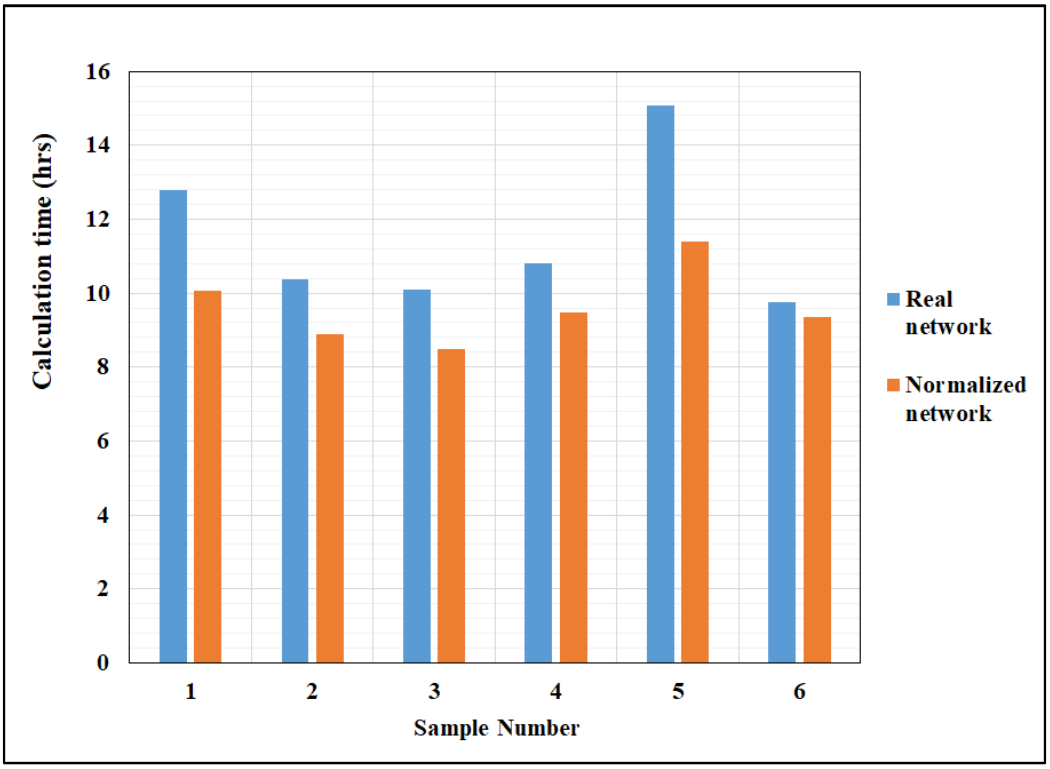

Figure 5.11 Comparison of simulation time between real and normalized network

As Figure 5.9 indicates, calculation time showed a lesser value when it simulates over the normalized network in comparison with the real network. This means that since all the links are having similar length in the normalized network, computer needs lesser memory for the calculation and accordingly the model has reached the optimization stage with a lesser time. For more details, let's consider the mathematical changes in the deterministic utility and value function matrices which are shown in Figure 5.12 and Figure 5.13 respectively. The values are respect to the hypothetical network considered in section 5.1 (taken as real network) and the normalized hypothetical network in section 5.3 (taken as normalized network).

Real network

$$\begin{pmatrix} 0 & e^{\frac{2\theta}{\mu}} & 0 & e^{\frac{0.5\theta}{\mu}} & 0 & 0 & \dots & \dots & \dots & \dots & \dots & \dots & 0 \\ 0 & 0 & 0 & 0 & e^{\frac{0.5\theta}{\mu}} & 0 & \dots & \dots & \dots & \dots & \dots & \dots & 0 \\ 0 & 0 & 0 & 0 & 0 & e^{\frac{\theta}{\mu}} & 0 & \dots & \dots & \dots & \dots & \dots & 0 \\ 0 & 0 & 0 & 0 & 0 & 0 & e^{\frac{3\theta}{\mu}} & 0 & \dots & \dots & \dots & \dots & 0 \\ \vdots & \dots & \dots & \dots & \dots & \dots & \dots & \dots & \dots & \dots & \dots & \dots & 0 \\ \vdots & \dots & \dots & \dots & \dots & \dots & \dots & \dots & \dots & \dots & \dots & \dots & 0 \\ \vdots & \dots & \dots & \dots & \dots & \dots & \dots & \dots & \dots & \dots & \dots & \dots & 0 \\ \vdots & \dots & \dots & \dots & \dots & \dots & \dots & \dots & \dots & \dots & \dots & \dots & e^{\frac{1}{\mu}(0)} \\ 0 & 0 & 0 & 0 & 0 & 0 & 0 & 0 & 0 & 0 & 0 & 0 & 0 \end{pmatrix}_{p \times p}$$

Normalized network

$$\begin{pmatrix} 0 & e^{\frac{\theta}{\mu}} & 0 & 0 & 0 & \dots & \dots & \dots & \dots & \dots & \dots & \dots & 0 \\ 0 & 0 & e^{\frac{\theta}{\mu}} & 0 & 0 & 0 & 0 & e^{\frac{\theta}{\mu}} & 0 & \dots & \dots & \dots & 0 \\ 0 & 0 & 0 & e^{\frac{\theta}{\mu}} & 0 & \dots & \dots & \dots & \dots & \dots & \dots & \dots & 0 \\ \vdots & \dots & \dots & \dots & \dots & \dots & \dots & \dots & \dots & \dots & \dots & \dots & 0 \\ \vdots & \dots & \dots & \dots & \dots & \dots & \dots & \dots & \dots & \dots & \dots & \dots & 0 \\ \vdots & \dots & \dots & \dots & \dots & \dots & \dots & \dots & \dots & \dots & \dots & \dots & 0 \\ \vdots & \dots & \dots & \dots & \dots & \dots & \dots & \dots & \dots & \dots & \dots & \dots & 0 \\ \vdots & \dots & \dots & \dots & \dots & \dots & \dots & \dots & \dots & \dots & \dots & \dots & e^{\frac{1}{\mu}(0)} \\ 0 & 0 & 0 & 0 & 0 & 0 & 0 & 0 & 0 & 0 & 0 & 0 & 0 \end{pmatrix}_{q \times q}$$

Figure 5.12 Element changes of the deterministic components matrices in between real and normalized network

p and q are the links of each network and the elements represent the deterministic utility of the forward link when moving from one link to other. Rows of the matrices represent the source links while columns are respected to the sinking link. As visualized by the valued elements in matrices of Figure 5.12, the deterministic components of the real network vary based on the observed link characteristics of each link. Meanwhile the valued elements of the matrix of normalized network contains the same value as the network is normalized. Both these matrices can be recognized as sparse matrices where most of the elements are zero. From the nonzero elements, the elements in the normalized matrix are similar to each other while the nonzero elements in the real network are having different values. This is benefited in the process of calculation and it gives a computational advantage. Let's visualize the elementary changes in the value function matrices in Figure 5.13 below.

Real network

$$\begin{pmatrix} \left(e^{\frac{\theta}{\mu}(2+\beta(1+\beta))} + e^{\frac{\theta}{\mu}}\left(e^{\frac{\theta}{\mu}(3+\beta)} + e^{\frac{\theta}{\mu}(4+\beta)}\right)^{\beta}\right)^{\beta} \\ \left(e^{\frac{\theta}{\mu}(1+\beta)}\right)^{\beta} \\ \left(e^{\frac{\theta}{\mu}}\left(e^{\frac{\theta}{\mu}(3+\beta)} + e^{\frac{\theta}{\mu}(4+\beta)}\right)^{\beta} + e^{\frac{\theta}{\mu}(2+\beta)}\right)^{\beta} \\ \left(e^{\frac{\theta}{\mu}(3+\beta)} + e^{\frac{\theta}{\mu}(4+\beta)}\right)^{\beta} \\ \left(e^{\frac{1}{\mu}(\theta+0)}\right)^{\beta} \\ \left(e^{\frac{\theta}{\mu}(3+\beta)} + e^{\frac{\theta}{\mu}(4+\beta)}\right)^{\beta} \\ \left(e^{\frac{1}{\mu}(\theta+0)}\right)^{\beta} \\ \left(e^{\frac{1}{\mu}(\theta+0)}\right)^{\beta} \\ \left(e^{\frac{1}{\mu}(\theta+0)}\right)^{\beta} \\ \left(e^{\frac{1}{\mu}(0+0)}\right)^{\beta} \\ \left(e^{\frac{1}{\mu}(\theta+0)}\right)^{\beta} \\ \left(e^{\frac{1}{\mu}(0+0)}\right)^{\beta} \\ \left(e^{\frac{1}{\mu}(0)}\right)^{\beta} \end{pmatrix}_{p \times 1}$$

Normalized network

$$\begin{pmatrix} \cdots \\ \cdots \\ \cdots \\ \cdots \\ \left(e^{\frac{\theta}{\mu}(1+\beta(1+\beta))}\right)^{\beta} \\ \left(e^{\frac{\theta}{\mu}(1+\beta)}\right)^{\beta} \\ \left(e^{\frac{\theta}{\mu}(1+\beta(1+\beta(1+\beta)))}\right)^{\beta} \\ \left(e^{\frac{\theta}{\mu}(1+\beta(1+\beta)}\right)^{\beta} \\ \left(e^{\frac{\theta}{\mu}(1+\beta)}\right)^{\beta} \\ \left(e^{\frac{1}{\mu}(\theta+0)}\right)^{\beta} \\ \left(e^{\frac{1}{\mu}(0+0)}\right)^{\beta} \\ \left(e^{\frac{1}{\mu}(0)}\right)^{\beta} \end{pmatrix}_{q \times 1}$$

Figure 5.13 Element changes of the value function matrices in between real and normalized network

The elements of the above matrices are represented the calculation relationships of determining the value function of each link. Origin links are represented at the top of the matrices while the last row represented the destination link. Hence the value function there is always zero by the definition. As indicated in the Figure 5.13 above, the value function elements with respect to the real network are always depend on each link cost and hence they are different from each other. In addition, they have a high complexity too. Meanwhile the respective elements in the normalized network, show a similar pattern even though they are different to each other. Since the link utility has normalized in the normalized network, calculation process becomes easier and can increase the computer efficiency. Even though the normalized network is extended with additional links, their decision making nodes remain unchanged as the real network. In this analysis, the number of links are kept same and same route choices were considered. Therefore, the calculation time showed a lesser value in comparison with the real network situation for the all considered samples.

In addition, the calculation speed of the model thoroughly depends on the performance of the computer used. Hence, different computer gives different calculation time for the same set of samples even though it produces the same result. Sometimes, there is an

uncertainty that even the same computer utilizes different period of time for simulating based on its usage during the period of simulation. Precisely, if a considerable amount of computer memory has been allocated for some other program, calculation time of the model could be increased. This was tested by simulating some samples twice under the different conditions, such as using the computer for usual works while model calculation is in progress and without using the computer for any other works while the simulation is going on. The results indicated that the difference in the calculation time is limited to few minutes. Since the total calculation time is around 10 hours for all samples, this effect can be easily neglected.

5.3.2 Performance based on scaled networks

The original networks are scaled by transforming the link lengths to an its own certain percentage. Accordingly, the link utilities will change from the original network. In the analysis, two networks were considered as scaling down the network to 50% and 75% by its link length. Then the simulations were done by using two samples and compared with the original network results. Sequential time discount rate was estimated together with two other parameters, travel time and right turn dummy variable (these variables are explained in detail in chapter 6). The results are tabulated and shown in Table 5.4 below.

Table 5.4 Estimation results of original and scaled networks

Sample 1						
Network	Original		Scaled to 75%		Scaled to 50%	
	Estimate	t-value	Estimate	t-value	Estimate	t-value
Travel Time	-0.120	-4.29	-0.160	-4.29	-0.240	-4.29
Right turn	-1.766	-6.15	-1.766	-6.15	-1.766	-6.15
β	0.337	-3.45	0.337	-3.45	0.337	-3.45
Lc		-292.4		-292.4		-292.4
LL		-220.6		-220.6		-220.6
ρ^2		0.25		0.25		0.25
Sample 2						
Network	Original		Scaled to 75%		Scaled to 50%	
	Estimate	t-value	Estimate	t-value	Estimate	t-value
Travel Time	-0.135	-4.73	-0.180	-4.73	-0.270	-4.73
Right turn	-2.244	-7.17	-2.244	-7.17	-2.244	-7.17
β	0.249	-4.00	0.249	-4.00	0.249	-4.00
Lc		-317.2		-317.2		-317.2
LL		-248.3		-248.3		-248.3
ρ^2		0.22		0.22		0.22

Lc is the value of the log likelihood function when all the parameters are zero and LL is the value of the log likelihood function at estimated parameters. As per the theory, the results should hold the equivalent differences property. Precisely, the choice probabilities of the alternatives should only depend on the differences in the systematic utilities of different alternatives and not their actual values. Accordingly, here, scaling of the network effect on the link length and hence its utility. Since the influence is affecting on all the links it doesn't make problems on the differences in the systematic utilities of different alternatives. Hence, sequential time discount rate should produce the same value as original network for all the scaled networks. The tested results above satisfied this condition.

In addition, since the link length was scaled the travel time has to be varied. Accordingly, the travel time parameter produced different values for scaled samples. Further, link length was decreased and simultaneously the link travel time also decreased. This variation has captured by the travel time parameter and accordingly, its value has decreased. Meanwhile, no change being done for the right turns and correspondingly, they are remaining same. Further, the value of the log likelihood function under the initial

and final conditions have not deviated from the original network. The log likelihood ratio also has not changed. This means, the scaling of the network has no influence on the model performance, except the directly affected parameters.

5.3.3 Performance based on extended networks

Performance of the $\beta -$ SRL model was tested with the extended networks and identified the characteristics of sequential time discount rate. Extended networks were created by adding a constant distance to each and every link in the network. Unlike in the process of scaling the network where link length of all links increased in same percentage, here each link is increased with different percentage to its own original length. Accordingly, the link utilities deviate from different percentage and sequential time discount rate will fluctuate. Under this analysis, link lengths were changed in three categories by adding 20m, 50 m and 100 m respectively and model was simulated. The obtained results are tabulated in Table 5.5 below.

Table 5.5 Estimation results of original and extended networks

Sample 1				
Network	Original	Add 20 m	Add 50 m	Add 100 m
β	0.337	0.319	0.271	0.217
t - value	-3.45	-3.74	-3.94	-3.92
Lc	-292.4	-288.0	-278.4	-271.2
LL	-220.6	-212.9	-206.3	-201.0
ρ^2	0.25	0.26	0.26	0.26
Sample 2				
Network	Original	Add 20 m	Add 50 m	Add 100 m
β	0.249	0.229	0.174	0.118
t - value	-4.00	-4.31	-4.26	-3.69
Lc	-317.2	-314.5	-309.4	-305.8
LL	-248.3	-238.2	-229.0	-221.4
ρ^2	0.22	0.24	0.26	0.28

The results shown in the Table 5.5 clearly indicate that the sequential time discount rate has decreased with the extended network. Further, the pattern keeps decreasing while the expanding of the link length is increased. Extending the link length from its original value by some constant length, make changes in the deterministic component in different percentages. Obviously, this could lead to a situation where the link choosing probability

is changed. But in this analysis, the same routes used in the original network were kept without changing. Therefore, the travellers are not using the downstream conditions well in selecting their next link in the decision-making process. Accordingly, the sequential time discount rate stays in lower values.

5.3.4 Performance based on number of links per trip

β −SRL model follows a link by link approach in estimating model parameters with respect to the travelers' route choice. Hence, understanding the model performance with different number of links per trip is important. Hence, simulations were carried out under three categories as trips having less than 25 links per trip, trips having links from 25 to 50 links per trip and trips having links over 50 per trip. Randomly sampled 20 trips were used as a sample and five independent samples were tested under each category. The simulated network was consisted with 4556 links and 2967 nodes. The resulted estimations of sequential time discount rate are tabulated in Table 5.6 below.

Table 5.6 Estimation results for trips having different number links per trip

For the trips having less than 25 links per trip					
Parameter	Sample 1	Sample 2	Sample 3	Sample 4	Sample 5
β	0.203	0.114	0.050	0.315	0.455
t - value	-2.46	-1.78	-1.25	-2.97	-2.12
Lc	-272.0	-239.5	-249.8	-319.9	-360.0
LL	-230.8	-219.2	-218.9	-223.4	-205.6
ρ^2	0.15	0.08	0.12	0.30	0.43
Sim. time (hr.)	26.2	19.2	44.8	27.5	21.9
For the trips having links between 25 to 50 per trip					
Parameter	Sample 1	Sample 2	Sample 3	Sample 4	Sample 5
β	0.113	0.320	0.063	0.081	0.068
t - value	-2.72	-3.11	-1.83	-2.25	-1.88
Lc	-430.1	-511.9	-438.7	-493.0	-478.6
LL	-404.6	-421.7	-395.4	-433.1	-430.2
ρ^2	0.06	0.18	0.10	0.12	0.10
Sim. time (hr.)	12.5	15.3	20.5	23.7	14.5
For the trips having links over 50 per trip					
Parameter	Sample 1	Sample 2	Sample 3	Sample 4	Sample 5
β	0.116	0.100	0.245	0.232	0.191
t - value	-3.90	-3.43	-5.07	-5.11	-5.00
Lc	-1067.0	-982.6	-1147.3	-1160.7	-1145.6
LL	-956.0	-866.7	-958.3	-988.9	-977
ρ^2	0.10	0.12	0.16	0.15	0.15
Sim. time (hr.)	22.9	20.8	17.3	19.0	19.5

Sequential time discount rate varies according to the selected routes in the sample and the network condition at that specific time. Before describing the variability of other entities, estimations of the sequential time discount rate are plotted in bar chart and shown in Figure 5.14 below.

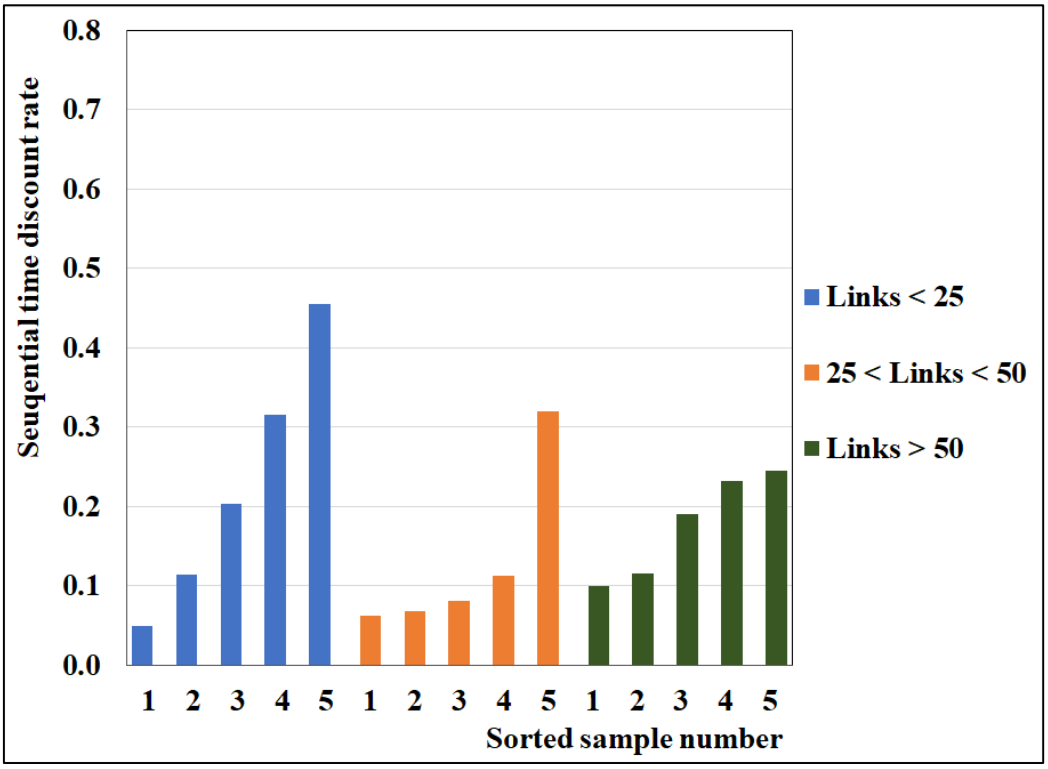

Figure 5.14 Variation of sequential time discount rate for samples having different number of links per trip

For the easiness of the visual observation, the estimated samples were sorted according to the value of the sequential time discount rate and plotted. Hence the Figure 5.14 shows the sorted sample number which is not equal to the sample number shown in the Table 5.6. As per the Figure 5.14 indicates, the estimations with respect to the trips having more than 50 links per trip showed more stability. The difference between the lowest and the largest estimation are 0.405, 0.257 and 0.145 respectively for less than 25 links, between 25 to 50 links and over 50 links per trip. The respective variances are 0.026, 0.012 and 0.004. In addition, t statistic values indicate high significance in the results of samples having links more than 50 per trip. Obviously, the log likelihood function calculates higher values when the number of links or the length of the trip is increased. This also can be visualized with the results appeared in Table 5.14. Calculation time varied significantly when the number of links become less in the trips. Further, it becomes much stable when the number of links per trip is increased. Since the calculation time is not significantly increased with the increase of number of links per trip, it is recommended to use trips with more links for better estimations.

5.4 Conclusions and discussions

Understanding mathematical characteristics and model performances are paramount importance in explaining model estimations under different network conditions. Hence this chapter was designed to scrutinize the matrix formations in intermediate steps of solving β −SRL model. In addition, the model performances were discussed under four

different scenarios. The value functions with respect to each link of the considered network can be determined by solving the system of non-liner equations with the sequential time discount rate. Hence, such a system of non-liner equations was determined based on a hypothetical network and their element basis changes under the key solving steps were discussed in detail.

In the next stage, the model performances were discussed based on normalized network, scaled network, extended network and number of links per trip. Route choice results based on a hypothetical real network proved that the choice probabilities are highly correlated with the respective link cost. In the lower values of sequential time discount rate, it was observed that the myopic decisions are dominating in selecting the links at different nodes. Meanwhile under higher values of sequential time discount rate, travelers were much willing to utilize the downstream utilities. These characteristics were changed with the normalized network which was created by adding nodes and links to the aforementioned real hypothetical network in such a way that it satisfied the network condition that the cost of all links is similar to each other. Correspondingly, the links were assigned with equal probabilities at decision making nodes under the myopic conditions. Meanwhile, route choice probabilities also observed to be normalized under the condition of sequential time discount rate was equal to one. The analyses were further carried out by using a real-world data and sequential time discount rate was estimated under the real and normalized network conditions. The results showed a lowering of sequential time discount rate, improvements in log likelihood ratio index, and reduction of simulation time in normalized network conditions in comparison with the real network conditions.

Further, the analysis based on scaled network showed that the results are holding the equivalent differences property between the alternatives. Precisely, the choice probabilities of the alternatives depended only on the differences in the systematic utilities of different alternatives and not their actual values. Accordingly, the model estimated the same value for the sequential time discount rate among all scaled networks. The extended networks were created by adding constant length to each link in the network. Unlike in the case of scaled network, here the link utilities changed by different percentages and accordingly, the route choice probabilities are changed. But the analysis was carried out by using the same route choices made during the normal network condition and hence a reduction of the sequential time discount was observed. Then the influence of the number of links per trip over the estimation of sequential time discount rate was tested by using three categories. Results showed that the model performance become more consistent and the estimations become more stable when estimating the samples having trips with their number of links per trip is more than 50 links.

6 Comparative analysis of travel behavior and sequential time discount rate

6.1 Introduction

Road networks are always vulnerable to adverse natural phenomenons such as earthquakes, hurricanes, tornados, floods, snowfalls and beyond. In terms of travel behavior is concerned, either of these hazards can be recognize in the form of a disaster, as they disturbed the normal travel behavior. Further, they often cause significant delays and operational irregularities in traffic networks. Hence, understanding network behavior in such abnormal conditions is important for transport planners to minimize the adverse impacts and regulate the traffic flows as soon as possible.

This chapter includes a comparative analysis of network behavior under two distinct and divergent disasters, the great east Japan earthquake and a torrential downpour. Earthquake is an unexpected event where panic behavior of travelers could be hypothesized given the complexity of the network and the massive crowd. Meanwhile, torrential downpour is an extreme weather condition which is expected to predict under the available weather forecasting systems, especially in Tokyo, Japan. It is expected that the majority of Tokyo people aware of daily weather forecasts and hence, a panic behavior is not assumed. Cools et al. (Cools, Moons, Creemers, & Wets, 2014) confirmed that the type of weather is significance and the changes in travel behavior in response to weather conditions are highly dependent on trip purpose.

Pacific coast of Tohoku, Japan was hit by a massive earthquake of magnitude 9.0 – 9.1 on the Richter scale at 14:46 hrs. in JST on Friday, 11th March 2011 and is often referred as the great east Japan earthquake or 2011 Tohoku earthquake. Even though the earthquake was occurred more than 100 km s away from the Tokyo, the trains and the Tokyo metropolitan expressway were suspended for safety checks and more than 5 million people were faced difficulties in returning home.

The torrential downpour was occurred around cities Shibuya, Minato, Shinagawa and Setagaya in Tokyo, on 23rd July 2013. Rainfall was started around 15:15 and ended around 16:35 JST. High intense rainfall (100 – 150 mm/h) caused a flash runoff which inundated some of the underpasses and depressions within the area up to a maximum flood height of 0.5 m. This caused difficulties for cars and taxis to move across and such road users had to choose alternative routes. Some of the such underpasses are shown in Figure 6.1. Under the both considered disasters, travelers were supposed to search for alternatives. But, the influence of the great east Japan earthquake is over the entire network while the issue under the torrential downpour was location specific.

Image source: http://www.geosense.co.jp/map/tool/geoconverter.php

Figure 6.1 Some of the effected underpasses

6.2 Data

Data collection techniques have been improved over the past six decades from face-to-face interviews or paper-and-pencil interviews to probe technology, which collects the GPS trajectories of trips (Shafique & Hato, 2016). Analysis of this chapter is made based on GPS observations of taxy trajectories collected on 11th and 18th March 2011 (on the occurrence day of the great east Japan earthquake and a day exactly one week after), and on 23rd and 30th July 2013 (the day that the torrential downpour was occurred and a day exactly one week after) in city of Tokyo, Japan. It is hypothesized that the demand was equilibrated to almost normal conditions after one week from the occurrence of the disasters and provide a better platform for comparison. Such hypothesize have made in the literature too (Dimitrou & Stathopoulos, 2016).

Site selected for the study under great east Japan earthquake is the area covered by the secondary mesh code 533946 (Iida K. , 2006) of the regional mesh (Statistics-Japan, 1996), which consisted 39,642 nodes and 54,211 links. The area covered by the secondary mesh code 533935 of the regional mesh, which consisted 31,142 nodes and 38,180 links was used for the analysis under the torrential downpour. Both areas are much closer to each other and lies within the city of Tokyo. Further, they are highly operated traffic networks and it is worth to analyze the travel behavior changes under disaster conditions. The respective areas are shown in Figure 6.2

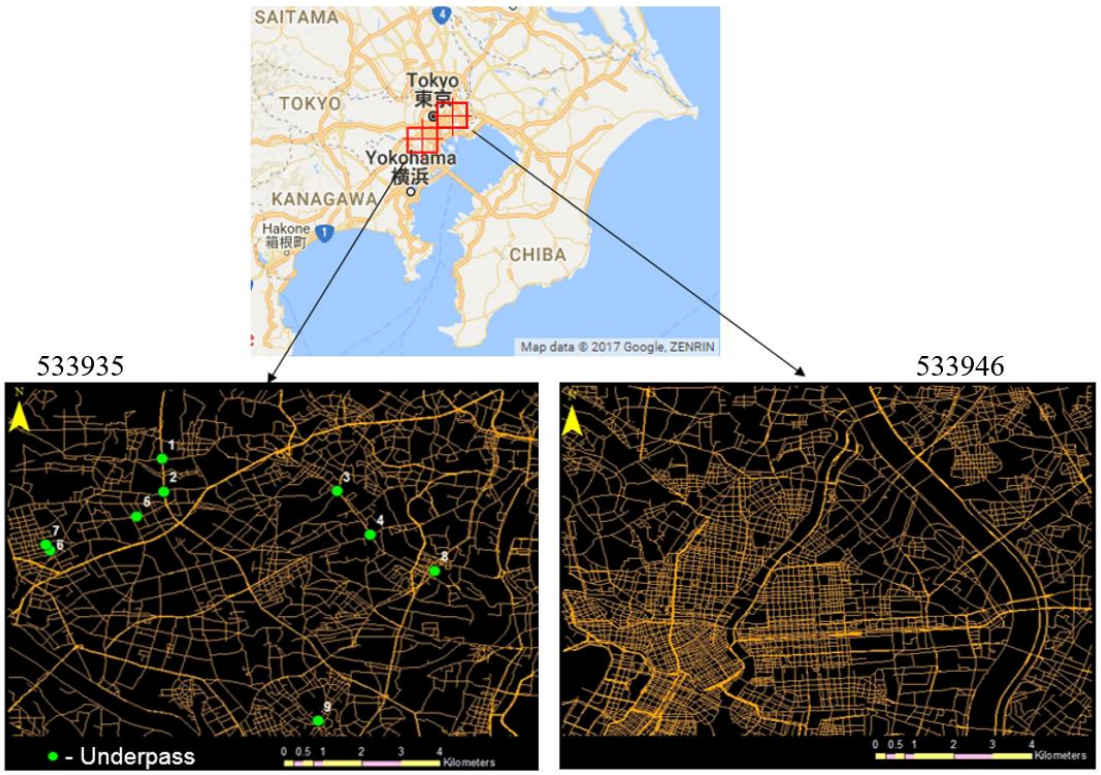

Figure 6.2 Study area under the torrential downpour (left) and the great east Japan earthquake (right)

Regional mesh is a square grid which divides the whole area of Japan into small mesh based on latitudinal and longitudinal lines. Primary mesh consists 40 minutes' latitude interval and one-degree longitude interval. The length of a side is about 80 km. The secondary mesh, which is used in this study consists 5 minutes in latitude interval, 7 minutes and 30 seconds in longitude interval. The length of a side is about 10 km.

The data set contained both occupied and non-occupied taxis for the analysis. In the contest of a non-occupied taxi, it can be either heading towards the customer's place for pick in, or it may be returning to its waiting place after dropping a customer, or driver may be heading towards his own personal business. In all these circumstances, it is hypothesized that the respective driver has a clear vision about where he is travelling. At each node where, a driver needs to take a decision on the choice of the next link, it is assumed that he/she maximizes the sum of instantaneous utility associated with current and next link, and the expected downstream utility. The recursive logit model is formulated based on this concept, and due to the validity of the concept in either of above cases, all the available data were used for the analysis.

The collected probe GPS taxi trajectories were map-matched based on the real road network data by using Dijkstra's algorithm (Dijkstra, 1959) for the shortest path. The taxi probe data were collected and provided by the vehicle information and communication system center (VICS), which is an organization that collects and provides drivers' road traffic information in Japan. Both events, the great east Japan earthquake and torrential

downpour were occurred during the afternoon session and accordingly, the analysis was carried out over four hours of period starting from 14:00 Japanese Standard Time (JST). The data set included taxi trips between 750 and 1400 in each hour and are presented in Table 6.1

Table 6.1 Hourly distribution of taxi trips

Date\Time period	14:00 – 15:00	15:00 – 16:00	16:00 – 17:00	17:00 – 18:00
11/03/2011 (Earthquake day)	789	760	915	1083
18/03/2011 (Normal day)	769	765	754	762
23/07/2013 (Rainy day)	977	1041	1396	1060
30/07/2013 (Normal day)	965	966	924	935

Number of taxi trips in Table 6.1 confirms the increase of taxi usage during extreme weather conditions, which is common for many disastrous networks. Normal taxis are equipped with radio communication systems from where drivers could collect up-to-date information about network behaviors. But under these situations, it is necessary to be noted that the drivers have not get information about downstream link conditions.

6.3 Trajectory behavior at damaged networks

Comparative analysis of trajectory behavior under the aforementioned disastrous networks and respective normal days were carried out through visualizing time-space diagrams, link speed variation maps, congestion index plots and right-turn ratio variability graphs.

6.3.1 Time space diagram

Individual taxi movements during disaster day and non-disaster day were visualized by plotting some selected taxi trajectories in time space diagrams. Essential criteria for comparing individual taxi trajectories are, their origin and destination must be much closer to each other and trips must be started within similar period of time. But, such trips are extremely difficult to find under these types of extraordinary situations. Four taxi trips showed in Figure 6.3, Figure 6.4, Figure 6.5 and Figure 6.6 were selected based on their close proximity in origin, destination and start time.

Figure 6.3 and Figure 6.4 show some sample time space diagrams of taxi trips occurred during the considered period after the earthquake and during its respective normal day respectively.

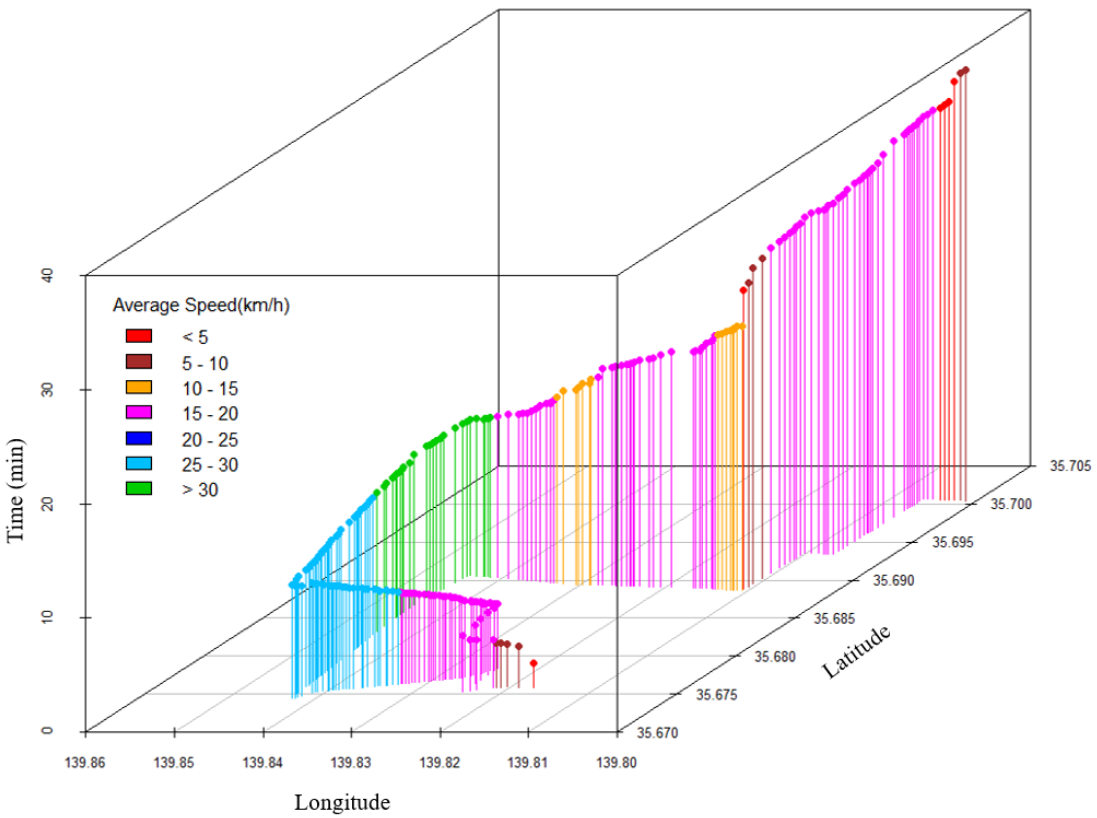

Figure 6.3 A sample taxi trajectory observed during the period of earthquake

Considering the taxi trip shown in Figure 6.3, most of the time it's speed is less than 20 km/h. Further, there are some stagnated points where the time axis increases without changing the space. Which means, the taxi might have stuck in a queue. Only a less portion of the trip has a speed over 25 km/h. In addition, comparatively with Figure 6.4 (below), the taxi has taken many number of turns. Precisely, 8 major turns where 5 out of that are right turns which drivers reluctant to take as Japan is a left driving country. The taxi has taken 38 minutes to reach its destination which is just 9.3 km s away.

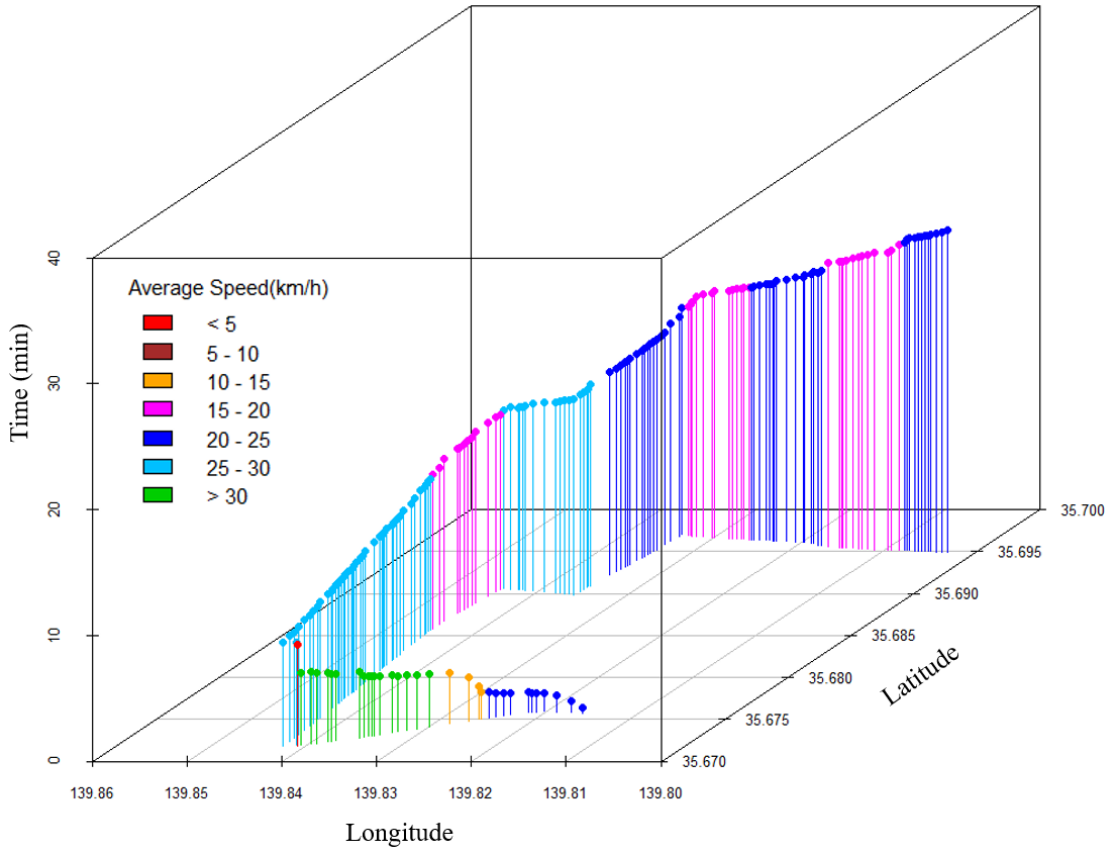

Figure 6.4 A sample taxi trajectory observed in respective normal day

According to the taxi trajectory shown in Figure 6.4, the taxi has maintained a speed above 20 km/h during most of the time of its trip while it was opposite in the Figure 6.3. Precisely, the average speed of the aforementioned taxi trip which was under the normal condition is 20.4 km/h while the average speed of the taxi trip under the disastrous condition is 14.7 km/h. Time axis of the both figures has kept under a same scale for the comparison purposes and they have taken 38 minutes and 25 minutes respectively under the disastrous condition and normal condition. Further, the taxi trip under the normal condition has taken only 4 major turns which is half of the turns in the disastrous condition.

Figure 6.5 and Figure 6.6 visualize two sample time space diagrams of taxi trips occurred during the considered period of torrential downpour and during its respective normal day respectively.

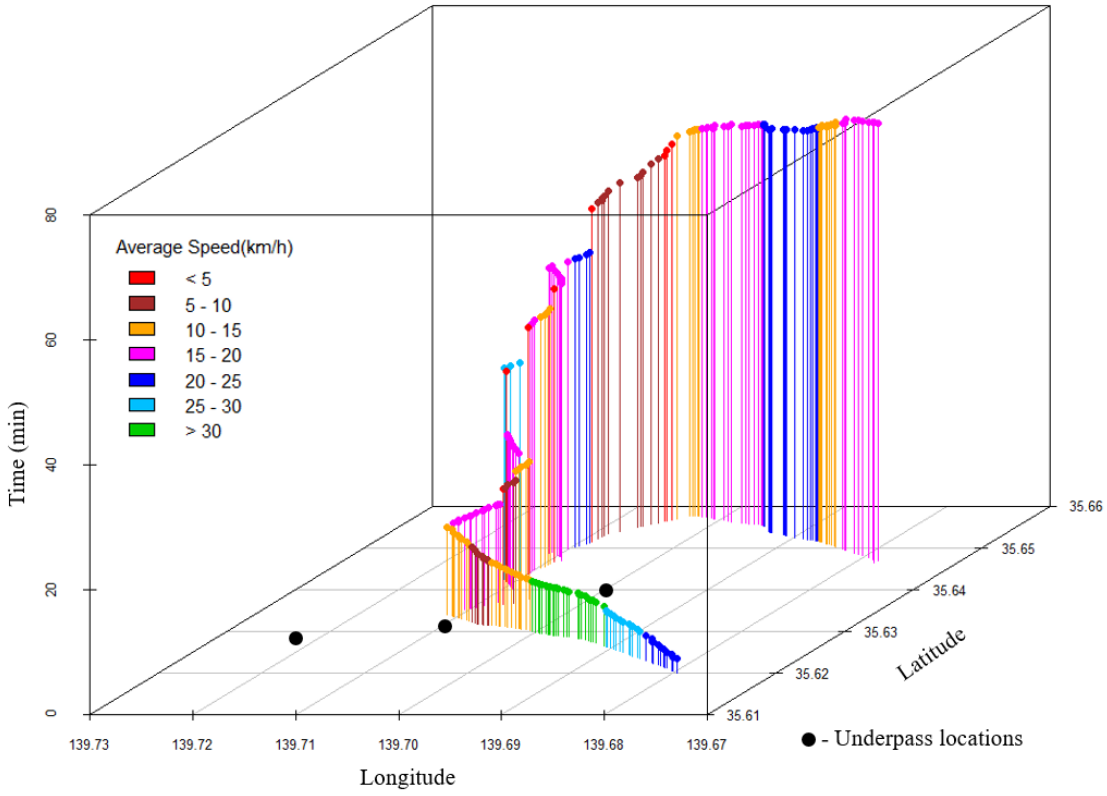

Figure 6.5 A sample taxi trajectory observed during the period of torrential downpour

Taxi trip visualized in the Figure 6.5 shows many stagnated points where it might have stuck in a queue and it illustrates the stop-move-stop behavior during the congestion. In addition, many portions of the trip have undergone a speed less than 20 km/h. Further it has taken longer time comparatively with the trip under the normal condition which is shown in Figure 6.6. Precisely, it has taken 70 minutes to reach just 10 km s under the congestion.

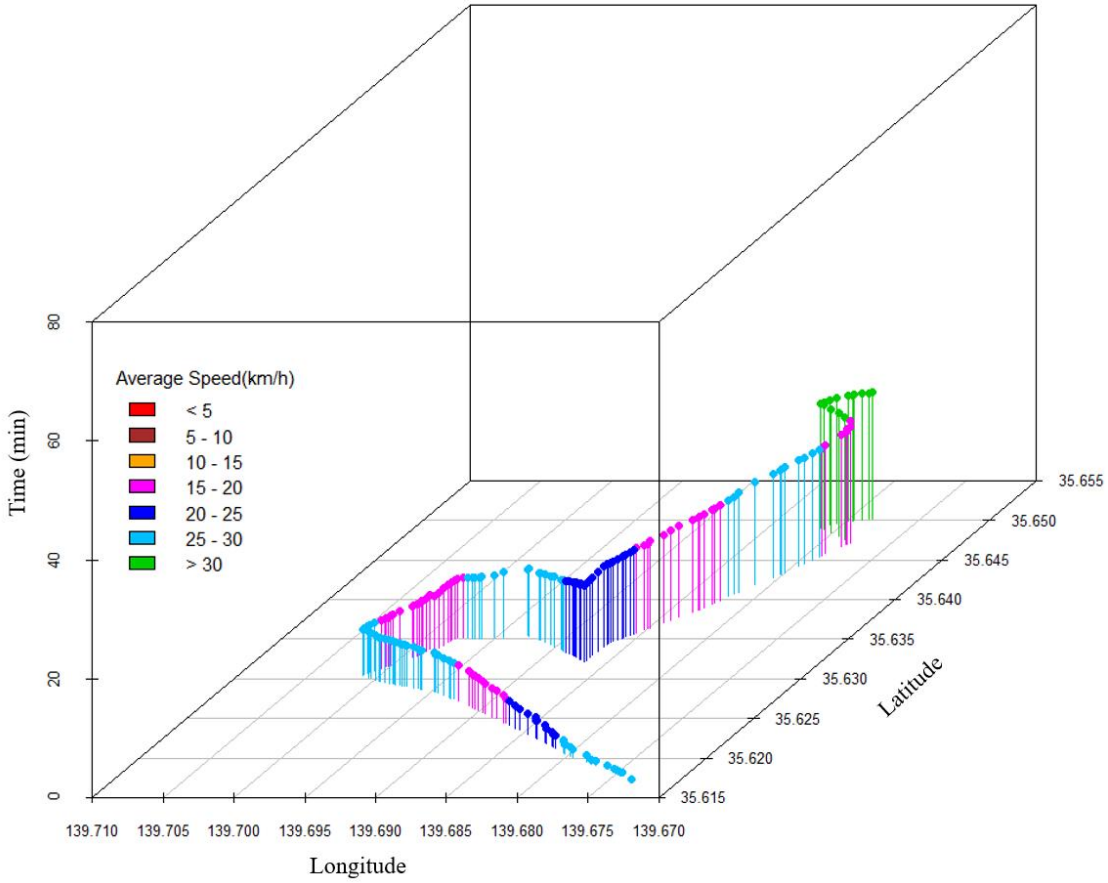

Figure 6.6 A sample taxi trajectory observed in respective normal day

Time axis of Figure 6.6 also kept in the same scale as Figure 6.5 for the comparison purpose. Hence, it can be clearly visualized that the trip under the normal condition has taken very less time comparatively. In addition, the taxi speed is over 20 km/h in many portions of the trip. Further, under the congested condition, the taxi has travelled about 10 km to reach the destination while it has taken about 7 km in the normal day. So, it is understanding that drivers have to go for additional miles when are choosing alternatives under the congestion. The other highlighting point is number of directional changes. Many directional changes can be visualized in Figure 6.5 under the congested condition while they are comparatively less in the normal day.

6.3.2 Route selection in congestion

In most of the choice models, consumers or subjects are assumed to follow the rational behavior. Which means, decision making process is based on making choices that result in the most optimal level of benefit or maximum utility for the consumer. When it comes to route choice, travelers are also expected to follow the same principle. Figure 6.7 and Figure 6.8 show some of the sample trips and respective link speed maps under the congestion occurred due to the great east Japan earthquake.

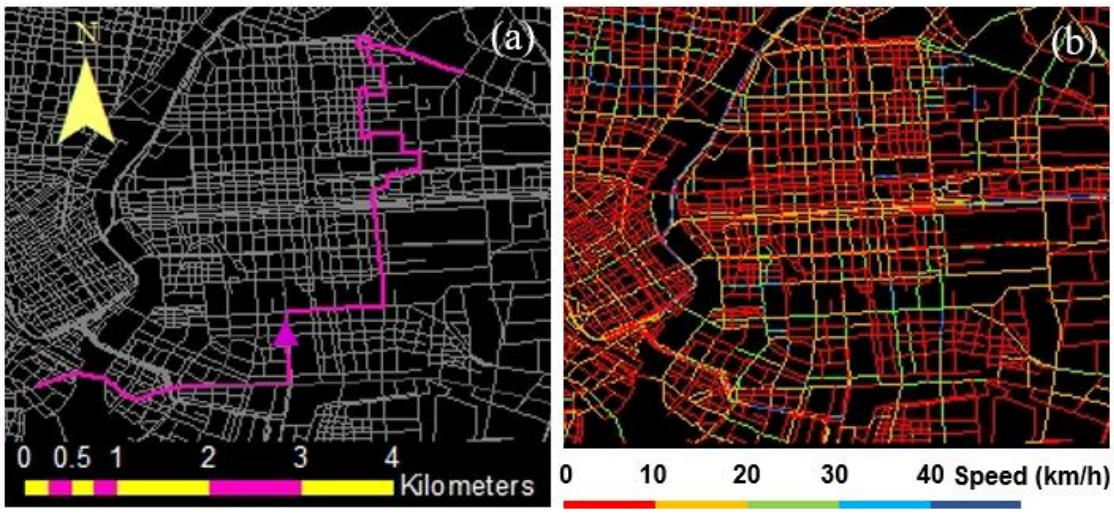

Figure 6.7 A sample trip_1 (a) and it's respective link speed map (b)

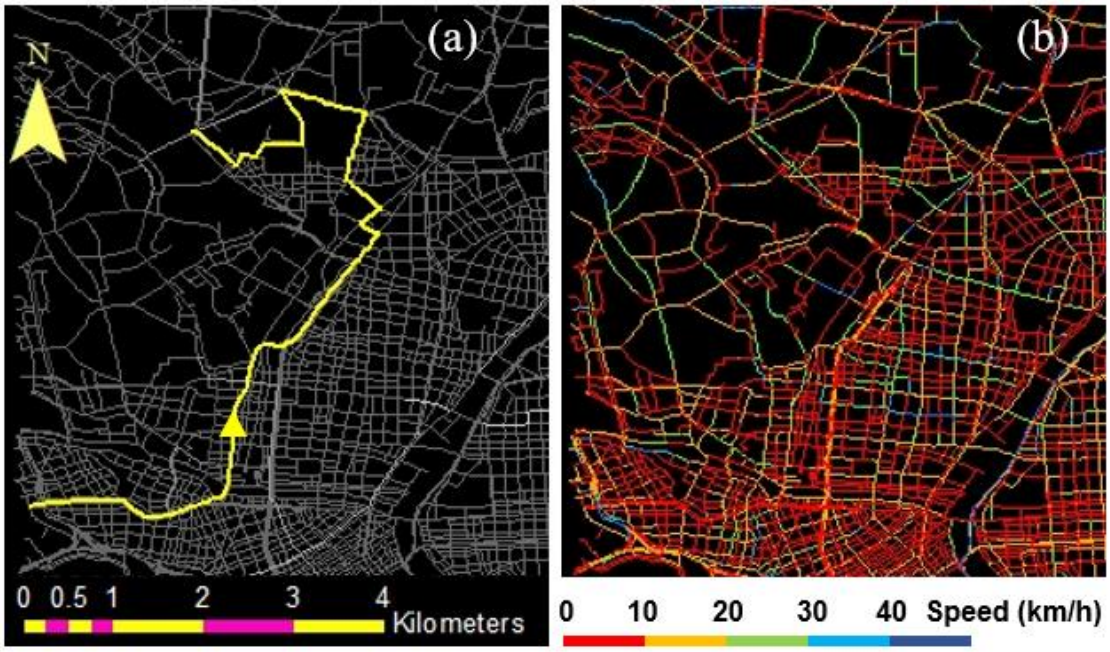

Figure 6.8 A sample trip_2 (a) and it's respective link speed map (b)

As both above figures (Figure 6.7 and Figure 6.8) illustrates, drivers have tried to find the lesser congested link in most of the times when they are supposed to make a link choice at each nodes. In other words, drivers have chosen the maximum utility links which makes the lesser travel time and supported the rational behavior. Similarly, taxi trips route selection characteristics under the torrential downpour also studied. Figure 6.9 and Figure 6.10 illustrates two of them.

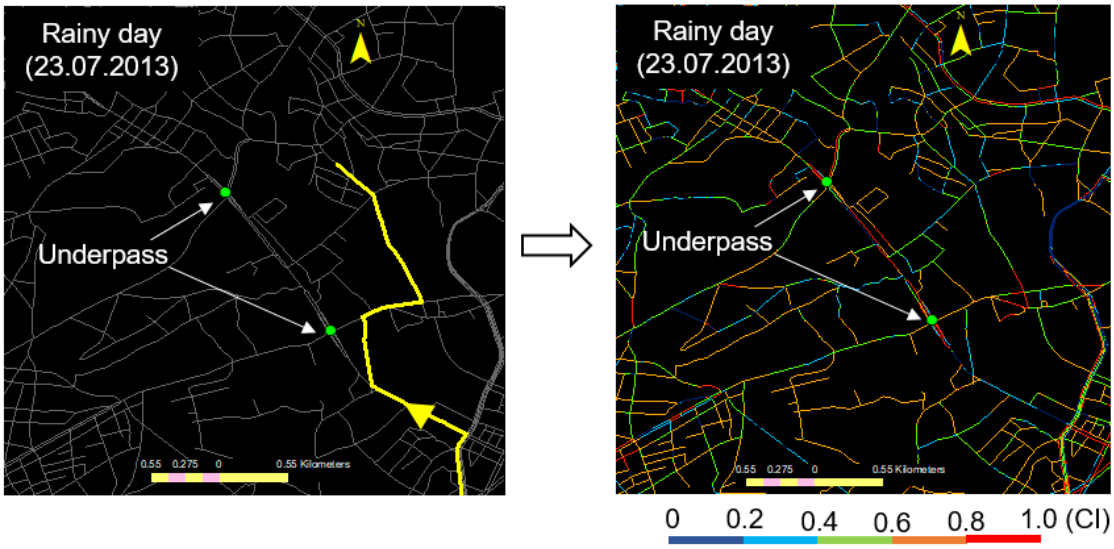

Figure 6.9 A sample taxi trip and its congestion index map on rainy day

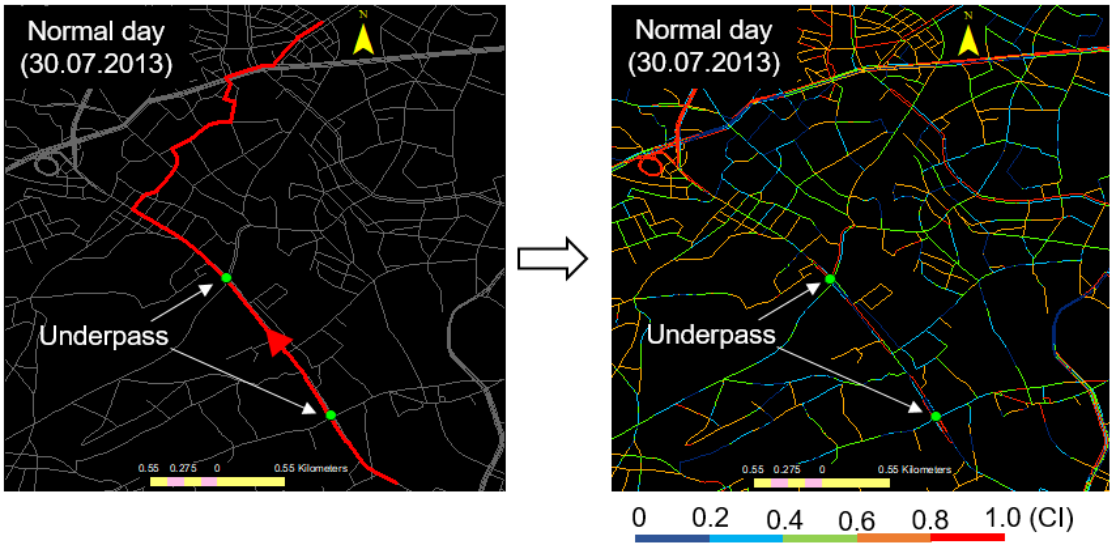

Figure 6.10 A sample taxi trip and its congestion index map on normal day

The taxi trip shown in the Figure 6.9 which is under the congestion of torrential downpour makes a right turn towards a lesser congested link with the vicinity of an underpass and avoids the underpass. Doing so, further it has to take two more major turns before reaching the destination. In a normal day, it would have been continuing through the nearest under pass and turn to right between the two under passes for reaching the destination. Correspondingly, in the taxi trip shown in the Figure 6.10, the taxi passes through both under passes and reach the destination. Hence, it is clear that in the rainy day, the taxi driver tries to avoid the congested under passes while they go through the under passes in normal days.

6.3.3 Link speed variation

Gathering of more than 5 million people who expected to return home as soon as possible after a shocking earthquake under the circumstances of trains and Tokyo metropolitan expressway were suspended for safety checks caused severe congestion in the road transport network. As a result, the link speeds are drastically dropped down. Figure 6.11 shows the comparison of average link speed between normal day and earthquake day from 14:00 to 16:00 hrs. while Figure 6.12 shows the similar plots for the period from 16:00 to 18:00 hrs.

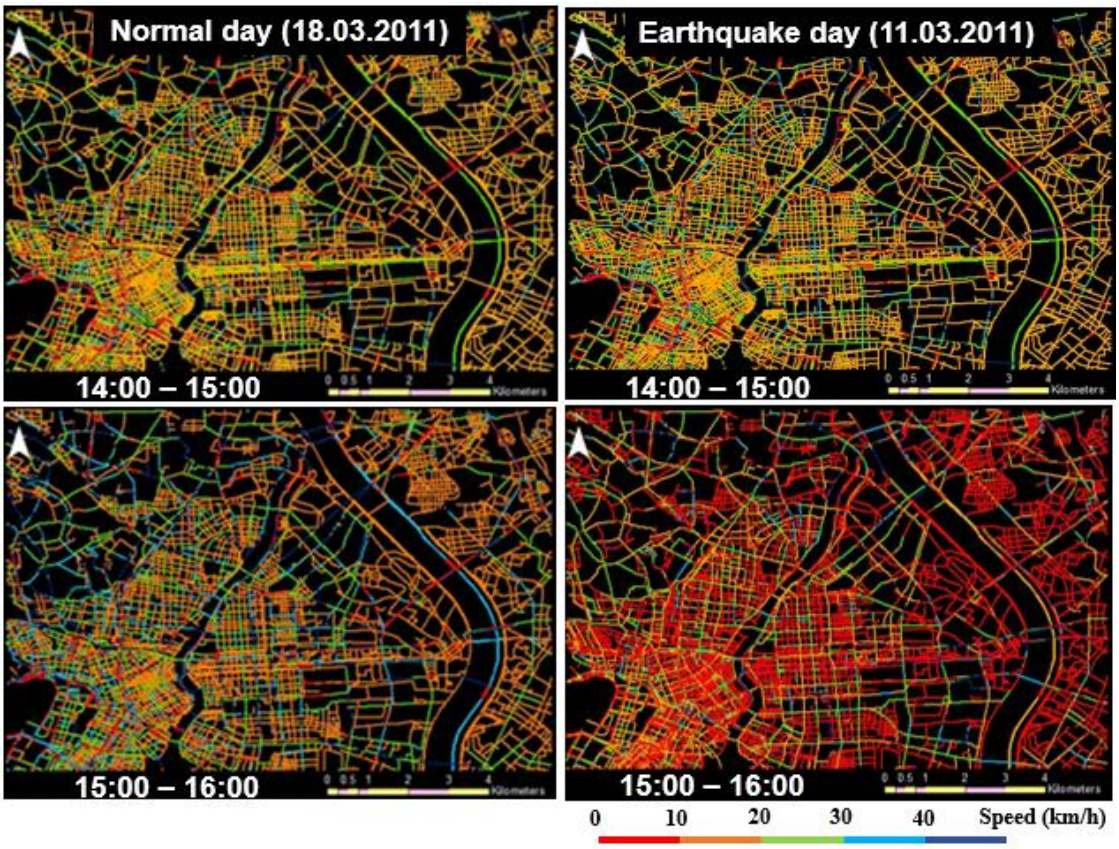

Figure 6.11 Link speed variability for the period from 14:00 to 16:00 hrs.

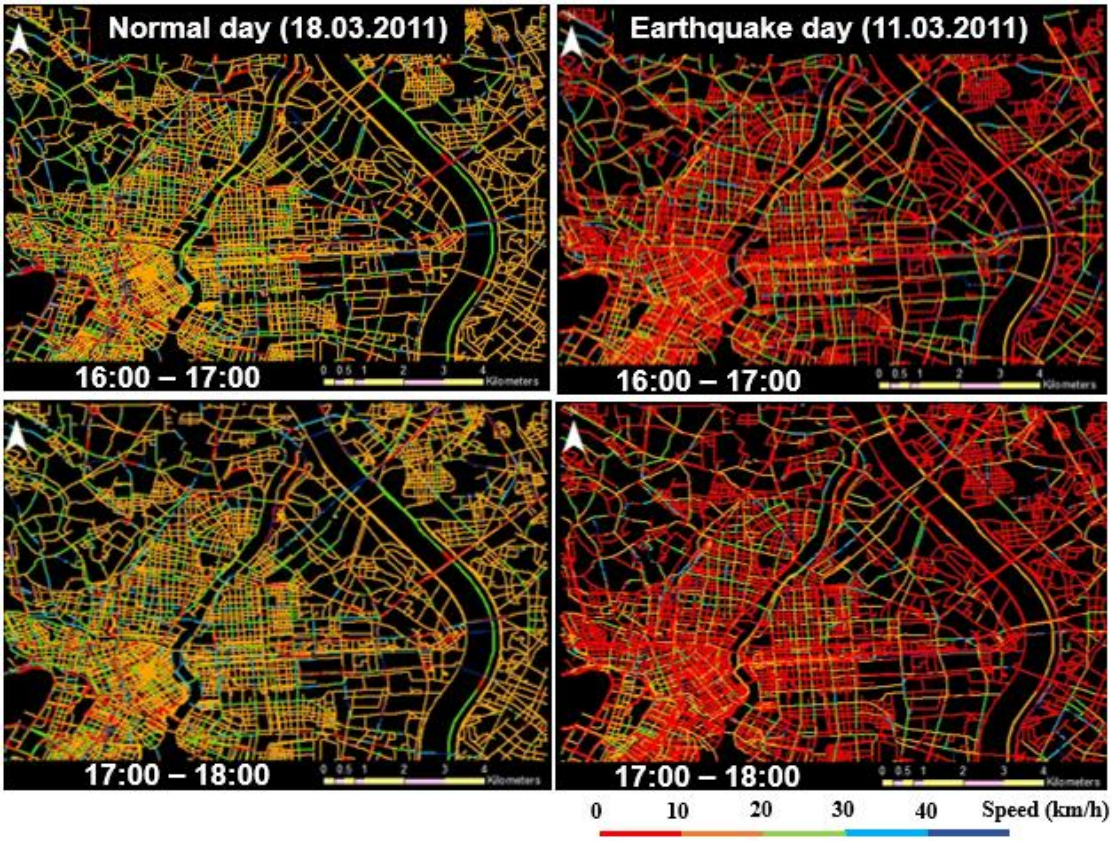

Figure 6.12 Link speed variability for the period from 16:00 to 18:00 hrs.

Figure 6.11 and Figure 6.12 evidenced the formation of congestion after the occurrence of the earthquake at 14:46 hrs. in JST. During the first hour which is from 14:00 to 15:00, there cannot observe much differences as it is less influenced due to the disaster. But, in the next three hours from 15:00 to 18:00, the figures clearly show the speed reduction of the links so as in the entire network. Meanwhile in the normal day, there cannot visualize any significant changes in the link speeds, other than some isolated links here and there, throughout the considered period.

In addition to the link speed maps, their frequency density distributions were plotted in order to understand the speed distribution during each hour and compared with normal day variations. Figure 3.13 showed the respective distributions from 14:00 hrs to 18:00 hrs.

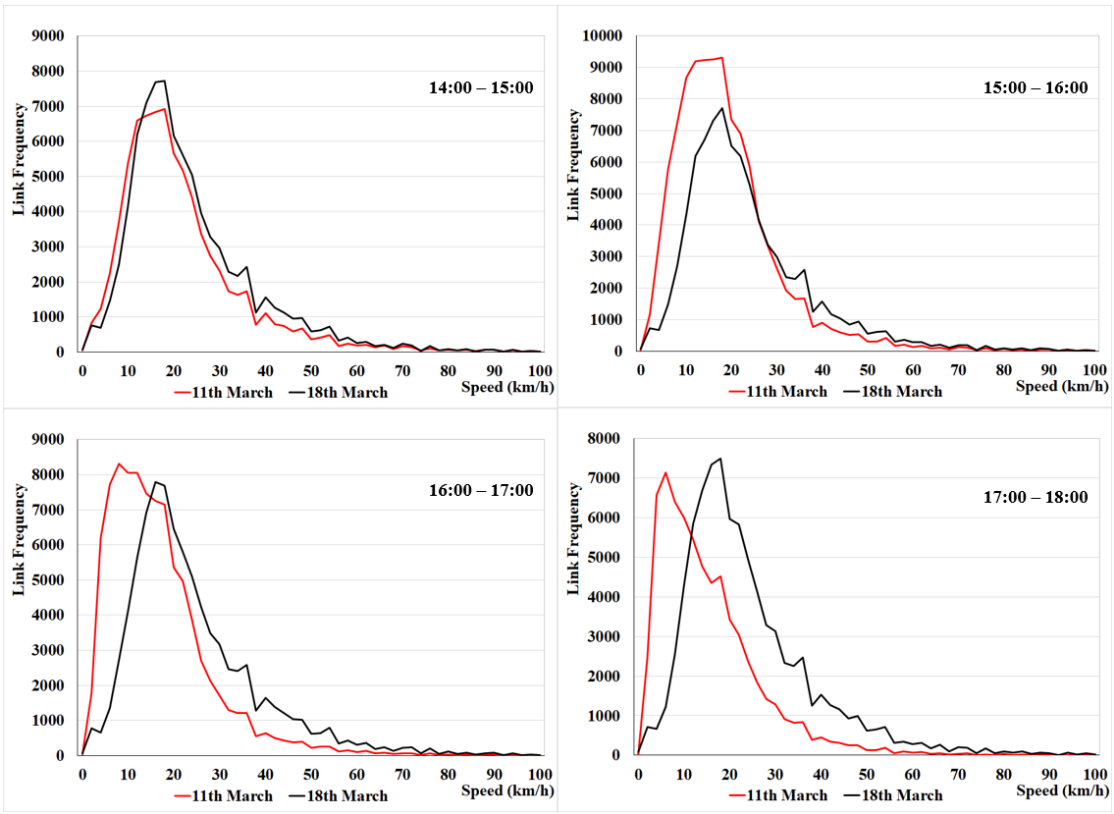

Figure 6.13 Frequency density of link's speed

As Figure 6.13 illustrates, from 14:00 to 15:00, link's speed frequency density curves do not show any significant differences between them as they are not much effected by the earthquake. When it moves to next hour, it clearly indicate that links with lesser speeds have increased while the links with higher speeds have decreased. Further, it showed an increase of link usage compare to the normal day. During the hour from 16:00 to 17:00, the distribution of the 11th March has shifted towards the left side of the plot showing that more links were suffering with low speeds. The peak of the plot of the 11th March has dropped up to 8 km/h by illustrating how severely congested the network between 16:00 to 17:00. Further speed down indicates in the next hour as well. Moreover, the analysis of link speed reduction patterns was supported by plotting the cumulative frequency of the link's speed. The respective plots are shown in Figure 6.14

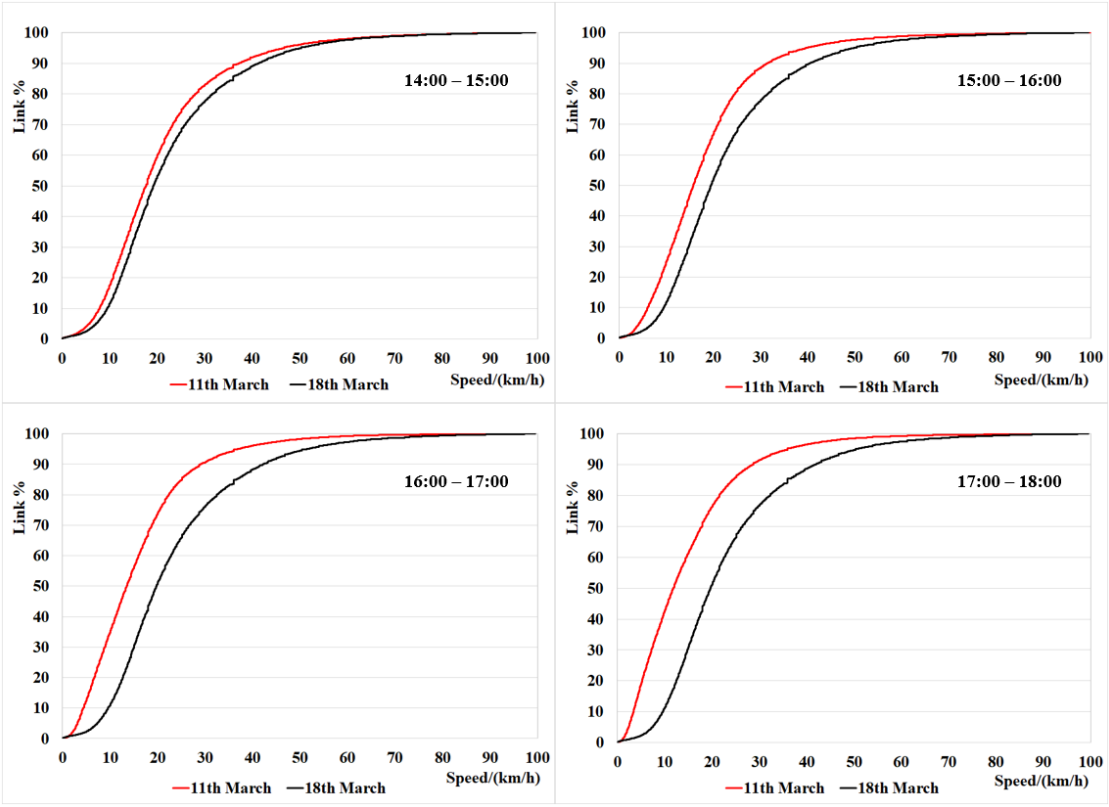

Figure 6.14 Cumulative frequency of link's speed

According to the Figure 6.14, from 14:00 to 15:00, cumulative link speed curves do not show any significant differences between them as they are not much effected by the earthquake. But, with the next hour onwards, the curves have started to separate from each other with the curve respected to disastrous day (red colour) moving towards the decreasing side of the speed. This indicates the increasement of lesser speed links compare to the normal conditions. The gap between the curves are continue to increase as the entire network got congested during the considered period.

Under disastrous condition where the traffic network get congested, it is important to understand the links variability under a certain threshold value of speed. Hence, variability of links having a speed less than 10 km/h was plotted and compared with normal day variation. The respective plot is shown in Figure 6.15

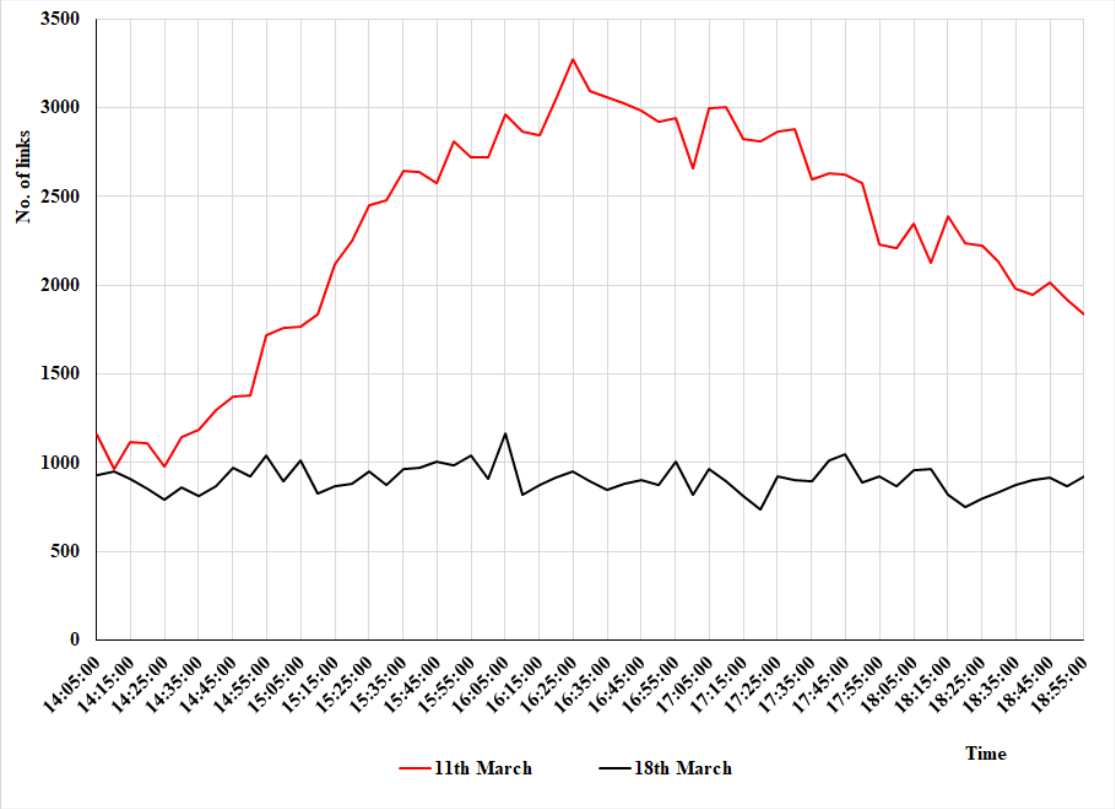

Figure 6.15 Variability of links having speed less than 10 km/h

Figure 6.15 clearly showed that the number of links having speed of less than 10 km/h starts to increase after the occurrence of earthquake, at 14:46 hrs. Then it reaches peak about 16:25 hrs and reduces thereafter. Meanwhile, no much fluctuations are observed in the normal day. Number of links with a speed less than 10 km/h become three times larger than the normal day after one and half hours from the occurrence of earthquake for the considered network and it indicates the severity of the congestion.

6.3.4 Analysis of congestion index variation

Unlike during the influence of the great east Japan earthquake, situation under the torrential downpour is location specific where the underpasses are presents (Figure 6.2). There are many evidences regarding underpass flooding around the world (Ali, 2018; Riva, 2017; Gerber, 2017; Wirth, 2018) but very less studies found in the literature in terms of travel behavior understanding, for the best of my knowledge. There are some studies, but their main focus was not studying the travel behavior (Patel, Patel, Patel, Trivedi, & Patel, 2017).

Congestion indexes (CI) were calculated on the links that were connected to the inundated areas for understanding the congestion at respective locations by using the relationship proposed by Dias et al. (Dias, Miska, Kuwahara, & Warita, 2009).

$$CI = \begin{cases} (V_{FF} - V)/V_{FF} & ; if\ V \leq V_{FF}\ and\ V_{FF} > 0 \\ 0 & ; if\ V > V_{FF} \end{cases} \quad (6.1)$$

where; V – average link speed and V_{FF} – free flow speed.

Free flow speed was calculated as the 85th percentile of all link speeds under the no weather influence condition. It was 40 km/h. The CI ranges are classified as; CI ≤ 0.2 is free flow, 0.2 < CI ≤ 0.4 is comfortable, 0.4 < CI ≤ 0.6 is medium, 0.6 < CI ≤ 0.8 is congested and CI > 0.8 is heavily congested. Calculated CI are plotted in the GIS platform. Figure 6.16 (a), (b) and (c) shows the comparison of CI of the links, for the period from 16:00 to 17:00 on 23rd July 2013, near the inundated sections 3, 4 and 8 respectively. Green colour circles indicate the exact locations of underpasses.

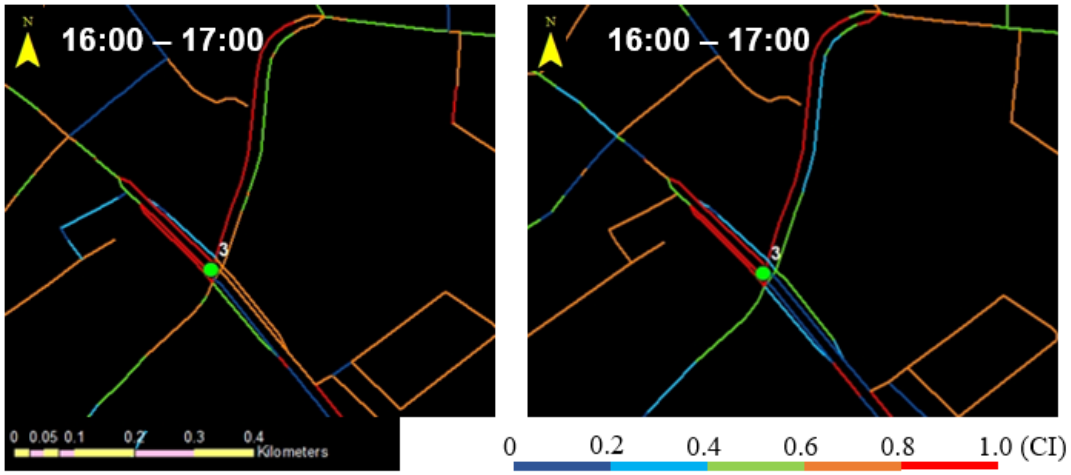

(a) Surround the under pass no. 3

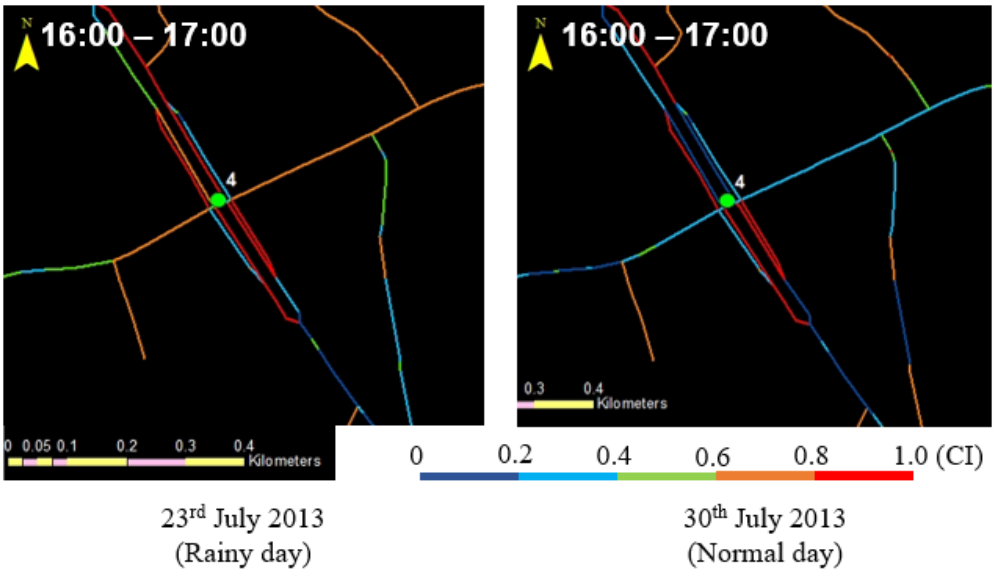

(b) Surround the under pass no. 4

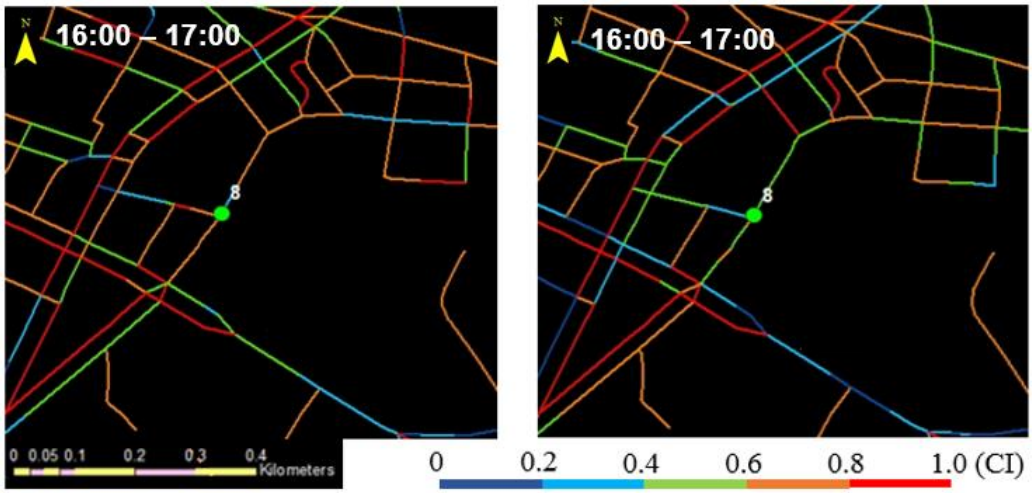

(c) Surround the under pass no. 8

Figure 6.16 Comparison of congestion indexes surround the underpasses

Figure 6.16 (a) and (b) show that some of the links near the underpass 3 and 4 were in free and comfortable zones during the normal day. But they have congested in the rainy day. In Figure 6.16 (c), the links through the underpass 8 were in comfortable and medium zones on normal day, whereas they were in congested and heavily congested zones in rainy day. These visual evidences prove that, congestion has formed after the rain, at surrounding links of the inundated locations. They are further supported with the route selection characteristics of drivers shown under the section 6.3.2

6.3.5 Right-turn ratio

With the inundation of the underpasses and depressions, drives were unable to use their normal routes. Accordingly, they had to search for alternatives that could usually cost more right turns. Since Japan is a left driving country, making right-turns is difficult and people reluctant to make right-turns. This become further headache during congestions. Hence, average right turn ratio per node was compared between the rainy day and the normal day. The respective plot is shown in the Figure 6.17

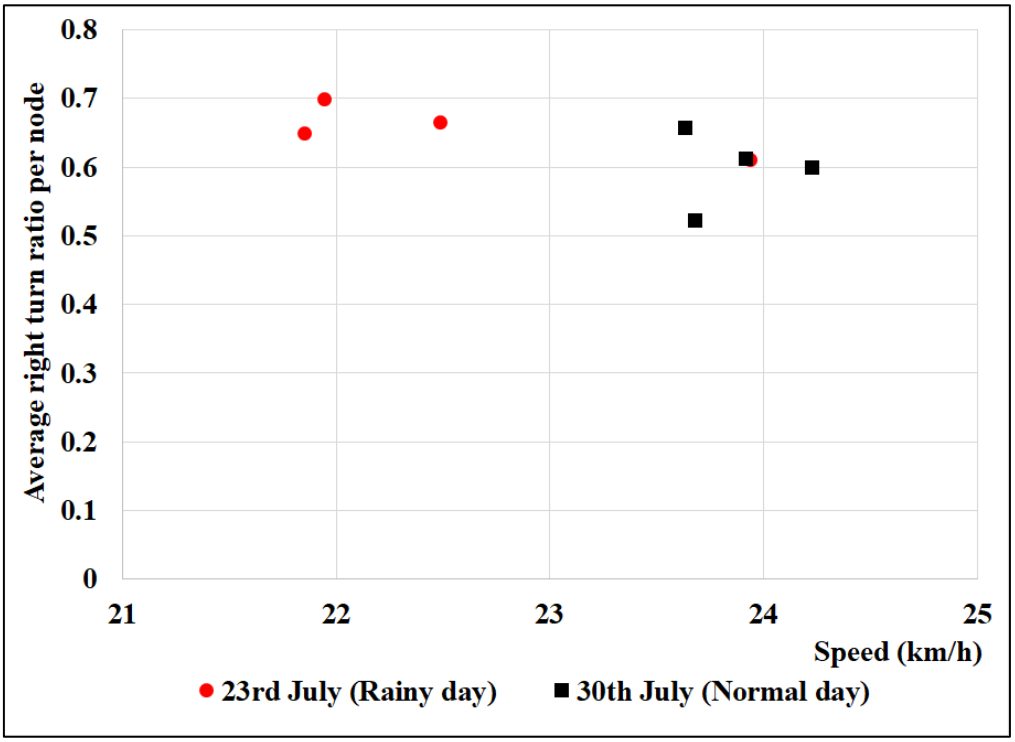

Figure 6.17 Variation of link speed with right turn ratio

Average right turn ratio was calculated by dividing the number of right turn links by total links at each node and taking the average over the entire network. As the Figure 6.17 illustrates, points refer to rainy day have higher right-turn ratio and lower speeds. While in normal day, the respective points have higher speeds and less right-turn ratios. This indicates the increase of number of right turns as a result of searching alternatives and hence reduction of the link speed. Along with that, it is important to consider the variation number of right turns per trip and it is visualized in Figure 6.18

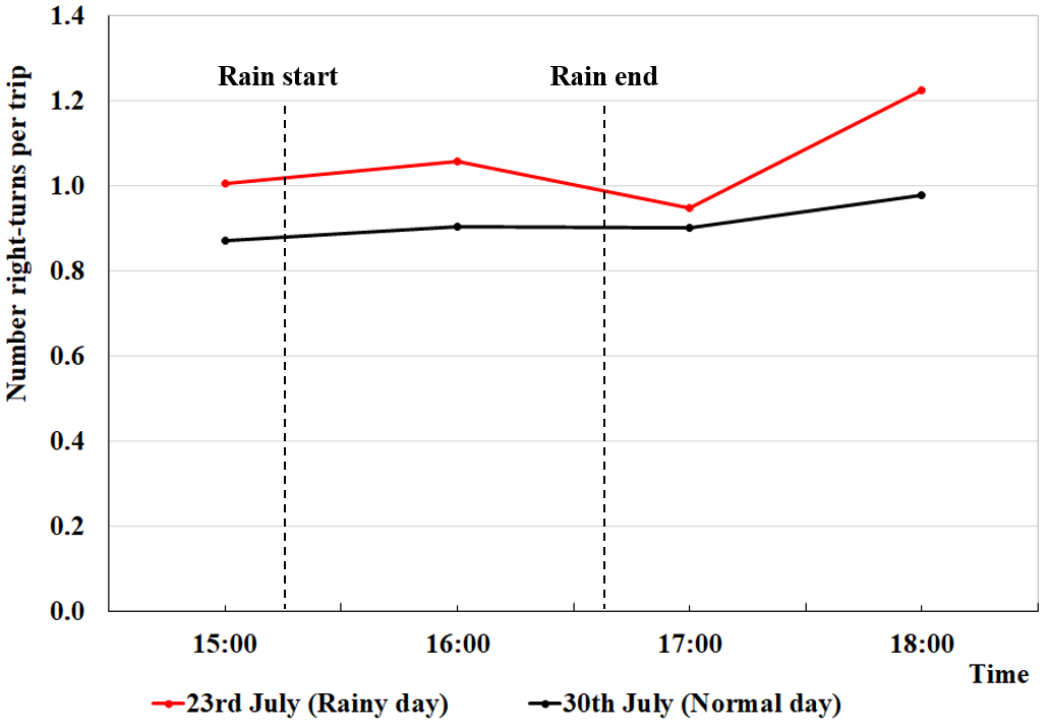

Figure 6.18 Variation of right-turns per trip with time

Unlike the great east Japan earthquake, the torrential downpour was not a sudden disaster. As the normal daily weather forecasts predicted, it is something known for the people. Correspondingly, by 15:00 hrs, it can be visualized that number of right-turns per trip is higher in the rainy day as the Figure 6.18 indicates. This can be hypothesized as people already know that, it will be a heavy rain and accordingly they tried to move quickly which result more taxi movements. Further, the number of right-turns per trip shows a little tendency of increasing with the beginning of the rainfall as people tend to move quickly taking different links and it decreases thereafter due to the congestion with the high rainfall. Later, it again increases after the rainfall as those who were waited begins to move.

6.4 Parameter estimation through β − SRL model and comparison

Sequential time discount rate (β) was estimated together with two other parameters, travel time (TT) and right turn dummy variable (RT) in β − SRL model by using the probe taxi data collected in Tokyo under the aforementioned disastrous conditions. Map matched data includes the sequential link combination of taxi trajectories and network data such as link combinations, right turns. The deterministic component of the instantaneous utility function was formulated as,

$$v(a_{j+1}|a_j) = \theta_{TT} TT_{a_{j+1}} + \theta_{RT} RT_{a_{j+1|a_j}} \quad (6.2)$$

where, TT_{a_j} is the travel time of link a_j in minutes. $RT_{a_{j+1|a_j}}$ represents the right turn dummy variable which equals to one if the turn from link a_j to a_{j+1} is a right turn with

an angle between 40^0 to 177^0 with respect to the direction of the link a_j and zero otherwise. θ is a parameter to be estimated. Two-step iterative method which includes maximization of the log-likelihood function and calculation of value function was adopted in the model estimation process. Hence, when the number of links in the network are increased, the aforementioned first step consumes more time. Therefore, it is necessary to reduce the network, for facilitating a smooth estimation process. Accordingly, two reduced areas were selected for the purpose of parameter estimation. Each area consisted 4608 and 3091 links respectively under the great east Japan earthquake and the torrential downpour. The estimation results are displayed in Table 6.2 and Table 6.3 for earthquake and torrential downpour respectively.

Table 6.2 Estimation results on great east Japan earthquake day and respective normal day

Date	**11th March 2011 (Great east Japan earthquake day)**							
Time	14:00 – 15:00		15:00 – 16:00		16:00 – 17:00		17:00 – 18:00	
	Est.	t-value	Est.	t-value	Est.	t-value	Est.	t-value
Travel Time	-0.244	-4.45	-0.238	-3.41	-0.122	-5.39	-0.016	-1.30
Right turn	-1.296	-4.89	-1.164	-3.15	-1.561	-7.24	-1.710	-7.52
β	0.536	-1.87	0.640	-0.60	0.219	-3.66	0.291	-4.20
Sample		584		294		861		1016
Lc		-411.234		-312.245		-389.897		-515.599
LL		-201.315		-94.673		-331.011		-425.087
ρ^2		0.510		0.697		0.151		0.175
Date	**18th March 2011 (Normal day)**							
Time	14:00 – 15:00		15:00 – 16:00		16:00 – 17:00		17:00 – 18:00	
	Est.	t-value	Est.	t-value	Est.	t-value	Est.	t-value
Travel Time	-0.384	-4.83	-0.314	-4.44	-0.216	-3.27	-0.173	-2.48
Right turn	-0.873	-3.50	-1.078	-3.73	-0.890	-3.44	-0.644	-2.32
β	0.548	-1.61	0.214	-2.76	0.555	-1.29	0.614	-0.76
Sample		406		347		350		305
Lc		-361.780		-182.014		-314.969		-379.916
LL		-157.813		-151.536		-154.906		-126.955
ρ^2		0.564		0.167		0.508		0.666

Table 6.3 Estimation results in torrential downpour day and respective normal day

Date	**23rd July 2013 (Torrential downpour day)**							
Time	14:00 – 15:00		15:00 – 16:00		16:00 – 17:00		17:00 – 18:00	
	Est.	t-value	Est.	t-value	Est.	t-value	Est.	t-value
Travel Time	-0.289	-4.65	-0.219	-4.81	-0.145	-4.87	-0.142	-4.70
Right turn	-0.598	-3.15	-0.345	-2.04	-0.529	-3.80	-0.844	-5.17
β	0.438	-2.24	0.295	-2.94	0.191	-4.01	0.326	-3.79
Sample		820		1085		1289		1347
Lc		-364.044		-372.180		-558.948		-546.656
LL		-258.284		-321.934		-514.953		-457.989
ρ^2		0.291		0.135		0.079		0.162
Date	**30th July 2013 (Normal day)**							
Time	14:00 – 15:00		15:00 – 16:00		16:00 – 17:00		17:00 – 18:00	
	Est.	t-value	Est.	t-value	Est.	t-value	Est.	t-value
Travel Time	-0.481	-4.99	-0.279	-3.57	-0.303	-4.26	-0.451	-4.56
Right turn	-0.651	-2.52	-0.292	-1.25	-0.927	-3.80	-0.879	-3.56
β	0.401	-2.28	0.031	-1.14	0.447	-2.22	0.685	-0.35
Sample		577		568		666		519
Lc		-210.282		-189.425		-289.759		-887.100
LL		-152.222		-177.513		-199.160		-162.593
ρ^2		0.276		0.063		0.313		0.817

In order to make a direct comparison between the estimated parameters in terms of their magnitude and pattern, they have to be estimated based on the same network. When the different networks are being used for the parameter estimation, only the distribution pattern can to be compared.

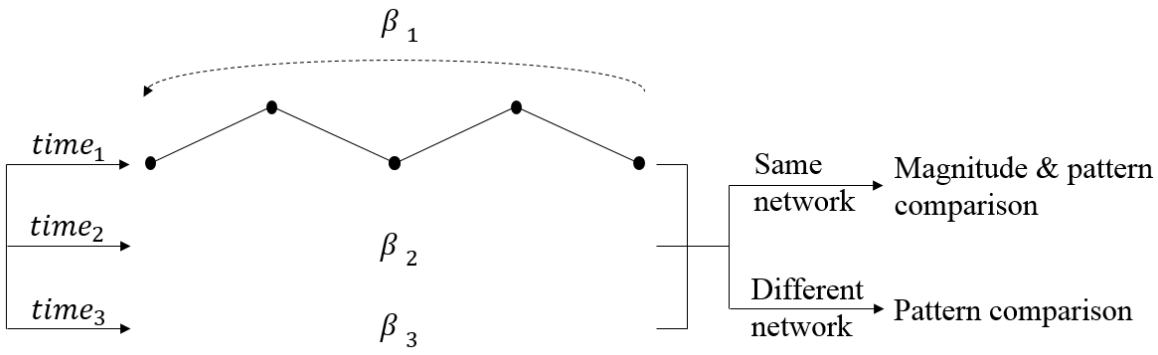

Figure 6.19 Schematic diagram of parameter comparison

6.4.1 Comparison of sequential time discount rate

Oscillation of drivers' decision-making process between myopic and global decisions is expected to illustrate through the variations of sequential time discount rate under the disastrous conditions. Since it identifies a fraction as travelers could utilize from the downstream utility up to the destination link, lower values indicate more myopic decision making behavior where the utility of the immediate links are given the priority for link choice while higher values more focused on global decision over the network. The variation of the estimated results of β are plotted, and shown in Figure 6.20

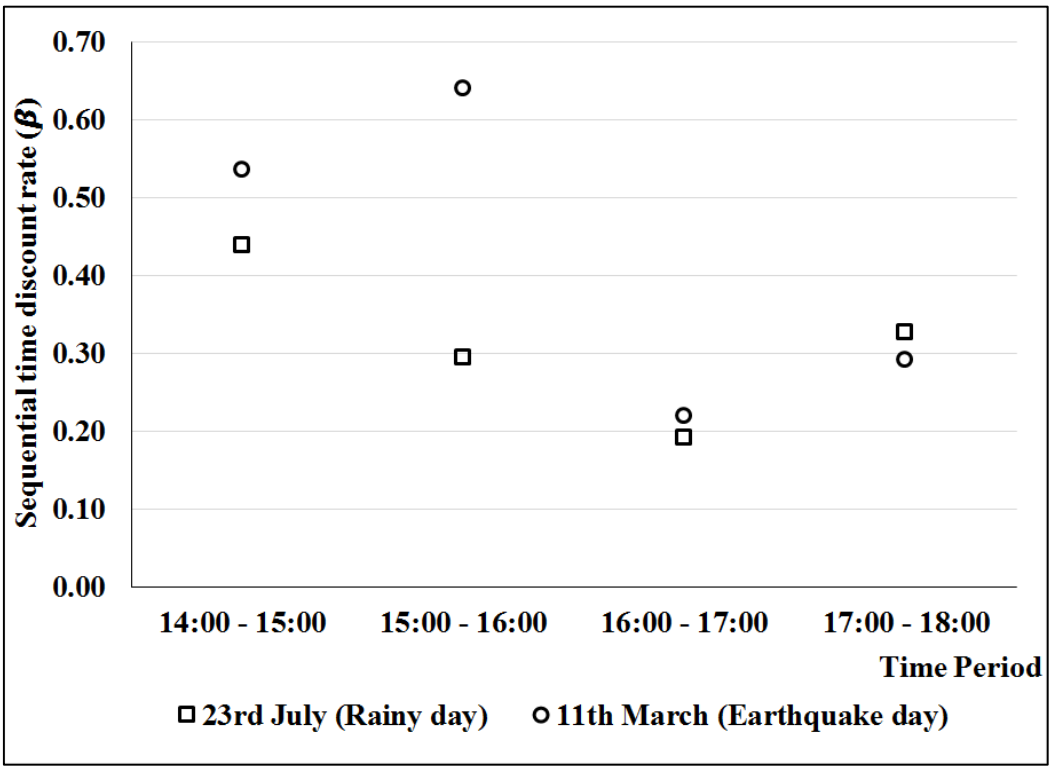

Figure 6.20 Variation of sequential time discount rate

It is expected that drivers would panic due to the unexpected massive earthquake, and unpredicted suspension of trains and Tokyo metropolitan expressway. Hence, they might have tried to maximize their global knowledge to choose links at the beginning and accordingly, the sequential time discount rate shows a higher value within the first hour after the earthquake. But, the heavy congestion forced them to turn in to the myopic decision process and as a result of that, the sequential time discount rate becomes lower in next hours. In the context of torrential downpour, the heavy rain would have been predicted under the normal weather forecasts and hence people knew that there will be a rain. But the intensity of the rainfall was high and the underpasses were inundated which could lead for the congestion. Correspondingly, the sequential time discount rate has gradually decreased as it was not suddenly congested. In a nutshell, under the both scenarios, sequential time discount rate has decreased and it reflects the changing tendency of drivers' decision-making behavior towards the myopic process in congested networks.

6.4.2 Comparison of travel time variable

As hypothesized, the estimated parameter values for travel time variable consistently indicate minus sign for all periods and are significant in most of the times. Since it was estimated together, the travel time parameter and the right turn dummy variable parameter, for the purpose of comparison, parameter ratios were considered. The ratio was determined as $\theta_{TT}/(\theta_{TT} + \theta_{RT})$, where θ_{TT} and θ_{RT} denote travel time parameter and right turn dummy parameter respectively. The calculated ratios are shown in Table 6.4

Table 6.4 Temporal variation of travel time parameter ratios

Period	Travel time ratio	
	11th March (earthquake day)	23rd July (rainy day)
14:00 – 15:00	0.158	0.326
15:00 – 16:00	0.170	0.388
16:00 – 17:00	0.072	0.215
17:00 – 18:00	0.009	0.144

The ratios are graphically presented in Figure 6.21

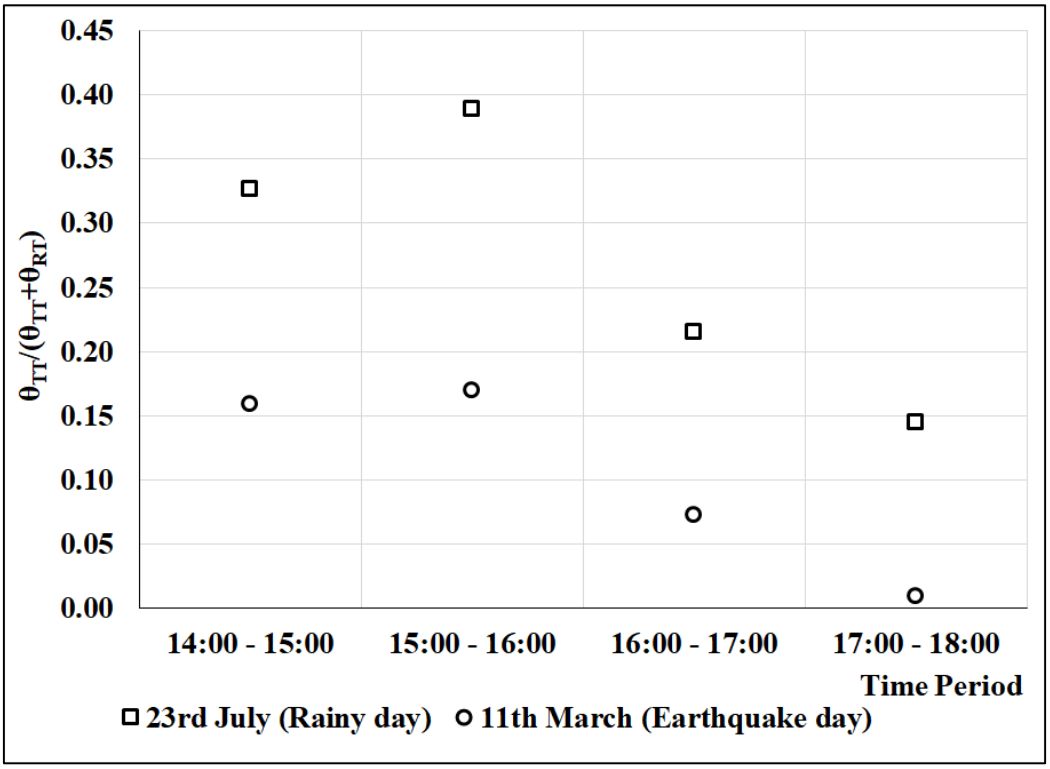

Figure 6.21 Variation of travel time parameter ratios

As per the Figure 6.21 indicates, the travel time parameter ratios under the both disaster circumstances follow a similar pattern. Both curves show little tendency of increasing with the occurrence of each disasters. This could illustrate the travelers' tendency for moving quickly to their destinations and accordingly, trying to evaluate the travel time properly before the congestion starts. Thereafter, both curves begin to decrease indicating that the difficulty of evaluating travel time properly under the congestions. The travel time parameter ratio under the great east Japan earthquake reaches almost zero during the time 17:00 to 18:00 hrs. indicate the heavy congestion occurred.

6.4.3 Comparison of right turn dummy variable

Japan is a left driving country and hence, turning right is always problematic for drivers and could be even worst under the disastrous conditions. Therefore, estimated parameters of right turn dummy variable too hypothesized to have negative signs. Precisely, parameters consistently indicated minus sign for all periods and are significant except one sample. As in the case of travel time parameter, here also, the parameter ratios were compared and are determined as $\theta_{RT}/(\theta_{TT} + \theta_{RT})$ for the right turn dummy variable. Calculated ratios are shown in Table 6.5

Table 6.5 Temporal variation of right turn dummy parameter ratios

Period	Right turn dummy parameter ratio	
	11th March (earthquake day)	23rd July (rainy day)
14:00 – 15:00	0.842	0.674
15:00 – 16:00	0.830	0.612
16:00 – 17:00	0.928	0.785
17:00 – 18:00	0.991	0.856

The graphical representation of the parameter ratios is presented in Figure 6.22

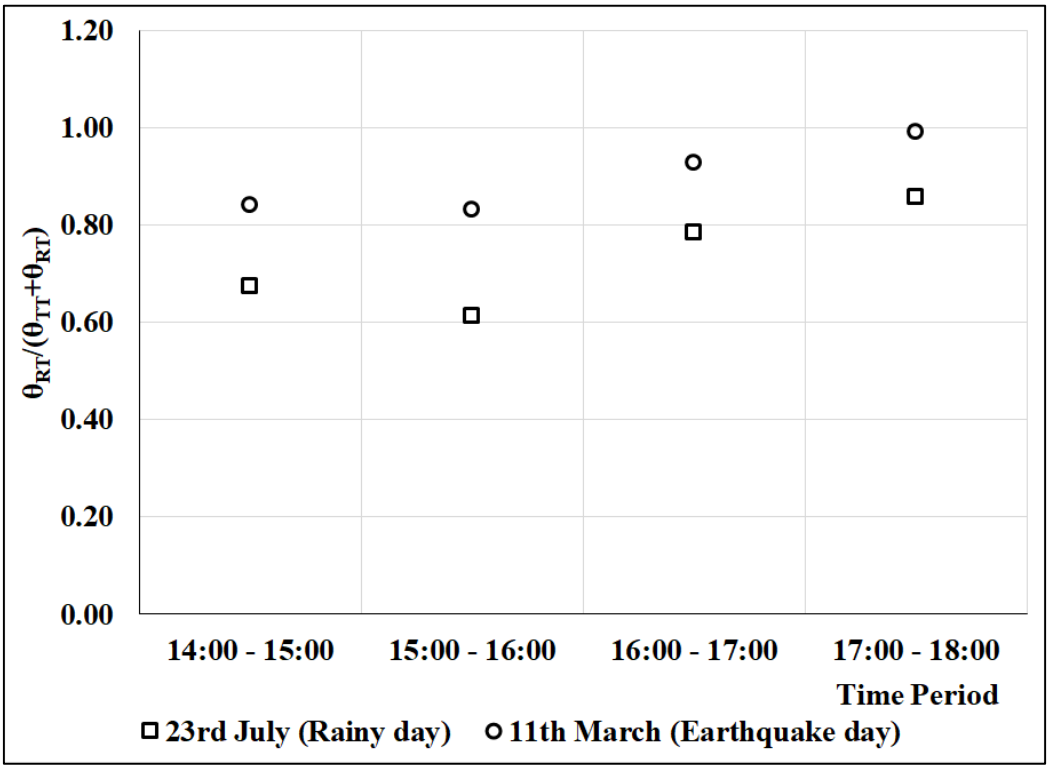

Figure 6.22 Variation of right turn dummy parameter ratios

As graphically visualized in Figure 6.22, right turn dummy parameter ratios follow a similar pattern under the both disasters. The patterns indicate marginal tendency of decreasing with the occurrence of the disasters and this refers to the phase where people trying to move quickly and it could happen more right turns. Thereafter it increases illustrating the difficulty of making right-turns under the congestions.

6.5 Conclusions and discussions

In this chapter, a comparative analysis of travel behavior in two distinct divergent disastrous networks was made by using GPS trajectories of probe taxi data collected in Tokyo under the influence of the great east Japan earthquake and a torrential downpour. Analyses were made by comparing each disaster day characteristics with respective normal day characteristics which is exactly one week after each disaster and also between both disasters themselves. Graphical illustrations were made in GIS and R platforms while parameter estimations were made by using β −SRL model.

Scrutinized time-space diagrams which include four dimensions of information such as travel time, latitude, longitude and taxi speed showed that drivers reached their destinations through longer paths, and slower speeds with many directional changes under both disastrous situations compared to their respective normal day trips. Two dimensional taxi trajectory plots visualized that drivers keen on to choose the lesser congested links in their link choice decisions which satisfied the concept of choosing maximum utility and the rational behavior.

Averaged link speed plots visualized a massive congestion after the great east Japan earthquake over the entire considered network. Frequency density distributions of link speed indicate the growth of less speed links. Precisely, the links with a lesser speed than 20 km/h increases within one hour from the occurrence of the great east Japan earthquake and speed drops further to less than 10 km/h within the next two hours. This was additionally supported by plotting the cumulative frequency of link speed which indicate the link percentages that drops at each speed levels comparatively to the respective normal day.

As it clearly shows a massive congestion after the occurrence of the earthquake, a threshold value for link speed was defined as 10 km/h and draw the variability of number of links having a lesser speed than the threshold value. The plot visualized that the respective links start to increase just after the occurrence of earthquake and reaches its peak about 16:25 hrs. JST and reduces thereafter. The number of links which were less than 10 km/h become three times larger than the normal day at its peak and it indicates the severity of the congestion occurred.

The influence of the torrential downpour was not over the entire network but instead, it was location specific which was around the inundated underpasses. Hence, congestion indexes of the surrounded links at the underpasses areas were calculated and visualized in the GIS platform. The results clearly showed that the links have congested around the underpasses which were not under congestion on the respective normal day.

Since Japan is a left driving country, making right turns become comparatively difficult under the congestions and therefore, variability of right turn ratios was compared against speed. As the number of right turns raise, the speed tends to decrease. Therefore, link speed was plotted against the average right turn ratios per node. The graph indicate that the right turn ratios are higher in the rainy day and correspondingly speed has reduced.

Making right turns are then further investigated by graphing number of right turns per trip against the time. The plot showed a little tendency of increasing with the beginning of rainfall as people used to move quickly with the bad weather. Then it drops in the next hour as the network get congested and increase later as the rainfall was over. Meanwhile, variation on the normal day shows a slight increasing trend as time moves from 14:00 to 18:00 in the afternoon.

Travel behavior under the aforementioned disasters were further investigated by estimating the parameters through the β −SRL model. Sequential time discount rate was estimated with travel time parameter and right turn dummy variable. Estimated values of β showed slight increasing trend with the occurrence of the earthquake as drivers would tried to maximize their global knowledge over the network for link choosing. But it drops then drastically due to the heavy congestion occurred with the suspended railway and Tokyo metropolitan expressway. The story was little different under the torrential downpour as it gradually decreased with the start of the rainfall. No panic situation was hypothesized under this scenario as rainfall would have predicted under the normal weather forecasts in Tokyo.

Variation of travel time parameter was presented as a ratio to the summation of right turn dummy variable parameter and travel time parameter itself. The curves follow a similar pattern under both disasters as it slightly increases in the immediate hour with the occurrence of disasters and decrease thereafter. This decreasing indicates the difficulty of evaluating travel time properly under the congestions. Severity under the earthquake was also been visualized in the graphs. Right turn dummy variable also presented as a ratio to the summation of travel time variable and right turn dummy parameter itself. The results showed closer patterns under both disasters and they were increasing with the time as congestion was occurred during both events. These trends illustrate the difficulty of making right turns under the congestions.

7 Conclusions and future works

This thesis evaluates the sensitivity, stability, performance and applicability of sequential time discount rate in understanding route choice behavior in different traffic networks. Sequential time discount rate was estimated as a parameter in β −scaled recursive logit model (Oyama, Chikamatsu, Shoji, Hato, & Koga, 2016). This chapter (7) provides an overview of the entire study discussed in aforementioned chapters.

7.1 Conclusions of the thesis

Chapter 3 explained the theoretical framework of recursive logit model (Fosgerau, Frejinger, & Karlstrom, 2013) and β − scaled recursive logit model (Oyama, Chikamatsu, Shoji, Hato, & Koga, 2016) in detail. Then the sensitivity of the sequential time discount rate on route choice probabilities was tested. Three different values of sequential time discount rate were used as $\beta = 0, \beta = 0.5\ and\ \beta = 1$ for understanding the deviations in link assignments under each condition by using a hypothetical network. Five scenarios as the original network conditions (Figure 3.2), introducing low cost links at the downstream, introducing high cost links at the downstream, introducing low cost links near the origin and introducing high cost links near the origin were used for the analysis. Route choice probabilities and link assignments under the recursive logit framework indicated that myopic decisions become crucial when the $\beta = 0$ and link choices being made based on the separated link costs. Further it clearly visualized the worst impacts of myopic decisions for route choosing by assigning larger flows to high costs links. This could lead to make heavy congestions in congested links. In addition, its further showed that making changes on link cost at downstream has no impact on the network assignments under the myopic decisions. Meanwhile higher values of sequential time discount rate always made the route choice decisions considering route-based decisions from origin to destination. Hence, it was clearly visualized that under the condition of $\beta = 1$, larger flows being assigned to low cost routes as they were given higher probabilities. As a conclusion, the analysis clearly showed the impact of sequential time discount rate on predicting link assignments under different circumstances.

Chapter 4 tested the stability of sequential time discount rate under different network settings. In usual practice in modeling route choice behavior, parameters are estimated by considering hourly periods of data. Since this could miss tiny variations of the network behavior in between the considered periods, stability of the sequential time discount rate was tested with the moving time. The results showed, that the β −SRL model is capable of estimating stable and reliable values for sequential time discount rate for the entire considered period of time. Finding the adequate minimum number of trips for stable estimation is always important for saving simulation time. Hence, model stability of estimating sequential time discount rate was evaluated under three categories as 10 trips, 20 trips and 30 trips. Visual observations together with statistical parameters illustrated that the 20 trips and 30 trips samples produced more stable results comparatively to the 10 trips samples. Besides, the asymptotic t test was performed and the resulted t values

were insignificant for all the considered samples and hence, it indicated that there are no significant differences between the estimated sequential time discount rates in each category. Precisely, the model estimations are stable. With this base, same sampling technique was tested by estimating in distinct networks such as different time zones, different networks and different size of trips. The overall results showed that β – SRL model estimate better results under all 03 categories while 20 trips and 30 trips samples always provide stable and reliable results compare to the 10 trips samples. Further, the improvements of the results from 10 trips samples to 20 trips samples was larger in comparison with the improvements from the 20 trips samples to the 30 trips samples.

Former part of the chapter 5 is utilized for explaining the mathematical characteristics of solving the value function in the β – SRL model while the latter part of the chapter described the model performances under different network settings. Since the value functions with respect to each link of the considered network can be determined by solving the system of non-liner equations of the sequential time discount rate, here we produced the element base changes of such a system of non-liner equations by using a hypothetical network. In the second half of the chapter 5, the model performances were discussed based on normalized network, scaled network, extended network and number of links per trip. Changes in the route choice probabilities from myopic decisions to route-based decisions were observed by changing the sequential time discount rate in a hypothetical network. These characteristics were changed with the normalized network where it assigned the links with equal probabilities at decision making nodes under the myopic conditions. Meanwhile, route choice probabilities also observed to be normalized under the condition of sequential time discount rate was equal to one. The analyses with the real world data showed a lowering of sequential time discount rate, improvements in log likelihood ratio index, and reduction of simulation time in normalized network conditions in comparison with the real network conditions. The analysis based on scaled network showed that the results are holding the equivalent differences property between the alternatives. Lower sequential time discount rates were observed in the extended networks as it kept the original route choices unchanged. The results based on the influence of the number of links per trip showed that the model performance become more consistent and the estimations become more stable when estimating the samples having trips with their number of links per trip is more than 50 links.

Comparative analysis of network behavior under two distinct and divergent disasters, the great east Japan earthquake and a torrential downpour was done at chapter 6 as a case study. Probe taxi data collected under the aforementioned disaster conditions and normal days as one week after each disaster were used for the analysis. Route choice characteristics were visualized by making a cross sectional analysis and travel behavior under each disastrous conditions were compared with a normal day variations. During both disasters that altered the normal city life, drivers had to change their original travel plans and choose alternatives. The sequential time discount rate was estimated together with two other parameters, travel time and right turn dummy variable in both circumstances. The estimated values of sequential time discount rate indicated the

transition of drivers' decision-making process from global decisions to myopic decisions. In addition, the estimated values of travel time parameter under both events indicated the difficulty for drivers to evaluate travel time properly, under the congestions. The estimations of right turn dummy variable showed an increasing difficulty of making right-turns under both disaster scenarios.

7.2 Future works

In chapter 3, network assignment results were determined by using a hypothetical network under the route choice probabilities of the β −scaled recursive logit framework. Unidirectional flows were utilized to visualize the network assignments. This steps need to be further extended up to a real network conditions with multidirectional flows and calculate network assignment results under varying sequential time discount rates. Since sequential time discount rate is estimated for a specific time frame, it can be further extended to visualized the timely varied network conditions. Various times of the day, different dates such as working days, weekends, public holidays can be analyzed.

As discussed in chapter 4 and chapter 5, calculation of sequential time discount rate is highly correlated with the number of trips and their links used in considered trips. In other words, there may be a relationship between the network density and link lengths with the sequential time discount rate. Therefore, it is worth to carry out a study under different densified networks and networks with different link lengths. Link lengths are different to each other always, but governing link sizes of the network can be identified by drawing cumulative frequency plots and model performances can be tested.

In chapter 6, parameter comparison was made based on estimations done in hourly basis. Hence, in order to more scrutinizing the travel behavioral patterns, it would be interesting to follow moving time method (chapter 4). Further, the comparison of disaster travel behavior was made by using the data of exactly one week after the disaster. It would be nice to analyze the travel behavior of few consecutive days before and after the disaster including one week before and after as well. But these analyses are permitted to the availability of probe taxi data which currently not available. In addition, taxi drivers are professional drivers and their network knowledge is high as they are highly familiar with the route network. Further, under the normal circumstances there is a current trend that almost all drivers use the applications like google maps for searching the best route. Hence it would be great to study the variations of sequential time discount rate when the route choice is being done between professional and non-professional drivers, using and without using applications for choosing route.

8 References

Ali, S. (2018, 05 27). *The Express Tribune*. Retrieved 05 27, 2018, from Karachi's eight underpasses underwater: https://tribune.com.pk/story/1447319/karachis-eight-underpasses-underwater/

Barker, K., Ramirez-Marquez, J., & Rocco, C. M. (2013). Resilience-based network component importance measures. *Reliability Engineering & System Safety, 117*, 89-97. doi:10.1016/j.ress.2013.03.012

Bekhor, S., & Prashker, J. N. (2001). Stochastic User Equilibrium Formulation for Generalized Nested Logit Model. *Transportation Research Record 1752*, 84-90.

Bekhor, S., Ben-Akiva, M. E., & Ramming, M. S. (2002). Adaptation of Logit Kernel to Route Choice Situation. *Transportation Research Record 1805*, 78-85.

Bellman, R. E. (1957). *Dynamic programming.* Princeton University Press.

Ben-Akiva, M., & Bierlaire, M. (1999). Discrete choice methods and their applications to short term travel decisions. In *Handbook of Transportation Science* (pp. 5-33). Boston, MA: Springer.

Ben-Akiva, M., & Lerman, S. (1985). *Discrete Choice Analysis Theory and Application to Travel Demand* (Vol. 9). MIT Press series in transportation studies.

Bharosa, N., Lee, J., & Janssen, M. (2010). Challenges and obstacles in sharing and coordinating information during multi-agency disaster response: Propositions from field exercises. *Information Systems Frontiers, 12*(1), 49-65. doi:10.1007/s10796-009-9174-z

Bickel, W. K., & Johnson, M. W. (2003). Delay discounting: A fundamental behavioral process of drug dependence. *Time and Decision*, 419-440.

Bolduc, D., & Ben-Akiva, M. (1991). A Multinomial Probit formulation for large choice sets. *6th Internatioanl conference on travel behaviour*, (pp. 243-258).

Bono, F., & Gutierrez, E. (2011). A network-based analysis of the impact of structural damage on urban accessibility following a disaster: the case of the seismically damaged Port Au Prince and Carrefour urban road networks. *Journal of Transport Geography, 19*(6), 1443-1455. doi:10.1016/j.jtrangeo.2011.08.002

Bovy, P. H., & Stern, E. (1990). *Route Choice: Wayfinding in Transport Networks.* Springer Netherlands. doi:10.1007/978-94-009-0633-4

Cantarella, G. E., & Watling, D. P. (2016). A general stochastic process for day-to-day dynamic traffic assignment: Formulation, asymptotic behaviour, and stability analysis. *Transportation Research Part B, 92*, 3-21. doi:10.1016/j.trb.2016.05.005

Cascetta, E., Nuzzolo, A., Russo, F., & Vitetta, A. (1996). A modified logit route choice model overcoming path overlapping problems. Specification and some calibration results for interurban networks. *Proceedings of the 13th*

International Symposium on Transportation and Traffic Theory, (pp. 697-711). Lyon, France.

Chang, S. E., & Nojima, N. (2001). Measuring post-disaster transportation system performance: the 1995 Kobe earthquake in comparative perspective. *Transportation Research Part A, 35*, 475-794.

Chapman, G. B., & Elstein, A. S. (1995). Valuing the Future: Temporal Discounting of Health and Money. *Medical Decision Making*, 373-386. doi:10.1177/0272989X9501500408

Cools, M., Moons, E., Creemers, L., & Wets, G. (2014). Changes in Travel Behavior in Response to Weather Conditions. *Transportation Research Record, 2157*, 21-28. doi:10.3141/2157-03

Dias, C., Miska, M., Kuwahara, M., & Warita, H. (2009). Relationship between congestion and traffic accidents on expressways: An investigation with Bayesian belief networks. *40th Annual Meeting of Insfrastructure Planning (JSCE).* Japan.

Dijkstra, E. W. (1959). A note on two problems in connexion with graphs. *Numerische Mathematik, 1*, 269-271.

Dimitrou, L., & Stathopoulos, A. (2016). Capturing System-wide Magnitude of Earthquakes' Effects on Urban Traffic Networks. *IFAC-PapersOnLine, 49*(3), 243-248. doi:10.1016/j.ifacol.2016.07.041

Dinh, D. D., & Kubota, H. (2013). Profile-speed data-based models to estimate operating speeds for urban residential streets with a 30 km/h speed limit. *IATSS Research, 36*(2), 115-122. doi:doi.org/10.1016/j.iatssr.2012.06.001

Donnell, E. T., Hines, S. C., Mahoney, K. M., & Porter, R. J. (2009). *Speed Concepts: Informational Guide.* Pennsylvania State University. Retrieved from https://safety.fhwa.dot.gov/speedmgt/ref_mats/fhwasa10001/

Faturechi, R., & Hooks, E. M. (2014). Travel time resilience of roadway networks under disaster. *Transportation Research Part B: Methodological, 70*, 47-64. doi:10.1016/j.trb.2014.08.007

Fosgerau, M., Frejinger, E., & Karlstrom, A. (2013). A link based network route choice model with unrestricted choice set. *Transportation Research Part B, 56*, 70-80. doi:http://dx.doi.org/10.1016/j.trb.2013.07.012

Frederick, S., Loewenstein, G., & O'Donoghue, T. (2002). Time Discounting and Time Preference: A Critical Review. *Journal of Economic Literature, 40*(2), 351-401. Retrieved from http://www.jstor.org/stable/2698382

Frejinger, E., & Bierlaire, M. (2007). Capturing correlation with subnetworks in route choice models. *Transportation Research Part B: Methodological, 41*(3), 363-378. doi:10.1016/j.trb.2006.06.003

Gao, B., Zhang, R., & Lou, X. (2016). Modeling Day-to-day Flow Dynamics on Degradable Transport Network. (W.-B. Du, Ed.) *PLOS ONE, 11*(12), 1-19. doi:10.1371/journal.pone.0168241

Gerber, C. (2017, 10 02). *Kokomo Tribune*. Retrieved 05 27, 2018, from Peru searches for cheaper fix to underpass flooding: http://www.kokomotribune.com/news/peru-searches-for-cheaper-fix-to-underpass-flooding/article_892e79be-a7b1-11e7-8182-276b5c6251c2.html

Giuliano, G., & Golob, J. (1998). Impacts of the Northridge Earthquake on Transit and Highway Use. *Transportation and Statistics, 1*(2), 1-20.

Green, L., Fristoe, N., & Myerson, J. (1994). Temporal discounting and preference reversals in choice between delayed outcomes. *Psychonomic Bulletin & Review, 1*(3), 383-389. doi:10.3758/BF03213979

Hamilton, K., Peden, A. E., Keech, J. J., & Hagger, M. S. (2018). Changing people's attitudes and beliefs toward driving through floodwaters: Evaluation of a video infographic. *Transportation Research Part F, 53*, 50-60. doi:https://doi.org/10.1016/j.trf.2017.12.012

Hara, Y. (2015). Behaviour analysis using tweet data and geo-tag data in a natural. *Transportation Research Procedia, 11*, 399-412. doi:10.1016/j.trpro.2015.12.033

Hashida, T. (2016). *Climate change monitoring report 2015.* Tokyo: Japan Meteorological Agency.

Hashim, I. H. (2011). Analysis of speed characteristics for rural two-lane roads: A field study from Minoufiya Governorate, Egypt. *Ain Shams Engineering Journal, 2*(1), 43-52. doi:doi.org/10.1016/j.asej.2011.05.005

Hato, E. (2007, August 1). *What is probe person technology*. Retrieved 4 23, 2018, from JSTE Probe Research Group: http://www.probe-data.jp/eng/about/index.html

Helton, W. S., Kemp, S., & Walton, D. (2013). Individual differences in movements in response to natural disasters: Tsunami and earthquake case studies. *Human factors and ergonomics society 57th annual meeting*, (pp. 858-862). doi:10.1177/154193121357186

Holyoak, N., & Taylor, M. A. (2006). Modelling trip timing behaviour and the influence of peak spreading. *Urban Transport and the Environment in the 21st Century, WIT Transactions on The Built Environment*, pp. 205-213. doi:10.2495/UT060211

Hou, Y., Sun, C., & Edara, P. (2012). A statistical test for 85th and 15th percentile speeds using the asymptotic distribution of sample quantiles. *Transportation Research Record*, 47-53. doi:doi.org/10.3141/2279-06

Huang, H., Liu, T., & H, Y. (2010). Modeling the evolutions of day-to-day route choice and year-to-year ATIS adoption with stochastic user equilibrium. *Journal of Advanced Transportation, 42*(2), 111-127. doi:10.1002/atr.5670420202

Hunter, T., Herring, R., Abbeel, P., & Bayen, A. (2009). Path and travel time inference from GPS probe vehicle data. *International Workshop on Analyzing Networks and Learning with Graphs.* Vancouver, Canada.

Iida, K. (2006, 01 11). *Geosense Inc*. (Geosense Corporation) Retrieved 10 20, 2016, from http://www.geosense.co.jp/map/tool/geoconverter.php

Iida, Y., Karauchi, F., & Shimada, H. (2000). Traffic management system against major earthquakes. *IATSS Research, 24*(2), 6-17. doi:10.1016/S0386-1112(14)60024-8

Iida, Y., Kurauchi, F., & Shimada, H. (2000). Traffic management system against major eathquakes. *IATSS Research, 24*(2), 6-17.

IPCC. (2015). *Climate Change 2014: Synthesis Report. Contribution of Working Groups I, II and III to the Fifth Assessment Report of the.* Geneva, Switzerland: IPCC. doi:ISBN 978-92-9169-143-2

Jenelius, E., & Mattsson, L. G. (2012). Road network vulnerability analysis of area-covering disruptions: A grid-based approach with case study. *Transportation Research Part A, 46*, 746-760. doi:10.1016/j.tra.2012.02.003

Jin, F., Yao, E., Zhang, Y., & Liu, S. (2017). Metro passenger's route choice model and its application considering perceived tranfer threshold. *PLOS ONE, 12*(9), 1-17. doi:https://doi.org/10.1371/journal.pone.0185349

Kattan, L., De Barros, A. G., & Saleemi, H. (2013). Travel behavior changes and responses to advanced traveler information in prolonged and large-scale network disruptions: A case study of west LRT line construction in the city of Calgary. *Transportation Research Part F, 21*, 90-102. doi:10.1016/j.trf.2013.08.005

Khan, M. H., Wisetjindawat, W., Fujita, M., & Suzuki, K. (2013). An Analysis of Probe Data on Traffic Congestion During the Typhoon Using GIS Application. *Eastern Asia Society for Transportation Studies, 9.*

Kim, C., Cheon, S. H., Choi, K., Joh, C. H., & Lee, H. J. (2017). Exposure to Fear: Changes in Travel Behavior During MERS Outbreak in Seoul. *KSCE Journal of Civil Engineering*, 2888-2895. doi:10.1007/s12205-017-0821-5

Kirby, K. N., & Marakovic, N. N. (1995). Modeling myopic decisions: Evidence for hyperbolic delay-discounting within subjects and amounts. *Organizational Behavior and Human Decision Processes*, 22-30. doi:10.1006/obhd.1995.1086

Knoop, V. L., Hoogendoorn, S. P., & Zuylen, H. V. (2010). Rerouting behaviour of travellers under exceptional traffic conditions – an empirical analysis of route choice. *Procedia Engineering, 3*, 113-128. doi:10.1016/j.proeng.2010.07.012

Koppelman, F. S., & Wen, C. (2000). The paired combinatorial logit model: properties, estimation and application. *Transportation Research Part B: Methodological*, 75-89. doi:10.1016/S0191-2615(99)00012-0

Lee, J. B., Zheng, Z., Kashfi, S., Chia, J., & Yi, R. (2013). Observation of Bus Ridership in the Aftermath of the 2011 Floods in Southeast Queensland, Australia. *9th Annual International Conference of the International Institute for Infrastructure Renewal and Reconstruction.* Brisbane.

Lee, S., Heydecker, B. G., Kim, J., & Park, S. (2017). Stability analysis on a dynamical model of route choice in a connected vehicle environment. *Transportation Research Procedia, 23*, 720-737. doi:10.1016/j.trpro.2017.05.040

Li, J., Ozbay, K., & Bartin, B. (2015). Effects of Hurricanes Irene and Sandy in New Jersey: traffic patterns and highway disruptions during evacuations. *Natural Hazards, 78*, 2081-2107. doi:10.1007/s11069-015-1820-9

Liao, T., Hu, T., & Ko, Y. (2018). A resilience optimization model for transportation networks under disasters. *Natural Hazards*, 1-21. doi:10.1007/s11069-018-3310-3

Liu, C., Susilo, Y. O., & Karlstrom, A. (2017). Weather variability and travel behaviour - what we know and what we do not know. *Transport Reviews*, 1-27. doi:10.1080/01441647.2017.1293188

Lu, Q. C., Zhang, J., & Rahman, A. B. (2017). The interrelationship between travel behavior and life choices in adapting to flood disasters. *Natural Hazards, 85*, 1005-1022. doi:10.1007/s11069-016-2617-1

Maghrebi, M., Abbasi, A., Rashidi, T. H., & Waller, S. T. (2015). Complementing travel diary surveys with twitter data: Application of text mining techniques on activity location, type and time. *18th International Conference on Intelligent Transportation Systems*, (pp. 208-213). doi:10.1109/ITSC.2015.43

Mai, T., Fosgerau, M., & Frejinger, E. (2015). A nested recursive logit model for route choice analysis. *Transportation Research Part B, 75*, 100-112. doi:http://dx.doi.org/10.1016/j.trb.2015.03.015

Manski, C. F. (1977). The structure of random utility models. *Theory and Decision, 8*(3), 229-254. doi:10.1007/BF00133443

Marsden, G., Anable, J., Shires, J., & Docherty, I. (2016). *Travel Behaviour Response to Major Transport System Disruptions.* International Transport Forum.

Maslac, M., Antic, B., Pesic, D., & Milutinovic, N. (2017). Behaviours of professional drivers: Validation of the DBQ for drivers who transport dangerous goods in Serbia. *Transportation Research Part F*, 80-88. doi:http://dx.doi.org/10.1016/j.trf.2017.08.001

Matherly, D., Langdon, N., Kuriger, A., Sahu, I., Wolshon, B., Renne, J., . . . Dixit, V. (2013). *A Guide to Regional Transportation Planning for Disasters*,

Emergencies, and Significant Events. Washington D.C.: National Cooperative Highway Research Program.

McFadden, D. (1974). Conditional logit analysis of qualitative choice behavior. In P. Zarembka, *Frontiers in econometrics* (pp. 105-142). New York: Academic Press.

McFadden, D. (1978). Modeling the choice of residential location. In *Spatial Interaction Theory and Planning Models* (pp. 75-96). North Holland, Amsterdam.

Meng, M., Zhang, J., Wong, Y. D., & Au, P. H. (2016). Effect of weather conditions and weather forecast on cycling travel behavior in Singapore. *International Journal of Sustainable Transportation*, *10*(9), 773-780. doi:10.1080/15568318.2016.1149646

Minhans, A. (2008). *Traffic Management Stratergies in Cases of Disasters.* Technische Universitat Darmstadt, Department of Civil Engineering and Geodesy. doi:10.13140/RG.2.1.5094.8560

Miwa, T., Sakai, T., & Morikawa, T. (2004). Route identification and travel time prediction using probe-car. *International journal of ITS research*, *2*(1), 21-28.

Mohamed, M., & Bromfield, N. F. (2017). Attitudes, driving behavior, and accident involvement among young male drivers in Saudi Arabia. *Transportation Research Part F*, *47*(http://dx.doi.org/10.1016/j.trf.2017.04.009), 59-71.

Nogal, M., O'Connor, A., Caulfield, B., & Martinez-Pastor, B. (2016). Resilience of traffic networks: From perturbation to recovery via a dynamic restricted equilibrium model. *Reliability Engineering & System Safety*, *156*, 84-96. doi:10.1016/j.ress.2016.07.020

Noordegraaf, D. M., & Annema, J. A. (2012). Employer Attitudes towards Peak Hour Avoidance. *European Journal of Transport and Infrastructure Research (EJTIR)*, *12*(4), 373-390.

Oh, Y., Chung, K., Park, S. H., Kim, C., & Kang, S. (2017). Evaluating the Impact of the Sudden Collapse of Major Freeway Connectors on Rapid Transit and Adjacent Freeway Systems: San Francisco Bay Area Case Study. *Applied Sciences*, 1-14. doi:10.3390/app7070726

Olson, M., & Bailey, M. J. (1981). Positive Time Preference. *Journal of Political Economy*, 1-25. Retrieved from http://www.jstor.org/stable/1837349

Othman, M. H., & Hamid, A. H. (2014). Impact of Flooding on Traffic Route Choices. *Sustainable Built Environment Symposium. 11*, pp. 1-9. SHS Web of Conferences. doi:10.1051/shsconf/20141101002

Oyama, Y., Chikamatsu, K., Shoji, Y., Hato, E., & Koga, M. (2016). Trajectory-oriented traffic management using sequential discount rate: a case study of the great east Japan earthquake. *11th ITS European congress.*

Patel, K., Patel, K., Patel, R., Trivedi, K., & Patel, D. M. (2017). Storm Water Drainage for Underpass. *International Journal for Innovative Research in Science & Technology, 3*(09), 23-29.

Prato, C. G. (2009). Route choice modeling: past, present and future research directions. *Journal of Choice Modeling, 2*(1), 65-100. doi:ISSN 1755-5345

Rawson, C. T. (2015). *Procedures for establishing speed zones.* Texas department of transportation.

Riva, S. (2017, 11 14). *The Phuket News*. Retrieved 05 27, 2018, from Samkong underpass flooding just bad timing: https://www.thephuketnews.com/samkong-underpass-flooding-just-bad-timing-64696.php#e8TbBaZUJCyo8sVo.97

Rust, J. (1994). Structural estimation of markov decision processes. In *Handbook of Econometrics* (pp. 3081-3143). Elsevier. doi:https://doi.org/10.1016/S1573-4412(05)80020-0

Samuelson, P. A. (1937). A Note on Measurement of Utility. *The Review of Economic Studies, 4*(2), 155-161. Retrieved from http://www.jstor.org/stable/2967612

Severens, J. L., & Milne, R. J. (2004). Discounting Health Outcomes in Economic Evaluation: The Ongoing Debate. *Value In Health, 7*, 397-401. doi:10.1111/j.1524-4733.2004.74002.x

Shafique, M. A., & Hato, E. (2016). Travel mode detection with varying smartphone data collection frequencies. *sensors*, 1-24. doi:10.3390/s16050716

Shafique, M. A., Hato, E., & Yaginuma, H. (2014). Using Probe Person Data for Travel Mode Detection. *Computer and Information Engineering, 8*(10), 1778-1782.

Si, Y., Weng, J., Chen, Z., & Wang, Y. (2014). Taxi Travel Purpose Estimation and Characteristic Analysis Based on Multi-source Data and Semantic Reasoning — A Case Study of Beijing. *Web Information Systems Engineering – WISE 2013 Workshops. 8182*, pp. 474-492. Springer, Berlin, Heidelberg. doi:10.1007/978-3-642-54370-8_40

Stanojevic, P., Lajunen, T., Jovanovic, D., Sarbescu, P., & Kostadinov, S. (2018). The driver behaviour questionnaire in South-East Europe countries: Bulgaria, Romania and Serbia. *Transportation Research Part F, 53*, 24-33. doi:https://doi.org/10.1016/j.trf.2017.12.011

Statistics-Japan. (1996). *Statistics Bureau*. (Ministry of Internal Affairs and Communications) Retrieved 10 26, 2017, from http://www.stat.go.jp/english/data/mesh/03.htm

Steenbruggen, J., Nijkamp, P., Smits, J. M., & Mohabir, G. (2012). Traffic incident and disaster management in the Netherlands: Challenges and obstacles in iformation sharing. *Networks and Communication Studies, 26*(3-4), 169-200. doi:10.4000/netcom.975

Sun, D., & Fu, L. (2007). Predicting bus arrival time on the basis of global positioning system data. *Transportation Research Record*, 62-72. doi:10.3141/2034-08

Train, K. E. (2003). *Discrete Choice Methods with Simulation.* New York: Cambridge University Press.

Uno, N., Karauchi, F., Tamura, H., & Iida, Y. (2009). Using bus probe data for analysis of travel time variability. *Journal of Intelligent Transportation Systems*, 2-15. doi:10.1080/15472450802644439

van Reeuwijk, L. P., & Houba, V. J. (1998). *Guidelines for Quality Management in Soil and Plant Laboratories.* Rome: International soil reference and information centre. Retrieved from http://www.fao.org/docrep/W7295E/w7295e08.htm#6 basic statistical tools

Vovsha, P., & Bekhor, S. (1998). Link-Nested Logit Model of Route Choice Overcoming Route Overlapping Problem. *Transportation Research Record 1645*, 133-142.

Watling, D., Milne, D., & Clark, S. (2012). Network Impacts of a Road Capacity Reduction: Empirical Analysis & Model Predictions. *Transportation Research Part A: Policy and Practice, 46*(1), 167-189. doi:10.1016/j.tra.2011.09.010

Wirth, M. (2018, 04 30). *Hastings Star Gazette*. Retrieved 05 27, 2018, from Underpass likely to close due to flooding: https://www.hastingsstargazette.com/news/traffic-and-construction/4437355-update-underpass-likely-close-due-flooding

Wolshon, B., Catarella-Michel, A., & Lambert, L. (2006). Louisiana Highway Evacuation Plan for Hurricane Katrina: Proactive Management of a Regional Evacuation. *Transportation Engineering*, *132*(1), 1-10.

Yai, T., Iwakura, S., & Morichi, S. (1997). Multinomial probit with structured covariance for route choice behavior. *Transportation Research Part B: Methodological, 31*(3), 195-207. doi:10.1016/S0191-2615(96)00025-2

Yan, L. C., Yang, S. S., & Fu, G. J. (2010). Travel Demand Model for Beijing 2008 Olympic Games. *Transportation Engineering*, *136*(6), 537-544.

Young, A. H., Mackenzie, A. K., Davies, R. L., & Crundall, D. (2017). Familiarity breeds contempt for the road ahead: The real-world effects of route repetition on visual attention in an expert driver. *Transportation Research Part F*. doi:https://doi.org/10.1016/j.trf.2017.10.004

Zhang, D., & Nagurney, A. (1996). On the local and global stability of a travel route choice adjustment process. *Transportation Research Part B: Methodological, 30*(4), 245-262. doi:10.1016/0191-2615(95)00034-8

Zhu, S., Levinson, D., Liu, H. X., & Harder, K. (2010). The traffic and behavioral effects of the I-35W Mississippi River bridge collapse. *Transportation Research Part A*, 771-784. doi:10.1016/j.tra.2010.07.001

Zhu, T., & Long, J. (2016). Travel Behavior of Morning Commute with Staggered Work Hours. *Procedia Engineering, 137*, 796-805. doi:10.1016/j.proeng.2016.01.318

Zhuang, X. Y., Fukuda, D., & Yai, T. (2007). Analyzing inter-regional travel mode choice behavior with multi nested generalized extreme value model. *Journal of the Eastern Asia Society for Transportation Studies, 7*, 686-699.

Zimmermann, M., Mai, T., & Frejinger, E. (2017). Bike route choice modeling using GPS data without choice sets of paths. *Transportation Research Part C, 75*, 183-196. doi:http://dx.doi.org/10.1016/j.trc.2016.12.009

Appendix A

The t values resulted from the asymptotic t test carried out between the estimations of 10 trips, 20 trips and 30 trips samples during the period of morning peak are presented here (Section 4.3.31).

Table A.1 t values of asymptotic t test carried out between the estimations of 10 trips samples during the morning peak

Sample	1	2	3	4	5	6	7	8	9	10
1										
2	0.01									
3	-0.15	-0.14								
4	0.00	-0.01	0.16							
5	-0.09	-0.09	0.04	-0.09						
6	0.02	0.02	0.17	0.03	0.11					
7	-0.05	-0.05	0.11	-0.05	0.05	-0.07				
8	-0.21	-0.19	-0.06	-0.22	-0.09	-0.23	-0.17			
9	0.01	0.01	0.17	0.01	0.11	-0.01	0.06	0.23		
10	0.16	0.15	0.28	0.17	0.23	0.14	0.20	0.32	0.15	

Table A.2 t values of asymptotic t test carried out between the estimations of 20 trips samples during the morning peak

Sample	1	2	3	4	5	6	7	8	9	10
1										
2	0.32									
3	0.41	0.10								
4	0.23	-0.11	-0.21							
5	0.31	-0.01	-0.11	0.10						
6	-0.09	-0.39	-0.47	-0.30	-0.38					
7	-0.10	-0.40	-0.48	-0.32	-0.39	-0.01				
8	0.48	0.16	0.05	0.28	0.18	0.54	0.55			
9	0.14	-0.17	-0.26	-0.07	-0.16	0.22	0.23	-0.32		
10	-0.13	-0.45	-0.53	-0.36	-0.44	-0.03	-0.02	-0.61	-0.26	

Table A.3 t values of asymptotic t test carried out between the estimations of 30 trips samples during the morning peak

Sample	1	2	3	4	5	6	7	8	9	10
1										
2	-0.12									
3	0.06	0.20								
4	0.04	0.17	-0.02							
5	-0.02	0.09	-0.09	-0.07						
6	0.12	0.25	0.06	0.07	0.14					
7	-0.04	0.07	-0.11	-0.09	-0.02	-0.16				
8	0.01	0.13	-0.06	-0.04	0.03	-0.11	0.05			
9	-0.02	0.10	-0.09	-0.07	0.00	-0.15	0.02	-0.03		
10	-0.20	0.09	-0.29	-0.26	-0.18	-0.34	-0.15	-0.22	-0.19	

Appendix B

The t values resulted from the asymptotic t test carried out between the estimations of 10 trips, 20 trips and 30 trips samples during the period of day peak are presented here (Section 4.3.3.2).

Table B.1 t values of asymptotic t test carried out between the estimations of 10 trips samples during the day peak

Sample	1	2	3	4	5	6	7	8	9	10
1										
2	0.03									
3	-0.27	-0.21								
4	0.01	-0.03	0.30							
5	0.04	0.02	0.14	0.03						
6	0.01	-0.02	0.27	0.01	-0.03					
7	-0.08	-0.09	0.25	-0.10	-0.07	-0.10				
8	-0.04	-0.06	0.27	-0.05	-0.05	-0.05	0.05			
9	-0.11	-0.11	0.20	-0.12	-0.08	-0.12	-0.03	-0.08		
10	0.01	-0.02	0.26	0.01	-0.03	0.00	0.09	0.05	0.11	

Table B.2 t values of asymptotic t test carried out between the estimations of 20 trips samples during the day peak

Sample	1	2	3	4	5	6	7	8	9	10
1										
2	-0.01									
3	0.11	0.11								
4	0.02	0.02	-0.10							
5	-0.19	-0.17	-0.25	-0.19						
6	-0.07	-0.06	-0.16	-0.08	0.13					
7	-0.10	-0.08	-0.19	-0.10	0.09	-0.03				
8	-0.18	-0.16	-0.25	-0.18	0.00	-0.12	-0.09			
9	0.01	0.01	-0.10	0.00	0.19	0.07	0.10	0.18		
10	-0.09	-0.07	-0.18	-0.09	0.10	-0.02	0.01	0.10	-0.09	

Table B.3 t values of asymptotic t test carried out between the estimations of 30 trips samples during the day peak

Sample	1	2	3	4	5	6	7	8	9	10
1										
2	-0.08									
3	-0.21	-0.14								
4	-0.18	-0.12	0.03							
5	-0.28	-0.22	-0.09	-0.12						
6	-0.29	-0.23	-0.10	-0.13	-0.01					
7	-0.10	-0.03	0.12	0.09	0.20	0.21				
8	-0.10	-0.02	0.13	0.10	0.21	0.22	0.00			
9	-0.07	0.00	0.14	0.11	0.21	0.23	0.03	0.02		
10	-0.01	0.07	0.21	0.18	0.29	0.30	0.09	0.09	0.06	

Appendix C

The t values resulted from the asymptotic t test carried out between the estimations of 10 trips, 20 trips and 30 trips samples during the period of evening peak are presented here (Section 4.3.3.3).

Table C.1 t values of asymptotic t test carried out between the estimations of 10 trips samples during the evening peak

Sample	1	2	3	4	5	6	7	8	9	10
1										
2	-0.09									
3	-0.02	0.23								
4	-0.05	0.15	-0.10							
5	-0.05	0.20	-0.08	0.03						
6	-0.04	0.19	-0.06	0.04	0.01					
7	-0.09	0.01	-0.24	-0.15	-0.20	-0.19				
8	-0.07	0.12	-0.16	-0.06	-0.10	-0.10	0.12			
9	-0.09	-0.01	-0.24	-0.16	-0.21	-0.20	-0.02	-0.13		
10	-0.01	0.20	0.02	0.10	0.08	0.07	0.20	0.14	0.21	

Table C.2 t values of asymptotic t test carried out between the estimations of 20 trips samples during the evening peak

Sample	1	2	3	4	5	6	7	8	9	10
1										
2	-0.03									
3	-0.01	0.02								
4	-0.18	-0.23	-0.21							
5	-0.17	-0.20	-0.19	0.04						
6	0.02	0.03	0.02	0.07	0.06					
7	-0.11	-0.11	-0.11	0.10	0.07	-0.05				
8	-0.05	-0.02	-0.04	0.19	0.17	-0.03	0.08			
9	0.00	0.04	0.02	0.19	0.17	-0.02	0.11	0.05		
10	-0.07	-0.06	-0.07	0.16	0.14	-0.04	0.05	-0.04	-0.08	

Table C.3 t values of asymptotic t test carried out between the estimations of 30 trips samples during the evening peak

Sample	1	2	3	4	5	6	7	8	9	10
1										
2	-0.29									
3	-0.02	0.32								
4	0.03	0.24	0.05							
5	-0.06	0.29	-0.04	-0.08						
6	0.04	0.37	0.06	-0.01	0.11					
7	-0.14	0.22	-0.14	-0.14	-0.10	-0.20				
8	0.03	0.12	0.04	0.02	0.05	0.02	0.08			
9	-0.19	0.17	-0.19	-0.17	-0.16	-0.26	-0.06	-0.09		
10	-0.02	0.28	0.00	-0.05	0.04	-0.06	0.12	-0.04	0.17	

Appendix D

The t values resulted from the asymptotic t test carried out between the estimations of 10 trips, 20 trips and 30 trips samples based on the trips with delay time less than five minutes are presented here (Section 4.3.4.1).

Table D.1 t values of asymptotic t test carried out between the estimations of 10 trips samples with trip delay time less than five minutes

Sample	1	2	3	4	5	6	7	8	9	10
1										
2	-0.07									
3	-0.01	0.07								
4	-0.08	-0.02	-0.08							
5	-0.08	-0.01	-0.08	0.01						
6	-0.04	0.02	-0.04	0.04	0.04					
7	-0.04	0.03	-0.03	0.04	0.04	0.00				
8	0.03	0.06	0.04	0.07	0.06	0.05	0.05			
9	-0.02	0.06	-0.01	0.07	0.07	0.03	0.02	-0.04		
10	-0.09	-0.03	-0.09	-0.01	-0.02	-0.05	-0.05	-0.07	-0.08	

Table D.2 t values of asymptotic t test carried out between the estimations of 20 trips samples with trip delay time less than five minutes

Sample	1	2	3	4	5	6	7	8	9	10
1										
2	-0.07									
3	0.07	0.13								
4	0.08	0.15	0.01							
5	-0.09	-0.02	-0.15	-0.16						
6	-0.13	-0.07	-0.19	-0.20	-0.05					
7	-0.14	-0.07	-0.19	-0.21	-0.06	-0.01				
8	-0.06	0.00	-0.12	-0.13	0.02	0.06	0.07			
9	0.08	0.14	0.01	0.00	0.16	0.20	0.20	0.13		
10	0.05	0.12	-0.02	-0.03	0.13	0.17	0.18	0.10	-0.02	

Table D.3 t values of asymptotic t test carried out between the estimations of 30 trips samples with trip delay time less than five minutes

Sample	1	2	3	4	5	6	7	8	9	10
1										
2	-0.06									
3	0.02	0.08								
4	-0.04	0.02	-0.06							
5	-0.22	-0.17	-0.23	-0.19						
6	-0.11	-0.06	-0.13	-0.08	0.12					
7	-0.17	-0.12	-0.18	-0.14	0.05	-0.07				
8	-0.08	-0.02	-0.10	-0.04	0.16	0.04	0.10			
9	-0.10	-0.04	-0.11	-0.06	0.14	0.02	0.09	-0.02		
10	-0.15	-0.10	-0.17	-0.12	0.08	-0.04	0.03	-0.08	-0.06	

Appendix E

The t values resulted from the asymptotic t test carried out between the estimations of 10 trips, 20 trips and 30 trips samples based on the trips with delay time between 5 to 10 minutes are presented here (Section 4.3.4.2).

Table E.1 t values of asymptotic t test carried out between the estimations of 10 trips samples with trip delay time between 5 to 10 minutes

Sample	1	2	3	4	5	6	7	8	9	10
1										
2	0.00									
3	0.01	0.01								
4	0.02	0.01	0.00							
5	-0.20	-0.17	-0.02	-0.16						
6	0.01	0.01	0.00	0.00	0.19					
7	-0.07	-0.06	-0.01	-0.07	0.22	-0.08				
8	-0.03	-0.03	-0.01	-0.04	0.22	-0.05	0.05			
9	-0.15	-0.13	-0.02	-0.13	0.09	-0.16	-0.14	-0.16		
10	0.01	0.01	0.00	-0.01	0.20	-0.01	0.08	0.04	0.16	

Table E.2 t values of asymptotic t test carried out between the estimations of 20 trips samples with trip delay time between 5 to 10 minutes

Sample	1	2	3	4	5	6	7	8	9	10
1										
2	0.08									
3	0.09	-0.01								
4	-0.05	-0.11	-0.12							
5	-0.04	-0.10	-0.11	0.02						
6	0.08	0.01	0.02	0.11	0.10					
7	-0.13	-0.14	-0.17	-0.08	-0.09	-0.14				
8	0.04	0.01	0.01	0.04	0.04	0.01	0.05			
9	0.06	0.01	0.02	0.08	0.08	0.01	0.10	0.00		
10	0.03	-0.06	-0.06	0.08	0.06	-0.06	0.15	-0.03	-0.05	

Table E.3 t values of asymptotic t test carried out between the estimations of 30 trips samples with trip delay time between 5 to 10 minutes

Sample	1	2	3	4	5	6	7	8	9	10
1										
2	0.06									
3	0.07	-0.01								
4	-0.04	-0.08	-0.09							
5	0.05	0.00	0.01	0.06						
6	0.06	0.00	0.00	0.08	-0.01					
7	0.02	-0.05	-0.05	0.05	-0.04	-0.05				
8	0.06	0.00	0.01	0.07	0.00	0.00	0.05			
9	0.05	0.01	0.01	0.06	0.00	0.01	0.04	0.00		
10	0.05	0.01	0.01	0.06	0.00	0.01	0.04	0.00	0.00	

Appendix F

The t values resulted from the asymptotic t test carried out between the estimations of 10 trips, 20 trips and 30 trips samples based on the trips with delay time greater than 10 minutes are presented here (Section 4.3.4.3).

Table F.1 t values of asymptotic t test carried out between the estimations of 10 trips samples with trip delay time greater than 10 minutes

Sample	1	2	3	4	5	6	7	8	9	10
1										
2	-0.20									
3	-0.17	0.08								
4	-0.15	0.14	0.06							
5	-0.15	0.16	0.09	0.02						
6	0.01	0.09	0.08	0.07	0.07					
7	-0.21	-0.02	-0.12	-0.17	-0.20	-0.09				
8	-0.14	0.14	0.08	0.03	0.01	-0.07	0.17			
9	-0.20	0.00	-0.09	-0.14	-0.17	-0.09	0.02	-0.15		
10	-0.15	0.13	0.06	-0.01	-0.03	-0.07	0.16	-0.03	0.13	

Table F.2 t values of asymptotic t test carried out between the estimations of 20 trips samples with trip delay time greater than 10 minutes

Sample	1	2	3	4	5	6	7	8	9	10
1										
2	0.32									
3	0.32	0.07								
4	0.24	-0.10	-0.16							
5	0.31	-0.01	-0.08	0.09						
6	-0.12	-0.41	-0.40	-0.35	-0.41					
7	-0.14	-0.43	-0.41	-0.37	-0.42	-0.02				
8	0.27	0.09	0.03	0.15	0.10	0.33	0.34			
9	0.16	-0.16	-0.21	-0.07	-0.16	0.27	0.29	-0.19		
10	-0.22	-0.52	-0.46	-0.49	-0.52	-0.06	-0.03	-0.36	-0.39	

Table F.3 t values of asymptotic t test carried out between the estimations of 30 trips samples with trip delay time greater than 10 minutes

Sample	1	2	3	4	5	6	7	8	9	10
1										
2	-0.13									
3	0.06	0.18								
4	0.04	0.17	-0.02							
5	-0.03	0.11	-0.08	-0.07						
6	0.11	0.23	0.05	0.06	0.13					
7	-0.05	0.08	-0.11	-0.09	-0.03	-0.15				
8	0.01	0.14	-0.05	-0.04	0.03	-0.10	0.06			
9	-0.03	0.11	-0.08	-0.07	0.00	-0.13	0.03	-0.03		
10	-0.23	-0.10	-0.27	-0.26	-0.20	-0.31	-0.18	-0.24	-0.21	

Appendix G

The t values resulted from the asymptotic t test carried out between the estimations of 10 trips, 20 trips and 30 trips samples based on the trips made at Toyosu area are tabulated here (Section 4.3.5.1).

Table G.1 t values of asymptotic t test carried out between the estimations of 10 trips samples based on the trips made at Toyosu area

Sample	1	2	3	4	5	6	7	8	9	10
1										
2	0.09									
3	-0.25	-0.24								
4	-0.22	-0.23	0.02							
5	-0.06	-0.13	0.18	0.15						
6	-0.16	-0.19	0.08	0.05	-0.10					
7	-0.35	-0.31	-0.13	-0.15	-0.28	-0.19				
8	-0.30	-0.28	-0.08	-0.10	-0.24	-0.15	0.04			
9	-0.03	-0.11	0.22	0.19	0.02	0.13	0.33	0.28		
10	-0.04	-0.11	0.20	0.18	0.02	0.12	0.31	0.26	-0.01	

Table G.2 t values of asymptotic t test carried out between the estimations of 20 trips samples based on the trips made at Toyosu area

Sample	1	2	3	4	5	6	7	8	9	10
1										
2	-0.06									
3	-0.09	-0.03								
4	-0.03	0.04	0.07							
5	0.02	0.08	0.12	0.05						
6	0.03	0.10	0.14	0.07	0.02					
7	0.00	0.07	0.10	0.03	-0.02	-0.04				
8	-0.03	0.03	0.07	0.00	-0.05	-0.07	-0.03			
9	-0.01	0.05	0.09	0.02	-0.03	-0.05	-0.01	0.02		
10	-0.06	0.00	0.03	-0.04	-0.09	-0.11	-0.07	-0.04	-0.06	

Table G.3 t values of asymptotic t test carried out between the estimations of 30 trips samples based on the trips made at Toyosu area

Sample	1	2	3	4	5	6	7	8	9	10
1										
2	-0.15									
3	-0.03	0.13								
4	-0.08	0.08	-0.05							
5	-0.16	0.00	-0.13	-0.08						
6	-0.04	0.12	-0.01	0.04	0.13					
7	-0.15	0.01	-0.12	-0.07	0.01	-0.12				
8	-0.01	0.15	0.02	0.08	0.17	0.03	0.15			
9	-0.18	-0.02	-0.15	-0.10	-0.02	-0.15	-0.03	-0.18		
10	-0.11	0.05	-0.08	-0.03	0.06	-0.07	0.05	-0.11	0.08	

Appendix H

The t values resulted from the asymptotic t test carried out between the estimations of 10 trips, 20 trips and 30 trips samples based on the trips made at Musashino area are tabulated here (Section 4.3.5.2).

Table H.1 t values of asymptotic t test carried out between the estimations of 10 trips samples based on the trips made at Musashino area

Sample	1	2	3	4	5	6	7	8	9	10
1										
2	0.07									
3	0.06	0.01								
4	0.06	0.01	0.00							
5	0.06	0.01	0.00	0.00						
6	0.06	-0.01	-0.02	-0.02	-0.02					
7	0.04	0.02	0.01	0.01	0.01	0.02				
8	-0.08	-0.13	-0.11	-0.11	-0.11	-0.13	-0.07			
9	0.05	0.02	0.01	0.01	0.01	0.02	0.00	0.08		
10	0.05	0.02	0.01	0.01	0.01	0.02	0.00	0.07	0.00	

Table H.2 t values of asymptotic t test carried out between the estimations of 20 trips samples based on the trips made at Musashino area

Sample	1	2	3	4	5	6	7	8	9	10
1										
2	0.04									
3	0.01	-0.02								
4	0.05	0.01	0.03							
5	0.04	0.01	0.03	0.00						
6	0.03	0.00	0.02	-0.02	-0.02					
7	0.03	-0.01	0.01	-0.02	-0.02	-0.01				
8	0.01	-0.03	-0.01	-0.04	-0.04	-0.03	-0.02			
9	0.04	0.02	0.03	0.01	0.01	0.02	0.03	0.04		
10	0.04	0.02	0.04	0.01	0.01	0.02	0.03	0.04	0.00	

Table H.3 t values of asymptotic t test carried out between the estimations of 30 trips samples based on the trips made at Musashino area

Sample	1	2	3	4	5	6	7	8	9	10
1										
2	0.03									
3	0.01	-0.03								
4	0.05	-0.01	0.04							
5	0.01	-0.03	-0.01	-0.04						
6	0.04	-0.01	0.03	-0.01	0.04					
7	0.04	0.00	0.04	0.00	0.04	0.01				
8	0.01	-0.03	0.00	-0.04	0.00	-0.03	-0.04			
9	0.04	0.00	0.03	0.01	0.04	0.02	0.00	0.03		
10	0.04	-0.01	0.03	-0.01	0.04	0.00	-0.01	0.03	-0.01	

Appendix I

The *t* values resulted from the asymptotic *t* test carried out between the estimations of 10 trips, 20 trips and 30 trips samples based on the trips made at Akihabara area are tabulated here (Section 4.3.5.3).

Table I.1 *t* values of asymptotic *t* test carried out between the estimations of 10 trips samples based on the trips made at Akihabara area

Sample	1	2	3	4	5	6	7	8	9	10
1										
2	0.04									
3	0.15	0.11								
4	-0.08	-0.12	-0.20							
5	0.18	0.15	0.05	0.23						
6	0.04	0.00	-0.12	0.12	-0.15					
7	0.12	0.08	-0.04	0.19	-0.09	0.09				
8	0.14	0.12	0.05	0.18	0.01	0.12	0.07			
9	0.05	0.05	0.03	0.06	0.02	0.05	0.03	0.01		
10	0.08	0.03	-0.09	0.15	-0.13	0.04	-0.05	-0.11	-0.04	

Table I.2 *t* values of asymptotic *t* test carried out between the estimations of 20 trips samples based on the trips made at Akihabara area

Sample	1	2	3	4	5	6	7	8	9	10
1										
2	-0.11									
3	-0.19	-0.10								
4	-0.21	-0.13	-0.02							
5	-0.07	0.05	0.15	0.18						
6	0.00	0.10	0.17	0.19	0.06					
7	-0.35	-0.31	-0.23	-0.22	-0.35	-0.31				
8	-0.15	-0.05	0.06	0.08	-0.10	-0.14	0.28			
9	-0.05	0.07	0.18	0.20	0.02	-0.04	0.37	0.12		
10	0.03	0.11	0.15	0.16	0.08	0.03	0.24	0.13	0.07	

Table I.3 t values of asymptotic t test carried out between the estimations of 30 trips samples based on the trips made at Akihabara area

Sample	1	2	3	4	5	6	7	8	9	10
1										
2	0.02									
3	0.18	0.16								
4	0.21	0.19	0.03							
5	0.21	0.20	0.04	0.01						
6	0.04	0.02	-0.14	-0.17	-0.17					
7	0.02	0.00	-0.16	-0.19	-0.20	-0.02				
8	0.23	0.22	0.09	0.05	0.04	0.20	0.22			
9	0.18	0.16	0.01	-0.03	-0.04	0.14	0.16	-0.08		
10	0.23	0.21	0.07	0.04	0.03	0.19	0.21	-0.01	0.07	